The Immobilization of Copper in Peatlands: Characterizing the Interactions Between Copper and Natural Organic Matter

by

Matt D. Boag

A Thesis
presented to
The University of Guelph

In partial fulfillment of requirements
for the degree of
Master of Science
in
Chemistry

Guelph, Ontario, Canada

ABSTRACT

THE IMMOBILIZATION OF COPPER IN PEATLANDS: CHARACTERIZING THE INTERACTIONS BETWEEN COPPER AND NATURAL ORGANIC MATTER

Matt D. Boag **Advisors:**

University of Guelph, 2017 **Susan Glasauer, Scott Smith**

Organic soils cover large areas of Canada's north and are vital to biogeochemical cycling. Near northern mining operations, organic soils of peatlands sequester potentially toxic metals. There is evidence that remobilization of metals takes place during cycles of freezing and thawing, which can be expected to cause seasonally elevated concentrations of metals in water discharging from peatland environments. This thesis investigates the potential seasonal export of metals from peat during freeze-thaw cycling. By characterizing different size fractions of natural organic matter and the respective complexes they form with copper, it was determined that freezing and thawing produces trends of increasing binding capacity and decreasing binding affinity in natural organic matter. Copper binding properties were also compared using two techniques commonly used to study organic matter; those being ultrafiltration and chemical extraction. It was determined that organic matter $\leq$ 5 kDa does not exhibit equal characteristics to chemically extracted fulvic acid.

Acknowledgements

I would like to thank both my supervisors, Dr. Susan Glasauer and Dr. Scott Smith, for their ongoing support, patience and direction throughout my entire Master's experience. Susan, I thank you for your ongoing encouragement and ability to challenge the status quo which forced me to think outside of the box and question unforeseen directions for my project. I have always appreciated your ability to relate our findings back to real world applications, which added value to everything I have learned. Scott, I thank you so much for the generous amounts of time you spent with me and for your ongoing efforts to improve my knowledge and technical expertise in Analytical Chemistry. It has been an extremely worthwhile endeavor and I will continue to use and expand on what you have taught me throughout the rest of my career.

I would like to thank Dr. Tremaine for his great questions, feedback and ongoing guidance as a member of my committee. Your contributions helped me to establish expectations and prepare myself for the later stages of my project. Your class was also one of the most rewarding challenges I have received throughout my University education.

I would also like to thank everyone who helped me complete my project in the University of Guelph, Environmental Sciences Department. To Shuo and Isaiah, I thank you both for your hard work throughout our small collaborations, assistance in the lab, and company on our frequent trips to Luther Marsh. To Peter Smith, I thank you for always being there as a resource and your assistance in the preliminary stages of my project. To Dr. James Longstaffe, I very much appreciate you letting me use the instruments in your lab and the intriguing questions you proposed I

contemplate for my project. To Dr. Evans, I thank you for your time and help in assessing whether environmental modeling was right to pursue for my project.

I would also like to thank Dr. Francois Caron for allowing me to use his ultrafiltration apparatus and the time spent teaching me how to operate it. Without the generosity of your equipment and your kind guidance to get me started, my project would be completely different than it is today.

Finally, I thank my parents for always being there in my times of stress and fatigue. Your support and encouragement has enabled me to make it through this experience mentally and physically unscathed! I know that without you both, my experience throughout this time would have been drastically different.

Table of Contents

Glossary

NOM……...……..Natural Organic Matter

DOM……...……. Dissolved Organic Matter

TOC……Total Organic Carbon

FTC……...……. Freeze Thaw Cycle

EEMS…….....Excitation-Emission Matrix Spectroscopy

HA……...…...……Humic Acid

FA……...……Fulvic Acid

TRP…….……Tryptophan

TYR…….....Tyrosine

PARAFAC…….……. Parallel Factor Analysis

FOCUS……Fully Optimized Continuous Model

HMW……...High Molecular Weight

LMW……Low Molecular Weight

K_a……...Acid Dissociation Constant

L_T……. Total Ligand Binding Capacity

RO……. Reverse Osmosis

List of Figures

List of Tables

Introduction

1.1 Wetlands & NOM

1.1.1 Wetland Environments

Wetlands can be categorized as one of four different types: bogs, fens, swamps and marshes. The first three contain or are involved in creating peat, a form of decomposed organic matter derived from plants. One essential requirement for all wetland environments is that they contain poorly drained soils [1]. Further classification can be given by organic matter composition and hydrologic cycle. Organic matter can be defined as a carbon-based material originating from plant and cellular components [1]. Wetlands are classified as one of two main hydrologic cycles: minerotrophic or ombrotrophic; the former are groundwater-fed systems and the latter are rainwater-fed systems [2]. Typically, bog wetlands are ombrotrophic, while fens and swamps are minerotrophic [2]. One main reason for this is that bogs have a convex landscape, raised above the surrounding land surface, and as a result it is relatively hydrologically isolated from ground and surface waters. Due to this isolation, there is an insufficient quantity of mineral bases such as $CaCO_3$ required to neutralize the acidity generated by the decomposing organic matter [2].

The end-products of organic decomposition are humic substances which contain acid-generating functional groups and result in bogs generally having a pH around 4 [3]. The Wylde Lake Bog at Luther Marsh, where the samples for this study were taken, is classified as a bog wetland [4].

The high concentration of decomposed organic matter produces oxidizing and reducing zones. Reducing zones are typically the result of microbes consuming oxygen more rapidly than can be replaced below the oxidized surface zone [5]. Further decomposition of organic matter is therefore

impeded by a lack of oxygen, and organic matter which is highly resistant to additional decomposition. Peat from bogs is predominantly comprised of this resistant fraction, and is of specific interest to this project. Organic matter in peat makes up approximately 80% of its composition, with the rest attributed to mineral matter and water [5]. In contrast, mineral soils are the exact opposite. In mineral soils aerobic conditions predominate, replenishing oxygen rapidly and as a result there is a lower composition of organic matter [8].

1.1.2 Humic Substances

One widely distributed component of natural organic matter (NOM) is humic substances [6]. Humic substances are dark coloured, heterogenous organic compounds which are the product of chemically transformed organic matter or are fractions which are highly refractory and cannot be decomposed by microbes. Humic substances are categorized into three fractions which are based on their chemical reactivity and size: humic acid, fulvic acid and humin. Humic acids typically have a molecular weight between 1000-100000 Da and are soluble at pH values greater than 2 [10]. Fulvic acids have a molecular weight between 200-2000 Da, are soluble at all pH values and have a higher oxygen to carbon ratio then humic acid [7]. Humin is the fraction which is insoluble at all pH values [5]. The structures of humic acid and fulvic acid are illustrated in Figures 1-2 and 1-2 below.

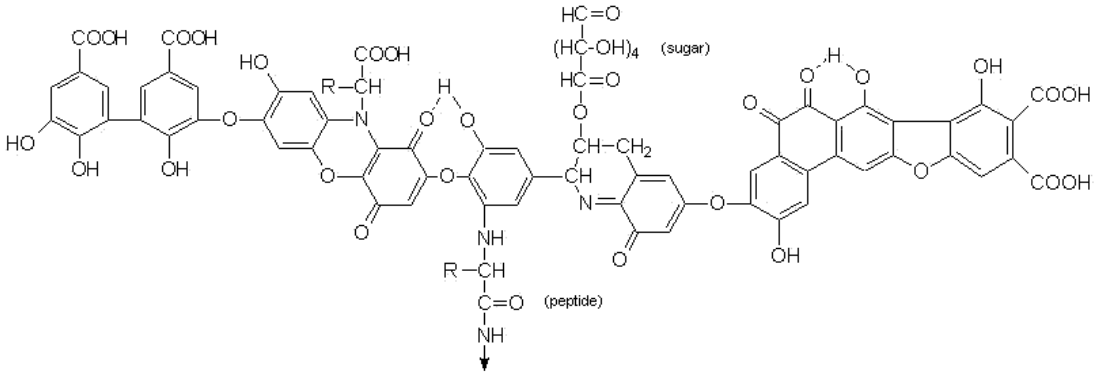

Figure 1-1. Model structure of humic acid according to Stevenson; R can be alkyl, aryl or aralkyl [8].

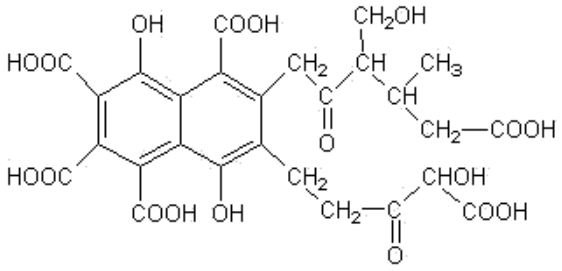

Figure 1-2. Model structure of fulvic acid according to Buffle et al. [9].

It is important to note that the structures above are model compounds and that different fractions of humic substances will exhibit chemical variability. They will share varying degrees of aromaticity and functional group composition; however, no molecule is the same and there is no single defined structure for any fraction [10]. Humic substances can be regarded as supramolecular associations in NOM environments, which form intermolecular complexes through H-bonding and hydrophobic interactions [11, 12].

In terms of solubility, it has been shown that fulvic acid forms complexes with metals that are more soluble while humic acid has the potential to form insoluble complexes [16]. Fulvic acid molecules are soluble at all pH values, they are smaller in size and have a higher content of functional groups [16]. Despite their limited solubility, all fractions of humic substances are very effective at complexing different metals. Defining metal-humic interactions is one of the major motivations for this study, and is a topic of research that is still relatively poorly understood despite decades of investigation.

1.1.3 Soil Solution Chemistry

The definition of soil solution chemistry tends to vary slightly depending on its context. For the purpose of this research, soil solution chemistry will encompass interactions between the aqueous phase and all components associated, and in equilibrium with natural organic matter (NOM). Soil is comprised of a three-phase system consisting of solids, liquids and gases. Soil solution chemistry attempts to describe interactions between these three phases, which include interactions between soil constituents such as mineral and organic particles, and dissolved species in the soil solution. The definition of dissolved species is any species that can pass through a 0.45μm filter. It is important to note that this study involves analyzing, solely, the dissolved fraction of NOM. Emphasis will be placed on the liquid phase, however, as a subset to the solid phase, colloidal particles play a critical role in the solution of soils as well. By definition, colloidal particles are any particle with a diameter of 0.01-10μm [17].

1.1.4 Soil Organic Matter

Soil organic matter (SOM) is composed of a complex mixture of chemical constituents with various ligand and chelating groups. Main groups include: keto, amino, hydroxyl, thiol, thioether, carboxyl and phosphonate groups; see Table 1 below [8].

Table 1-1. Common functional groups present in soil organic matter.

Functional Group Name	Chemical Structure	Reference
Keto	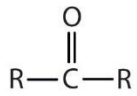	[18]
Amino	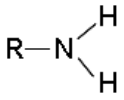	[19]
Hydroxyl	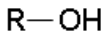	[19]
Carboxyl	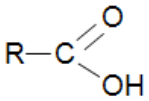	[19]
Thiol	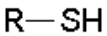	[19]
Thioether	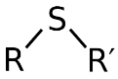	[20]
Phosphonate	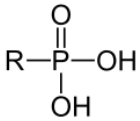	[21]

Functional groups found in SOM are highly immobile and serve largely as centers for ion exchange [8]. This is one of the main reasons why SOM is a primary source for cation exchange in soils, which plays an important role in metal-organic matter interactions [8]. Cation exchange capacity (CEC) is the quantifiable number of negative sites available for cation binding [21]. The CEC is an important property of soil for the binding of elements that occur as soluble cations in pore water. Anion exchange capacity is the opposite.

1.1.5 Origin of NOM

Understanding how NOM is formed can offer insight not only into the structure of NOM, but also how it will interact with metals and its redox properties. NOM can be classified as either autochthonous or allochthonous. Autochthonous NOM is produced through processes that are present in the soil environment [22]. Specifically, this means that they are derived from non-woody plant sources and processes involved in microbial metabolism. This type of NOM will have a much lower proportion of aromatic groups compared to aliphatic compounds, and will therefore have a decreased reducing capacity per unit of carbon [23]. Conversely, allochthonous NOM represents NOM which is not produced in the soil environment of interest [24]. This type of NOM is predominantly produced from woody plants and has a much higher proportion of aromatic groups in comparison to aliphatic ones; this results in an increased reducing capacity per unit of carbon [24].

1.2 Climate Change & Freeze Thaw Impacts

The impact of climate change on wetlands in northern Ontario is a motivation for this study. Approximately 14% of Canada's land surface consists of wetlands, with an area of approximately 1,300,000 km^2 [25] . These wetlands hold approximately 150 billion tonnes of carbon [26]. Specifically, the boreal and subarctic wetland regions of Canada cover at least 1100000 km^2, which comprises approximately 85% of the total area of wetlands in Canada [25]. Massive volumes of water pass through these wetlands containing low level concentrations of metals derived naturally or from mining activity discharge. Changes to the climate are of interest because they may impact the natural equilibrium of these environments. Specifically, there is concern for an increase in metal transport through wetlands.

In the past years, because of the rising temperatures, there has been an emphasis placed on understanding the changes affecting surface water flows at upper latitudes. Specifically, there has been a projected annual increase in temperature and precipitation, and a decrease in snowfall; see Table 1-2 below [27, 28].

Table 1-2. Forecasted temperature, precipitation and snowfall for upper latitudes taken from the Churchill airport meteorological station [28].

	Temperature – Air (°C)		Precipitation (mm)		Snowfall (mm)	
Period	Projected	Observed	Projected	Observed	Projected	Observed
1971-2000	-6.6	-6.8	385	426	148	167
2041-2070	-3.5	-	455	-	159	-
2071-2100	-1.4	-	476	-	140	-

As seen in the table above, the result of these climate related changes is an overall increase in temperature (+5.2 °C) and precipitation (+91 mm) and a decrease in snowfall (-8 mm). Precipitation has the biggest impact on bogs because that is their primary source of water. These projections raise a concern for wetlands during winter months. Warmer and drier winters may lead to an increase in the frequency of soil freeze-thaw cycles (FTCs) [29]. To elaborate, drier winters may decrease snowpack, producing less insulated soil [29]. Without this insulation, warmer winters could result in soil temperatures closer to zero, thereby enabling more frequent fluctuations between freezing and thawing conditions [29]. The reason FTCs are of interest is that they can change the hydrologic fluxes of wetlands, affecting carbon cycling and potentially metal transport as well. One example of how carbon cycling can be affected is that freezing and thawing of different peat soils has been shown to increase dissolved organic carbon (DOC) concentrations at different depths of different soils profiles, as shown in Figure 1-3 below. This is of concern because research has shown that certain metals, specifically copper, become mobile in the presence of increased DOC [30, 31]. Also, to reiterate what was mentioned in Section 1.1.2, attention should be given to fulvic acid in this context since it is known to form soluble complexes with metals

[16]. Soluble metal complexes are of concern because they are typically more bioactive than colloidal complexes, and can have toxic effects against species and microorganisms which may be sensitive to increased concentrations of metal release [32].

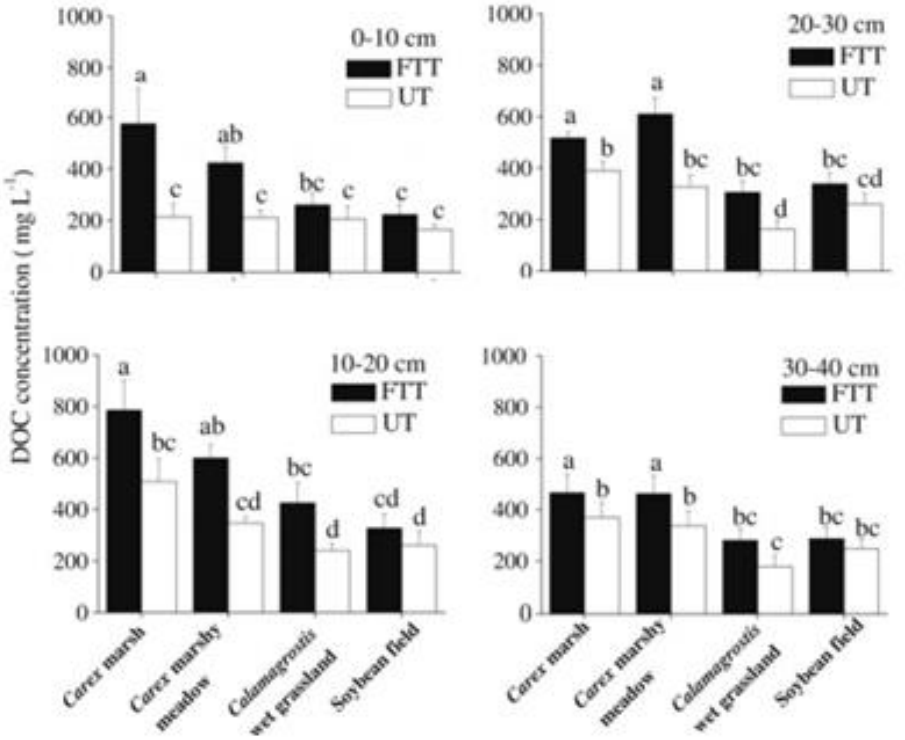

Figure 1-3. Freeze-thaw (FTT) and untreated (UT) comparison of DOC levels in samples of peat soils, at various depths. Taken from [33].

1.3 Redox Chemistry of Natural Organic Matter Systems

1.3.1 NOM, Microbial Metabolism & Electron Shuttling

There has long been supporting evidence that both NOM and microorganisms in NOM environments control redox chemistry in wetland environments [34]. A variety of studies have demonstrated that the same microbes are ubiquitous in NOM systems [35, 36, 37, 38]. We know

that NOM and soil microorganisms are linked through pathways that facilitate the shuttling of electrons. There is a perpetual cycle of electron shuttling that will continue to be maintained as long as there is NOM present. In these cycles microbes will metabolize NOM as a fuel source, and utilize a final electron acceptor (e.g. O_2) to complete the reduction cycle at the end of the pathway.

To provide some perspective in the context of wetland environments, consider an anoxic system with Fe(III) oxide minerals as one example [39]. Since the system is anoxic, there is a very low concentration of oxygen, which characteristically act as a primary electron acceptor. Naturally, microorganisms in this system will process and oxidize NOM as an energy source. However, without oxygen present the Fe(III) oxide will act as an electron acceptor in this microbial process and be reduced to Fe (II) oxide [39]. Microbial degradation of NOM will continue as long as there is sufficient Fe(III) oxide or other available oxidants to accept electrons. If there are no oxidants available, the microbial processing of NOM will be halted.

1.3.2 Redox-Active NOM Constituents

1.3.2.1 Quinone and Quinone-like Moieties

The most common moieties found in NOM systems that take part in reversible redox reactions are quinones and quinone-like moieties, illustrated in Figure 1-4 below.

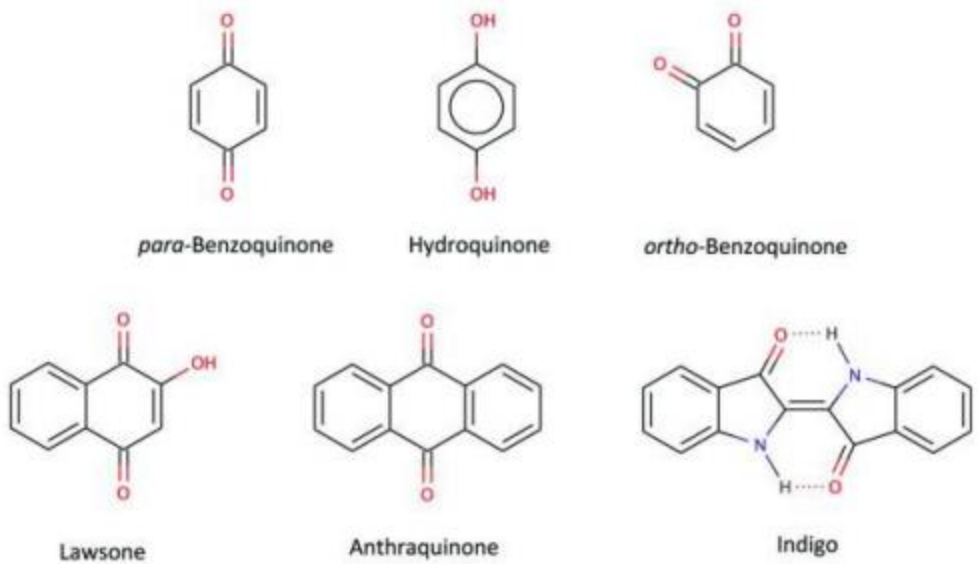

Figure 1-4. Structure of common quinone species found in NOM systems [40].

It should be noted that none of the molecules above have been specifically identified in NOM individually. Instead, they share strong structural similarities to moieties that are found in NOM molecules, which exhibit quinone-like redox behavior.

Although outside of the scope of this study, it is interesting that these moieties play an even larger role relative to natural redox processes when considering one-electron transfer reactions to semiquinone-type free radical intermediates, illustrated in Figure 1-5 below.

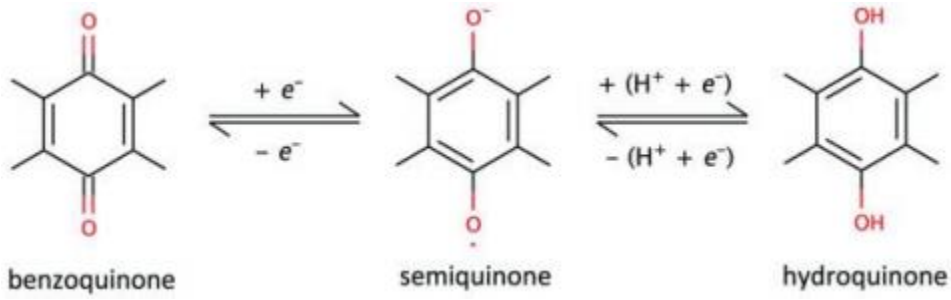

Figure 1-5. Structural diagram of the redox reaction of a quinone compound, to the free-radical semi-quinone intermediate, to the fully reduced hydroquinone [40].

The presence of semi-quinone radicals in NOM has previously been identified by electron paramagnetic resonance (EPR) [40]. The same can be said to a smaller degree for carbon-centered aromatic radicals. Under basic conditions, semi-quinone-type radicals will dominate. As one might assume, and as Figure 1-5 above depicts, pH plays an important role in the redox properties of NOM samples, with redox activity increasing as pH rises [40].

1.3.2.2 Sulfur

Quinone moieties are not the only molecules which can affect the redox chemistry of NOM. Sulfur moieties, although less abundant, contribute to reversible redox reactions as well. Past research has determined that dissolved sulfide, impacts redox reactions of fulvic acid and quinone molecules by generating addition products with phenolic groups; as shown in Figure 1-6 below [41, 34]. Sulfide linkages present in wetlands have also been observed to reduce NOM [42].

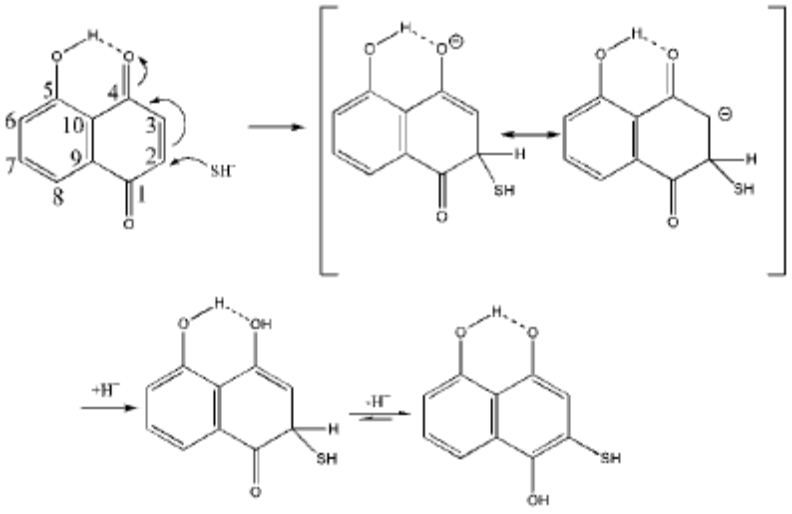

Figure 1-6. Addition reaction mechanism of bisulfide with quinone-like molecule [43].

1.3.2.3 Nitrogen

Nitrogen, although not well studied in the context of NOM redox chemistry, is an interesting element. It is often present in amide and amine form, and solid-state ^{13}C and ^{15}N NMR has demonstrated that it is also present, while in much lower quantities, in heterocyclic moieties [44]. Amides and free amino acids may potentially play a unique role in the overarching properties of NOM and its structural conformation. This is due to the fact that amide molecules typically have a net positive charge in NOM systems, opposite to the majority of NOM which will have a net negative charge [45]. However, this is a difficult element to study due to the lability of nitrogen species in environmental settings [46].

1.4 Metals and Metal Interactions in NOM

1.4.1 Metals in Soils

All soils contain metals which are related to the specific characteristics and geology of the parent material and atmospheric deposition [30]. Because metals cannot be degraded, they are persistent, and it is important to understand their mobility in soil. The mobility of metals is controlled by a number of factors, and is ultimately dependent on the metal and soil environments of interest; although general trends do occur. Some major factors that control metal mobility include: oxidation states of the metals, adsorption and complexation mechanism's, changes in pH, redox potential of the soil environment, and soil composition [2]. Some of these factors will be discussed in detail later in this review. All of these have the ability to change over time due to the progression of organic matter degradation, remediation, climate and weathering processes [30].

Metals in soil environments are considered to be a in free or colloid-bound state. A 'free metal' is in its uncomplexed ionic form or in soluble complexes with organic or inorganic ligands. A complex is defined as a binding arrangement between metals and ligands to create a defined geometrical pattern [47]. Total metal concentration is the sum of all three of these states: free uncomplexed metal, soluble metal complexes and colloid-bound metal. Examples of inorganic ligands that form complexes with metals are: SO_4^{2-}, Cl^-, OH^-, PO_4^{3-}, NO_3^- and CO_3^{2-} [47]. Examples of organic ligands include: low molecular weight aliphatic hydrocarbon chains, aromatic groups, humic acid, fulvic acid, and amino acids [47]. Free Cu in the aqueous phase of soils, typically occurs as the following species: Cu^{2+}, $CuCO_3$, $CuOH^+$ [48]. Metal complexes can be described by formation constants to determine their concentration under specific environmental conditions [48]. One caveat to this is that there is difficulty in describing the relationships for organic ligand

complexes due to the large variability of organic ligands. Generally, the aqueous fraction and those that are in equilibrium with it are the most important when predicting metal mobility [47].

1.4.3 Metal Organic Matter Complexations

Metals are known to form various with functional groups such as: phenol, amino, phosphoryl, thiol and alcohol groups; as previously presented in Table 1-1 [49]. These interactions are based on the specific relationships and properties of functional groups present in the soil environment. In sphagnum peat, humic and fulvic acids comprise the main metal binding ligands, which are predominantly carboxylic and phenolic groups [50].

Metals can be found in diffuse ion associations, also referred to as outer sphere complexes. Such complexes are defined as the exchangeable state of metals. These types of associations are surrounded by water molecules which are not directly bonded to SOM ligands [47]. The ions typically accumulate at the interface of charged particles through electrostatic interactions. The interactions are reversible and largely independent of the electronic configuration of the metal ion and the functional groups [47]. This gives rise to a large reserve of potentially mobile metals [51, 52].

In contrast to outer sphere complexes, metals also form inner sphere complexes. Inner sphere complexes are metals bonded directly via ligand exchange to functional groups in the soil, with no association of water molecules [47]. This type of mechanism is termed “specific adsorption”, in which the word specific implies a difference in the energy of complexation. These associations are fundamentally different from the exchangeable fraction in that these metals form ionic and

covalent bonds with the charged sites of the soil [47]. For this reason, electronic configuration of the metal and functional ligand of the organic matter are much more important due to the high bonding energy. Inner sphere complex metals are known to be mainly immobile due to their strong associations and unaffected by high concentrations of other cations due to the large energy differences [47].

Studies using sphagnum peat show uptake of metals ions following this trend: Pb > Cu > Ni > Cd > Zn, which follows the Irving-Williams series [50]. Cu binding is largely characterized by phenolic sites and is unique from other metals in that it has been shown to form ring shaped complexes with multidentate chelating compounds [50]. However, the complexes that Cu ions form in peat have high-spin configurations, meaning electrons will occupy all orbitals first and then pair up, regardless of the energy of the orbital [50]. Cu often results in very stable complexes in peat relative to other metals [50].

1.4.4 Factors Affecting Metal Behaviour in Soils

1.4.4.1 Effect of Complex Formation

Metal cations, as previously stated, can form complexes with both organic and inorganic ligands. These complexes can yield a net positive, neutral, or negatively charged molecule. Complex formation impacts the binding of an element to a substrate. For example, if the positive charge of a metal decreases due to complexation, specific adsorption to negative sites is reduced. This is important because complexation of metals and NOM is controlled largely by the composition of metal binding sites as well as compatible soluble organic ligands. In general, the stabilities of metal-organic complexes are ordered in the sequence of Hg>Cu>Ni>Pb>Co>Zn>Cd [53]. Copper

forms stable bonds with organic complexes relative to other metals. This trend in stability can influence the mobility of metals as well, as shown by Amrhein, who demonstrated that the mobility of Cu, Ni, and Pb in the presence of DOM increases [54].

1.4.4.2 Effect of pH

The pH of a soil environment can affect several metal retention mechanisms including: adsorption, precipitation, complex formation and oxidation/reduction reactions [2]. As a general rule, metal binding to organic matter typically increases with pH. Cationic metals generally follow this trend because there is an increase in negatively charged binding sites in NOM with an increase in pH. The opposite effect is therefore observed as pH decreases. This is largely attributed to metal cations competing with higher concentrations of H^+ and Al^{3+} ions at lower pH values [47]. In peat, the effect of pH is essentially dependent on the composition of functional groups found in binding ligands. The majority of these functional groups can be classified as weak acids, meaning the stability of the complex will be pH dependent. This helps explain why associations of cations increase in media as the pH increases, cationic metal retention typically reaches a maximum at pH>7 [8].

1.4.4.3 Effect of Ionic Strength

Ionic strength is the strength of the electric field in a solution, determined by the concentration and charge number of electrolytes in that solution [55]. Metal binding by humic matter has been shown to decrease with ionic strength [55]. This can be explained due to complexation reactions involving species of the opposite charge. As ionic strength increases, species of the opposite charge have

their electrostatic attraction shielded by neutral salts, resulting in an overall decrease in attraction. As the ionic strength increases, the shielding effect becomes greater.

1.4.4.4 Effect of Redox Potential

Many metals found in soils can exist in multiple oxidation states. Metals with multiple redox states can gain or lose electrons if suitable oxidants or reductants are present. These states are directly related to the redox potential of the soil environment. Redox potential can be defined in this setting as the availability of electrons or the measure of electrochemical potential in a NOM system [55]. Electrochemical potential can be correlated with information regarding anoxic and oxic soil environments. In anoxic soil environments, oxygen is consumed faster than it is supplied to the soil (e.g. water-logged soils), resulting in a reducing environment [56]. The opposite is true for oxic conditions, which sustain an oxidizing environment (e.g. well – drained 14 soils) [56]. For these reasons, NOM from bog peat is typically in a reduced state. Interestingly, copper is still commonly found in the Cu (II) state under typical environmental conditions [57, 58].

1.5 Organic Matter Characterization

This section will provide the reader with information pertaining to organic matter characterization techniques used in the fields of soil science and geochemistry. This was an important aspect of this project as there is still large debate around the optimal approach to studying NOM. It is therefore important that this section also serve to justify why the methods of characterization for this project were selected. There will be an emphasis placed on conventional extraction techniques, common substitutes and less common techniques which show potential for future application.

One of the simplest approaches to characterizing NOM would be to visually discern differences in its physical characteristics. An example would be characterizing a sample by its visibly distinguishable components of plant debris (e.g. roots or plant branches) and contrasting it to a sample which is highly degraded and therefore has no observable constituents. While this approach would only offer qualitative information, the main goal of such a comparison would be to gain insight into the differences in biochemical transformations. As one might imagine, this method of characterization does not offer detail into the different classes of compounds – for example different classes of biomolecules – which could be present in the multiple phases of soil transformation.

One way to characterize NOM more precisely is to describe the chemical properties of specific phases in soil. Soil OM is divided into humic substances and non-humic substances [59]. Plant debris and its different sub-classes of organic molecules are classified as non-humic substances. The remaining amorphous components, which are not discernable as plant debris and cannot be recognized as a class of organic compounds, are classified as humic substances [59].

The method of approach depends on the goals of the study. NOM systems are tremendously complex and it is advised that samples be analyzed either in situ or by extraction, purification and fractionation techniques.

1.5.1 Extraction of SOM

There are a number of techniques which facilitate characterization of OM in situ. In "Methods of Soil Analysis" D. Sparks explains that these range from detailed chemical characterizations to separation of OM fractions based on broad chemical properties [60]. However, to reiterate, NOM systems can be complex and the removal of any one constituent may affect the state of NOM or how it interrelates with the rest of sample.

To elaborate on the previous point, a topic of controversy is the modification of organic matter in extraction techniques. This is concerning because there is the potential to alter the organic matter's structure as well as produce unwanted artifacts. However, these effects can be somewhat mitigated by selecting appropriate extraction reagents. An example of this could be the use of neutral pyrophosphate as a milder reagent, as opposed to the commonly used sodium hydroxide [60]. The one caveat to this compromise is that there can be a decreased yield of extracted NOM when using milder reagents [61].

Most soil extraction methods aim to raise the pH of the sample, therefore removing any multivalent cations from negatively charged functional sites in the process. The base extractant competes with these cations for exchange sites. A large proportion of these cations will be replaced with the counterion of the base (e.g. NaOH is comprised of OH^- and its counterion Na^+). As the pH rises and more cations are dissociated from their binding sites, intramolecular repulsion expands the organic macromolecules. This allows water molecules to solvate polar groups, disrupting

intermolecular interactions, and in turn solubilizing the organic matter so that it can be extracted [60].

Whitehead and Tinsley originally proposed four criteria that the solvent should possess if used as for the extraction of SOM [61]. These include: 1) high polarity and high dielectric constant to support the dispersion of charged molecules; 2) small molecular size to infiltrate humic substances; 3) properties to disrupt pre-existing hydrogen bonds, enabling alternate groups to create humic-solvent hydrogen bonds 4) properties which facilitate the removal and immobilization of metallic cations.

Stevenson outlines four alternative criteria that the entire extraction process should represent [62]. 1) The extraction should yield isolation of unaltered constituents. 2) Extracts have no inorganic impurities like clay or polyvalent cations. 3) The extraction should be complete, thereby ensuring representation of fractions from the entire molecular weight range. 4) The process should be universally valid for all soil types.

1.5.2 Fractionation of Soil Organic Matter

Fractionating a sample of humic substances does not yield pure homogenous compounds but instead it produces fractions with a narrower range of physical or chemical properties than the original sample. There are a number of different fractionation techniques. These are based on

characteristics such as differences in solubility, molecular size and electrostatic charge within a system [63]. They are summarized below.

1.5.2.1 Fractionation Based on Solubility

The solubility of humic substances is not only pH dependent but also depends on the cation concentration, other solutes and the choice of solvents. These factors can be used individually or in combination to fractionate organic matter.

1.5.2.2 pH Fractionation

As previously mentioned in Section 1.5.1, pH can be manipulated to solubilize and precipitate out fractions of humic substances. This is the basis of the classic soil extraction of humic acid and fulvic acid. The degree to which the pH is changed can result in narrower or wider fractions [64]. However, due to the variety of functional and structural properties in these molecules, it is probable that sub-fractions will yield substantially similar chemical characteristics.

1.5.2.3 Salting Out

Both the intramolecular and intermolecular potential depends on salt concentration. This means an increase in salt concentration will decrease intermolecular charge repulsion and result in increased condensation of macromolecules and an exclusion of solvent molecules. This will produce a shrinking effect on the diffuse double layer which controls electric potential surrounding a charged

surface [65]. This would therefore produce less intermolecular charge repulsion and facilitate coagulation of organic matter molecules [65].

1.5.2.4 Fractionation Based on Molecular Size

As a result of the vast intermolecular associations in organic matter systems, it can be challenging to impose well defined molecular size characterizations. However, ultrafiltration, gel permeation chromatography and electrophoresis are methods which have had success when used on organic matter samples [60].

1.5.3 Filtration Separation

Membrane separation technology is becoming a popular alternative to common methods of soil OM characterization. Major benefits include: no supplementary materials or reagents required, constant and automatic operation, generally inexpensive [66, 67]. Filtration separation techniques can also be characterized by different size ranges and the applied force that is used. Most common filtration techniques include: microfiltration, ultrafiltration, nanofiltration and reverse osmosis. This project makes use of microfiltration and ultrafiltration separation. Microfiltration separates particles ranging from 0.1-10 μm and ultrafiltration separates particles ranging from 1-100 nm in size [66]. The typical driving pressures to force the solvent to flow through the membrane in ultrafiltration are in the range of 10 to 100 psi [67].

Typically, microfiltration and ultrafiltration membranes are produced from some type of polymeric material. These may include: polyamide, polysulphone, cellulose-acetate, or polycarbonate materials [66]. Inorganic membranes are rarely used due to their high costs; however they are utilized when separations need to be performed at a smaller pore size range, at high temperatures, or if there is potential for resistance to fouling. Inorganic membrane material may include: aluminum-oxide, silica glass or ceramic material [66].

There are three main types of filtration. The first is referred to as dead-end filtration. In this type of filtration, the sample is put under pressure and not disturbed otherwise. The second is referred to as stirred dead-end filtration. This is the same as dead-end filtration, except the sample is stirred with a stir bar. The third type of filtration is referred to as cross-flow filtration. In this technique, the solution is pumped tangentially (i.e. travels parallel to the membrane) over the membrane [66]. In each case transmembrane pressure is the force that drives the solution and permeable molecules through the membrane [67].

1.5.4 Gel Permeation Chromatography

Separation of organic matter is facilitated by the pore properties found within the beads of gel permeation columns. Pore size is of main interest, and is a result of the degree to which the polymers making up the gel are cross linked [60]. The process works by imposing a size constraint on the space between the pores that make up the column. When a sample is passed through the column with a solvent, larger molecules typically move through the column faster because they are too large to pass through individual pores, and instead travel around the beads entirely. In

contrast, smaller molecules will take longer to pass through the column since they will penetrate and travel slowly through the smaller pore sizes. Pore shape can also elicit differences in the time it takes for molecules to pass through the column. The range of the separation will depend specifically on size properties of the column. The selection of the column should also factor in properties of the solute, ensuring that the column is inert to the solute molecules so there are no additional chemical or physical interactions that occur during the separation [60].

1.5.5 Electrophoresis

Electrophoresis is another technique that makes use of the size properties of organic matter molecules to characterize a system. The process involves denaturing or unfolding molecules in the sample so that they can be analyzed at the same mass to charge ratio. This is then followed by dissolving these molecules in a gel medium, in which an electrical current is passed through. This causes movement of the molecules as a function of their charge, shape and size. As a result, smaller molecules will typically pass through the gel pores faster than larger ones do. The particular sizes of the samples are analyzed by comparison to a molecular weight ladder or a similar gel-injected standard [68].

Electrophoresis can also make use of pH gradients which are integrated into the gel. This specific type of separation is termed electrofocusing, which takes advantage of each individual molecule's isoelectric point [68]. The isoelectric point is the pH at which there is no longer any charge on the molecule, and as a result there is no attractive force to pull the molecule through the gel. It is worth

noting that when using this type of technique, a constant pore size is usually applied so that the samples are solely separated based on charge.

1.5.6 Characterization by Spectroscopic Methods

Spectroscopic techniques can offer valuable insight into important molecular components of soil systems, such as the composition of functional moieties in NOM. However, these techniques are not entirely comprehensive, and are best used in tandem with other techniques, or combined with additional data to provide an overall characterization

1.5.6.1 UV-Visible Spectroscopy

Both UV-Visible and fluorescence spectroscopy are used in this project. One of the main reasons is that this technique effectively identifies electronic transitions of bonding electrons from 200-400 nm (UV region) and 400-800 nm (visible region). This makes this technique ideal for identifying moieties in soil samples with unbound electrons. Such moieties include carbonyl groups, conjugated C-C groups, as well as groups with the presence of O, N and S [60].

The reason these techniques are typically used in tandem with other data is because UV-visible data cannot elucidate specific compounds in organic matter samples. Its purpose is to provide the relative concentration of various chromophores. Research in this field has shown that as the wavelength decreases, there will typically be an increase in absorbance [60].

A common technique used for studying NOM is to relate the absorbances at 465 nm and 665 nm to one another to confer information about the degree of aromaticity. This is denoted as the E_4/E_6 ratio [69, 70]. Important to note is, because organic matter chemistry is a function of pH, the identifiable components in NOM samples are also pH dependent. Interestingly, the E_4/E_6 ratio decreases as the pH increases, and conversely it will also decrease at pH values lower than 5.5 [69, 70]. Absorbance is also dependent on ionic strength.

1.5.6.2 Fluorescence Spectroscopy

Radiation which is absorbed in UV-Visible frequency range is also released as electromagnetic radiation, or as heat energy. Fluorescence is a result of the former producing an emission of light with wavelengths that are longer than the incident light.

Fluorescence spectroscopy is quite effective at characterizing soluble organic matter in soil systems because it more sensitive and selective than UV-Vis spectroscopy. It is able to identify humic-like, fulvic-like, and protein-like moieties. Components of the humic-like and fulvic-like fractions have previously been identified by 5 excitation/emission wavelengths. In past research done by Kramer et al., ratios of 320nm/425nm have represented interactions with simple aromatics and hydroxyquinolones, 370nm/450nm have represented simple aromatics and flavones, 420nm/500nm have represented flavones, and 480nm/540nm and 500nm/550nm have represented common but unknown fluorophores signature to fluorescent intensities found in natural organic matter [71]. Protein like components in soil can be characterized by tyrosine peaks at 270-280nm/300-305nm, and tryptophan peaks at 270-280nm/340-350nm [71].

Important to note is that, when applied to soil systems, only a small proportion of chemical groups will fluoresce. Due to the fact that organic matter in soil samples can absorb light over a range of wavelengths, it is very likely that molecules will actually reabsorb emitted fluorescence light. This is a form of inner filtering, which can make attaining fluorescence difficult. Fortunately, researchers such as T. Ohno et al. have shown that absorbance spectroscopy can be used as to help correct for this [72].

1.5.6.3 *Infrared Spectroscopy*

Infrared spectroscopy (IR) takes advantage of characteristic absorption frequencies associated with molecular vibrations that occur between bonded atoms in a sample. The measured frequencies can be used to discern different atoms and their binding characteristics. One downfall to this technique, similar to other spectroscopic techniques, is that it is not sensitive enough to detect low concentrations of specific functional groups which would aid in differentiating complicated samples of NOM.

This technique can be fully utilized when comparisons of a sample spectrum can be made to reference standards. Conclusions can therefore be drawn from the differences in each spectrum. IR can also be utilized by comparing unaltered samples to chemically altered samples. Commonly, the main benefit one might be interested in is attaining information related to functional groups such as aromatic, aliphatic and quinone groups [60].

Spectra produced by IR will not provide any well-defined structural information. Instead the spectra will offer a wide breadth of information including a range of different chemical moieties. It is therefore an effective technique at describing overall functional group composition, and should be used in tandem with other techniques to provide a full description when studying soil systems.

1.5.6.4 Nuclear Magnetic Resonance

Nuclear Magnetic Resonance (NMR) characterizes samples based on specific magnetic properties of atomic nuclei. An isotope will have a magnetic moment and angular momentum if it has an odd number of protons and/or neutrons. This can be referred to as a nonzero spin. In contrast, isotopes with an even number of protons and/or neutrons will have a total spin of zero. The most commonly studied nuclei are ^{-1}H and ^{-13}C.

Again, there are difficulties when applying NMR to organic matter soil samples. With liquid state NMR, the first concern is the amount of sample required (i.e. 100-200 mg), and the second major concern is that water, which is typically present in samples, will interfere with ^{-1}H NMR [60]. However, solid state NMR does not suffer from the same limitations and has both a better sensitivity and signal to noise ratio. Solid state cross-polarization magic angle spinning-nuclear magnetic resonance (CPMAS-NMR) is most commonly utilized to characterize NOM [73, 74].

Like other spectroscopic techniques, one cannot fully characterize NOM samples with this method of analysis. Rather NMR serves to provide a comparison of functional group compositions in samples.

1.6 Objective of This Study

This thesis addresses two main themes; (1) the assessment and characterization of the effects that multiple freeze-thaw cycles have on NOM present in wetland pore water and (2) a comparison of results from two different approaches used to study NOM: ultrafiltration and chemical extraction. The experimental objectives of this research were:

1. To characterize the quality of pore water NOM taken from Luther Marsh Wylde Lake Bog using ultrafiltration, acid-base titrimetry and fluorescence spectroscopy.
2. To assess the effects that freezing and thawing have on pore water NOM, using ultrafiltration, acid-base titrimetry and fluorescence spectroscopy.
3. To assess the effects that multiple freeze-thaw cycles have on peat, specifically examining Cu binding strengths and capacities. This involved ultrafiltration, fluorescence spectroscopy and Cu ion selective electrode.
4. To assess the differences between an ultrafiltration and chemical extraction approach to studying NOM. This involved comparing the 5 kDa filtrate fraction from ultrafiltration separation, and the fulvic acid fraction from a humic-fulvic chemical extraction. Fluorescence spectroscopy and Cu ion selective electrode analysis were used to assess variability between the two approaches.

1.7 Hypotheses and Overview of Chapters

The focus of Chapter 2 is to outline preliminary experimentation used to establish optimal experimental parameters to characterize the effects, if any, that freezing and thawing have on pore water NOM. No formal hypotheses were made for these preliminary experiments. Objectives 1 and 2 were explained in this chapter. The results indicated no distinct differences between the control and treatment samples. This led to the conclusion that there is either no effect observed after freezing and thawing, there was insufficient NOM present to observe these effects, or that the freeze-thaw stimulus was insufficient to elicit any observable change.

Chapter 3 describes results using a revised experimental design, based on the findings explained in Chapter 2. The experimental set-up, including sample preparation and treatment, was changed. We hypothesized that because thawing of frozen peat has been shown to release DOM, and the dissolved fraction is more labile and therefore characteristic of smaller fulvic acid-like molecules, FTCs will generate a larger proportion of smaller molecular weight NOM [54, 75]. Additionally, previous research has shown an increase in DOC concentrations in the first three days of consecutive freezing and thawing of peat in FTC studies [76]. This was attributed to the decomposition of dead microorganisms and release of lysed small molecular weight sugars and amino acids [76, 77]. It was therefore also hypothesized that multiple FTCs will yield a larger proportion of protein-like fluorescent moieties from the pore water-peat mixtures. These two hypotheses led to another hypothesis that Cu binding capacity will be higher in samples which have undergone multiple FTCs, but the affinity will be lower. This is because it is expected that the ‘control’ samples will have a greater composition of NOM which is larger in size. Larger NOM

fragments resemble humic acid-like molecules which have been shown, generally, to have a higher affinity for Cu in comparison to fulvic acid [78, 79]. However, they only have approximately half the exchange capacity [80].

Chapter 4 focuses on comparing similar NOM samples from two different approaches to studying NOM. The 5 kDa filtrate fraction from ultrafiltration separation and the fulvic acid extract from a humic-fulvic extraction procedure were studied. As previously stated, fulvic acid molecules range from 200-2000 Da, and the 5 kDa filtrate fraction will contain molecules which are equal to or less than 5000 Da [7]. Relative to the overall range of NOM molecular weights present in pore water samples, this difference in size is considered small. It is therefore hypothesized that NOM in the 5 kDa filtrate fraction will have predominantly the same characteristics as fulvic acid molecules. Both NOM fractions will therefore yield equal fluorescent and copper binding properties.

1.8 Significance of Study

The ability to characterize DOM in bog pore water samples, as well as studying the effects that freezing and thawing has on DOM, will offer valuable insight into metal cycling in wetlands which has gone largely unstudied in this field. This information, most importantly, has the goal of aiding in assessing the risks and effects that climate change will have on wetlands. There is a specific interest in connecting the effects of climate change to copper mobility, NOM complexation, and thus its potential for toxicity.

There is a not only a need for understanding how NOM interacts with itself but with metals as well. Specifically, assessing the binding strength and capacity of copper in our samples can offer valuable information related to the remedial properties of wetlands. In particular, there is specific interest to regions which are in the vicinity of potential mining activity.

The combination of the first three objectives provide a foundation to assist risk assessors in predicting the fate and transport of Cu in environments that may be toxicologically threatened, or sensitive to increased concentrations of metals.

The fourth and final objective will establish a clear comparison between different approaches taken by different disciplines, in studying the same systems. Specifically, this involves comparing the two techniques: ultrafiltration and chemical extraction. For a field to progress, it is paramount that novel techniques and ideas be pursued to gain unprecedented information, while also ensuring that different scientific groups achieve reproducible results. Currently, there has been little information researched to indicate that results from one method of DOM characterization can be reproduced using another markedly different method of characterization. Dependent on the similarity of these results, this could potentially aid in the development of new techniques, or further solidify the use of traditional methods.

1.9 References

[1] Wright, A., "Environmental consequences of water withdrawals and drainage of wetlands," University of Florida, vol. 302, 2013.

[2] Shotyk, W., "Review of the inorganic geochemistry of peats and peatland waters," pp. 95-176, 1988.

[3] Atkins, W., "Some geochemical applications of measurements of hyrodgen ion concentration.," *Sci. Proc. R. Dublin Soc.*, vol. 19, pp. 455-460, 1930.

[4] Cheskey, E., Wilson, W., "Luther Marsh important bird area conservation plan," Ontario Ministry of Natural Resources, 2001.

[5] Gondar, D., "Copper binding by peat fulvic and humic acids extracted from two horizons of an ombotrophic peat bog," *Chemosphere*, vol. 63, pp. 82-88, 2006.

[6] Sutton, R., Sposito, G., "Molecular structure in soil humic substances: the new view," *Env. Sci. & Tech.*, vol. 39, pp. 23.

[7] Niessen, W., "Liquid Chromatography-Mass Spectrometry, Third Edition," CRC Press - Taylor & Francis, vol. 97, pp. 216.

[8] Stevenson, F., "Humus Chemistry; genesis, composition, reactions" Wiley Interscience, vol. Chapter 14, 1982.

[9] Buffle, J., "Measurement of complexation properties of humic acid and fulvic acid acids in natural waters with lead and copper ion-selective electrodes," *Anal. Chem.*, vol. 49, pp. 216-222, 1977.

[10] Hayes, M., Malcolm R., and Swift, R., "Humic Substances II: In Search of Structure," John Wiley & Sons, 1989.

[11] Piccolo, A., "The supramolecular structure of humic substances," *Soil Sci.*, vol. 166, pp. 810-832, 2001.

[12] Simpson, A., Kingery, W., Hayes, M., et al., "Molecular structure and associations of humic substances in the terrestrial environment," *Naturewissenchaften*, vol. 89, pp. 84-88, 2002.

[13] Jenkinson, D., "The turnover of soil organic matter in some of the Rothamsted classical experiments," *Soil Sci*., vol. 123, pp. 298-305, 1977.

[14] Hsieh, P., "Radiocarbon signatures of turnover rates in active soil organic carbon pools," *Soil Sci. Soc. Am. J*., vol. 57, pp. 1020-1022, 1993.

[15] Balesdent, J., "Soil organic matter turnover in long-term field experiments as revealed by carbon-13 natural abundance," *Soil Sci. Soc. Am. J*., vol. 52, pp. 118-124, 1988.

[16] Tan, K., "Humic matter in soil and the environment: principles and controversies," University of Georgia, Marcel Dekker Inc., 2003.

[17] Sposito, G., "The Chemistry of Soils," Oxford University Press, 1989.

[18] Timberlake, K., Introduction to Chemistry: General, Organic, and Biological, Prentice Hall; 10th Edition, 2008.

[19] Evanko, C., Dzombak, D., “Influence of Structural Features on Sorption of NOM-Analogue Organic Acids to Goethite” *Environ. Sci. Technol.*, vol. 32, pp. 2846-2855, 1998

[20] Manceau, A., et al., “Structure, bonding, and stability of mercury complexes with thiolate and thioether ligands from high-resolution XANES spectroscopy and first-principles calculations”, *Inorg. Chem*. Vol. 54, pp. 11776-11791, 2015

[21] Karlsson, T., Persson, P., Skyllber, U., “Complexation of copper(II) in organic soils and in dissolved organic matter − EXAFS evidence for chelate ring structures” E*nviron. Sci. Technol.*, vol. 40, pp. 2623–2628

[22] Christman, R., Shi, J., Wagoner, D., Sharpless, C., Fischer, E., Schupach, J. "A new method for characterizing aquatic organic matter," University of North Carolina: Chapel Hill, 1998.

[23] Kordel, D., Dassenakis, M., Lintelmann, J., Padberg, S., "The importance of natural organic material for environmental processes in waters and soils," *Pure Appl. Chem*., vol. 69, pp. 1571-1600, 1997.

[24] Tank, J., Rosi-Marshall, E., Griffiths, N., Entrekin, S, Stephen, M., "A review of allochtonous organic matter dynamics and metabolism in streams," *J. N. Am. Benthol. Soc*., vol. 29, pp. 61, pp. 118-146, 2010.

[25] Marsh, P., "Climate variability and change - wetlands," Environment and Climate Change Canada, National Water Research Institute, 2007.

[26] Roulet, N., "Peatlands, carbon storage, greenhouse gases, and the Kyoto protocol: prospects and significance for Canada," *Wetlands*, vol. 20, pp. 605-615, 2000.

[27] IPCC, "Climate Change 2007: Climate Change Impacts, Adaptation and Vulnerability Contribution of Working Group II to the Fourth Assessment Report of the IPCC," Cambridge University, 2007.

[28] Macrae, M., Brown, L., Duguar, C., Parrott, J., Petrone, R., "Observed and projected climate change in the churchill region of the hudson bay lowlands and implications for pond sustainability," *Arct. Antarc. Alp. Res.*, vol. 46, pp. 272-285, 2014.

[29] Henry, H., "Soil freeze-thaw experiments: trends, methodological weaknesses, and suggested improvements," *Soil. Biol. Biochem.*, vol. 39, pp. 977-986, 2007.

[30] W. Kalbitz, "Mobilization of heavy metals and arsenic in polluted wetland soils and its dependence on dissolved organic matter.," *Sci Total Environ*., vol. 209, pp. 27-39, 1998.

[31] Lockwood, B., "Leaching of copper and nickel in soil-water systems contaminated by bauxite residue (red mud) from Ajka, Hungary: the importance of soil organic matter," *Environ. Sci. Pollut. Res.*, vol. 22, pp. 10800-10810, 2015.

[32] Wells, M., Kozelka, P., Bruland, K., "The complexation of ‘dissolved’ Cu, Zn, Cd and Pb by soluble and colloidal organic matter in Narragansett Bay, RI," *Mar. Chem.*, vol. 62, pp. 203-217, 1998.

[33] Yu, X., Zou, Y., Jiang, M., Lu, X., Wang, G., "Response of soil constituents to freeze–thaw cycles in wetland soil solution," *Soil. Biol. Biochem.*, vol. 43, pp. 6, pp. 1308-1320, 2011.

[34] Dunnivant, F., Schwarzenbach, R., Macalady, D., "Reduction of substituted nitrobenzenes in aqueous solutions containing natural organic matter," *Environ. Sci. Technol*., vol. 26, pp. 2133-2141, 1992.

[35] Brune, M., Schink, B., Benz, M., "Humic acid reduction by Propionibacterium freudenreichii and other fermenting bacteria," *Appl. Environ. Microbio*., vol. 64, pp. 4507-4512, 1998.

[36] Lovley, D., Roden E., Gaw, C, et al., "Recovery of humic-reducing bacteria from a diversity of environments," *Appl. Environ. Microbio*., vol. 64, pp. 1504-1509, 1998.

[37] Coates, J., Phillips, P., Hayes, L., et al., "Humic substances as a mediator from microbially catalyzed metal reduction," *Acta. Hydrochim. Hydrobiol*., vol. 26, pp. 152-157, 1998.

[38] Lovley, D. Kashefi, K., Vargas, M., et al., "Reduction of humic substances and Fe(III) by hyperthermophilic microorganisms," *Chem. Geol.*, vol. 169, pp. 289-298, 2000.

[39] Tratnyek, P., Nurmi, J., "Electrochemistry of natural organic matter. division of environmental and biomolecular systems," *J. Am. Chem. Soc.*, 2011.

[40] Macalady, D., Walton-Day, K., "Redox chemistry and natural organic matter (NOM): geochemists' dream, analytical chemists' nightmare," *J. Am. Chem. Soc*, pp. 85-111, 2011.

[41] Schäfer, T., Mayer, B., Einsiedl, F., "Evidence for incorporation of H_2S in groundwater fulvic acids from stable isotope ratios and sulfur K-edge X-ray absorption near edge structure spectroscopy," *Environ. Sci. Technol.*, vol. 42, pp. 2439-2444, 2008.

[42] Zeyer, J., Lanz, K., Stierli, R., Schwarzenbach, P., "Quinone and iron porphyrin mediated reduction of nitroaromatic compounds in homogeneous aqueous solution," *Environ. Sci. Technol.,* vol. 24, pp. 1566-1574, 1990.

[43] Perlinger, J., Kalluri, V., Vekatapathy, R., Agnst, W., "Addition of hydrogen sulfide to juglone," *Environ. Sci. Technol*., vol. 36, pp. 2663-2669, 2002.

[44] Knicker, H., "Biogenic nitrogen in soils as revealed by solid-state carbon-13 and nitrogen-15 nuclear magnetic resonance spectroscopy," *J. Environ. Qual*., vol. 29, pp. 715-723, 2000.

[45] Wershaw, R., "Evaluation of conceptual models of natural organic matter (humus) from a consideration of the chemical and biological processes of humification," Scientific Investigations Report, U.S. Geological Survey, pp. 2004-5121, 2004.

[46] Sposito, G., Sutton, R., "Molecular structure in soil humic substances: The new view.," *Environ. Sci. Technol.*, vol. 39, pp. 9009-9015, 2005.

[47] Bledsoe, B., McLean, J., "Ground Water Issue - Behavior of Metals in Soils," US EPA, vol. 540, 1992.

[48] Driscoll, C., Otton, J., Iverfeldt, A., "Trace Metals Speciation and Cycling," Biogeochemistry of Small Catchments: A Tool for Environmental Research, 1994.

[49] Parikh, S., Goyne, K., Margenot, A., et al., "Soil chemical insights provided through vibrational spectroscopy," USDA-ARS, 2014.

[50] Kalmykova, Y., Stromvall, A., Steenari, B., "Adsorption of Cd, Cu, Ni, Pb and Zn on sphagnum peat from solutions with low metal concentrations," *J. of Haz. Mat.,* vol. 152, pp. 885-891, 2008.

[51] Silviera, D., Sommers, L., "Extractability of copper, zinc, cadmium, and lead in soils incubated with sewage sludge," *J. Environ. Qual*., vol. 6, pp. 47-52, 1977.

[52] Latterell, J., Dowdy, R., Larson, W., "Correlation of extractable metals and metal uptake of snap beans grown on soil amended with sewage sludge," *J. Environ. Qual*., vol. 7, pp. 435-440, 1978.

[53] Overcash, M., Pal, D., "Design of Land Treatment Systems for Industrial Wastes - Theory and Practice," Ann Arbor Science Publishers, 1979.

[54] Amrhein, C., Strong, J., "Effect of deicing salts on metal and organic matter mobility in roadside soils," *Environ. Sci. Technol*., vol. 26, pp. 703-709, 1992.

[55] Tipping, E., "Cation Binding by Humic Substances," Cambridge University Press, 2002.

[56] Russel, B., "EPA Environmental Engineering Sourcebook," CRC Press, 1996.

[57] Cempel, M., "Nickel: a review of its sources and environmental toxicology," *Polish. J. of Environ. Stud*., vol. 3, pp. 375-382, 2006.

[58] "Alberta Water Quality Guideline for the Protection of Freshwater Aquatic Life," Alberta Environmental Protection, 1996.

[59] Hayes, S., "The Chemistry of Soil Organic Colloids," Wiley-Intersci., pp. 179-320, 1978.

[60] Sparks, D., "Methods of soil analysis part 3 - chemical methods," *Soil Sci Soc Am J,* Inc., pp. 5, p. 1011, 1996.

[61] Whitehead, T., "Extraction of soil organic matter with dimethylformamide," *J. Soil Sci.,* vol. 97, pp. 34-42, 1964.

[62] Stevenson, S., "Humus Chemistry. Genesis, composition, Reactions 2nd ed.," John Wiley & Sons, 1994.

[63] Tipping, E., “Extraction of Humic Substances from Soil in Humic Substances in Sediment and Water”, Wiley-Interscience, 1985.

[64] Flaig, W., Beutelspacher, H., Rietz, E, “Chemical Composition and Physical Properties of Humic Substances: in Soil Components, Vol. 1, Organic Components”, New York: J. E. Gieseking, ed., Springer-Verlag, 1975.

[65] Hotze, E., Phenrat, T., Lowry, G., "Nanoparticle aggregation: challenges to understanding transport and reactivity in the environment," *J. Environ. Qual.*, vol. 10, pp. 1909-1924, 2010.

[66] Bowen, R., Jenner, F., "Theoretical description of membrane filtration of colloids and fine particles: an assessment and review," *Adv. Colloid Interface Sci.*, vol. 56, pp. 141-200, 1995.

[67] Shen, J., Probstein, R., "On the prediction of limiting flux in laminar ultrafiltration of macromolecular solutions," *Ind. Eng. Chem. Fundamen.*, vol. 16, pp. 4, pp. 459-565, 1977.

[68] Nobili, M., Bragato, G., Puigbo, A., "Characterization of electrophoretic fractions of humic substances with different electrofocusing behaviour," *Soil Sci.*, vol. 150, pp. 763-770, 1990.

[69] Chen, Y., Senesi, N., Schnitzer, M., "Information provided on humic substances by E4/E6 ratios," *Soil Sci. Soc. Am. J.*, vol. 41, pp. 352-358, 1977.

[70] Ghosh, K., Schnitzer, M., "UV and visible absorption spectroscopic investigations in relation to macromolecular characteristics of humic substances," *J. Soil. Sci.*, pp. 735-745, 1979.

[71] Kramer, J., Smith, S., "Fluorescence analysis for multi-site aluminum binding to natural organic matter," *Environ. Int.*, vol. 25, pp. 295-306, 1996.

[72] Ohno, T., "Fluorescence inner-filtering correction for determining the humification index of dissolved organic matter.," *Environ Sci Technol*., vol. 36, pp. 4, pp. 742-746, 2002.

[73] Wilson, M., Goh, K., "NMR spectroscopy of soils. Structure of organic material in sodium deuteroxide extracts from Patua Loam," *J. Soil Sci*., vol. 34, pp. 305-313, 1983.

[74] Wilson, M., Gillam, A., Collin, P., "Analysis of the structure of dissolved humic substances and their phytoplankton precursors by 1H and 13C nuclear magnetic resonance," *Chem. Geol.*, vol. 40, pp. 187-201, 1983.

[75] Wang, B.,"Organic and inorganic nitrogen leaching from incubated soils subjected to freeze–thaw and flooding," *Can. J. Soil Sci*., vol. 74, pp. 201-206, 1994.

[76] Yu, X., "Material Cycling of Wetland Soils Driven by Freeze–Thaw Effects," Springer - Northeast Institute of ¬Geography and Agroecology, Vols. 2190-5061.

[77] Grogan, P., Michelsen, A., Ambus, P., Jonasson, S., "Freeze–thaw regime effects on carbon and nitrogen gen dynamics in sub–arctic heath tundra mesocosms," *Soil Biol Biochem*, vol. 36, pp. 641-654, 2004.

[78] Ghabbour, E., Davies, G., "Humic Substances: Structures, Models and Functions" RCS Publishing, 2001, p. 161.

[79] Plaza, C., Senesi, N., Garcia-Gill, J., Polo, A., "Copper(II) complexation by humic and fulvic acids from pig slurry and amended and non-amended soils," *Chemosphere*, vol. 61, pp. 711-716, 2005.

[80] Pettit, R., "Organic matter, humus, humate, humic acid fulvic acid and humin: their importance in soil fertility and plant health" Texas A&M University, 2004.

[81] Theng, B., Tate, K, Becker-Heidmann, P., "Towards establishing the age, location, and identity of the inert soil organic matter of a spodosol," *Pflanzenernahr. Bodenk.*, vol. 155, pp. 181-184, 1992.

Chapter 2: Method Development

2.1 Abstract

The purpose of Chapter 2 is to present preliminary experiments used to refine experimentation, especially to develop an optimized method for characterizing soil/sediment pore water. The specific goals were to provide an initial characterization of pore water taken from Luther Marsh, and to establish how the samples should be prepared in order to simulate a realistic experimental system for studying the effects of freezing and thawing. NOM was processed by ultrafiltration and analyzed by TOC analysis to establish the distribution of high molecular weight (HMW) and low molecular weight (LMW) fractions. Results indicated that freezing and thawing lead to a relative increase in the composition of HMW NOM. The quality of the NOM was determined by acid-base titrations which provided information on the composition of acid functionals; and absorbance/fluorescence spectroscopy which provided information on the composition of fluorescent moieties. Titration data qualitatively showed similar results for all samples except LMW NOM which had an overall larger proton binding capacity and a larger composition of functional groups with a pK_a >8.5 per mg of carbon. Fluorescence results qualitatively indicated

that 1) all fractions represent predominantly humic-like molecules, and 2) the overall fluorescence characteristics increased after freezing and thawing, regardless of size.

2.2 Ultrafiltration

Ultrafiltration was used to separate NOM samples into high molecular weight (HMW) and low molecular weight (LMW) fractions. The material was first passed through a 0.45µm filter, yielding retentate (retained by filters) and filtrate (passing through filter) fractions. The retentate fraction was discarded and the filtrate fraction was filtered again using a 5 kDa pore size filter. This resulted in a second pair of filtrate and retentate fractions, providing a total of three fractions for analysis: the 0.45µm filtrate (<0.45 µm), the 5 kDa retentate (0.45µm – 5 kDa), and the 5 kDa filtrate (<5 kDa). A third step that included a 1 kDa pore size filter was attempted as well, however, an insufficient volume of pore water was able to pass through this pore size for subsequent analyses. The filtration process is illustrated in Figure 2-1 below.

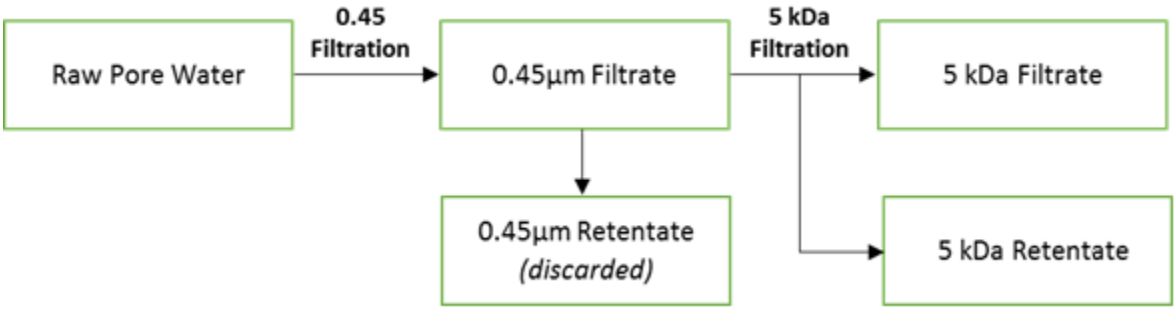

Figure 2-1. Flow chart illustrating the filtration process required to acquire the 0.45µm filtrate, 5 kDa filtrate, and 5 kDa retentate fractions used for subsequent analyses.

TOC analysis was used to determine the quantity of carbon in the LMW fraction, which is the component of NOM that is smaller than 5 kDa, and the quantity of the HMW fraction, which is the component of NOM that is between 0.45µm and 5 kDa.

In order to interpret the organic carbon fractions, it is important to understand that the 5 kDa retentate fractions contain both the HMW material, which is concentrated during the filtration process, and LMW NOM material which is smaller than the cut-off value of 5 kDa [1]. In order to accurately determine the quantity of NOM in both a LMW and HMW state, two corrections incorporating the mass balances and volumes of the different fractions must be performed to account for the smaller NOM material in the 5 kDa retentate fraction [1].

$$M_{HCorr} = C_{Ret} * V_{Ret} - C_{Filt} * V_{Ret} \qquad (2-1)$$

$$M_{LCorr} = C_{Filt} * V_{Filt} - C_{Filt} * V_{Ret} \qquad (2-2)$$

where M is the quantity of the carbon (mg), C is the concentration of carbon (mg C L^{-1}) in the sample or the fraction, and V is the volume (L) of the fraction. Subscript 'HCorr' is the corrected value for the material of sizes higher than the nominal cutoff value of the filter; 'LCorr' is the corrected value for the material of sizes lower than the nominal cut-off value of the filter, 'Ret' denotes the retentate fraction, and 'Filt' denotes the filtrate fraction.

2.2.1 Experimental Details

2.2.1.1 Sampling, Storage and Selection

Approximately 10 L of pore water was taken from Luther Marsh, Wylde Lake Bog at coordinates (43°54'20.4"N 80°24'21.9"W) on May 28, 2015. Sphagnum moss and other vegetation was removed from the top layer of the peat and a small hole approximately 1 ft^3 was dug. The holes filled rapidly with pore water, which was sampled by submerging pyrex bottles, ranging in volume from 500 mL to 2 L, completely under the water, and then capping the bottles while still submerged to ensure minimal headspace. Peat samples were taken from the decomposed vegetation at the sides of these holes above the redox transition zone, where the plant material exhibited different features of humified organic matter, plant debris and roots.

After the pore water was sampled, it was taken to the University of Guelph, Guelph, Ontario, where it was then wrapped with aluminum foil to minimize light exposure and stored at 4 ^oC.

2.2.1.2 Pre-treatment of Pore Water (Control and Freeze-Thaw Treatment)

Before samples were filtered with the initial 0.45µm hollow fiber filter, the pore water was passed through a 2-mm sieve to remove large plant debris, large fibers or roots. This is to ensure homogeneity among the samples, as well as to prolong filter lifetime and maintain optimal ultrafiltration performance.

The pore water samples designated as the 'freeze-thaw treatment' (FTC) were treated using the same initial steps, followed by freezing for 24 hours at -10 ^{o}C and thawing at room temperature (~20 ^{o}C) prior to filtration.

2.2.1.3 Ultrafiltration Apparatus Setup

The ultrafiltration apparatus setup, used with the 0.45µm filter and 5 kDa filter, is illustrated in Figure 2.2 below.

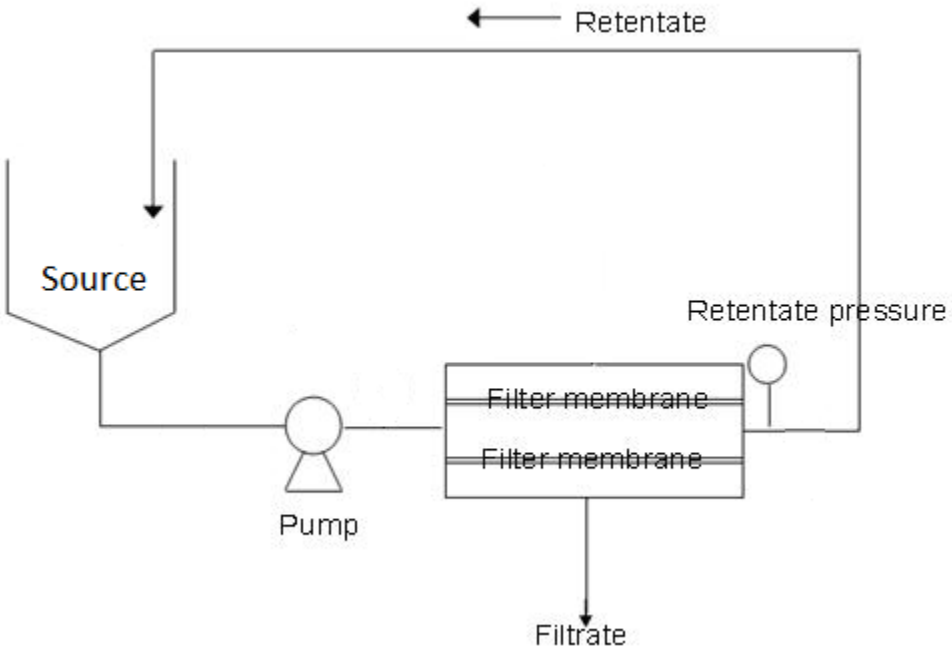

Figure 2-2. Schematic of the ultrafiltration apparatus set-up used for separating pore water samples taken from Luther Marsh.

Before filtration, all of the sampled pore water was decanted into a ~10L polypropylene bottle to provide a single homogenized source of pore water. The bottle had tubing attached at the base, which passed through a peristaltic pump and into the base of the 0.45µm polysulfone hollow fibre filter (A/G Technologies, Amersham Biosciences). The sample was processed and NOM particles smaller than the filter pore size flowed through the filter membrane before eluting through a spout approximately 1/3 of the way up the filter column. The spout was connected to 2L pyrex beaker by a polypropylene tube to collect the filtrate. Any organic matter in the pore water that exceeded the filter pore size would bypass the filter and flow through a spout at the top. Tubing at the spout directed the rejected flow past a pressure gauge and then back to the source intake. Pressure was maintained between 0.3-1.0 bar. The flow was cycled continuously in this way until the filtration was stopped.

2.2.1.4 Pre and Post Treatment, and Storage of Hollow Fiber Ultrafiltration Filters

Prior to filtering samples (i.e. pre-treatment), the source reservoir was filled with milli-Q water. The pump level was increased to the desired flow, not exceeding 15 psi. The retentate tube was placed in the sink or a disposal container and the filter was run for 30 minutes, the source reservoir was filled as needed. The retentate tube was then placed back into the source and water was recirculated for 15 minutes. To sanitize the apparatus these steps were repeated with a solution of 30 mL of 5% (~1.5 mL) NaOCl per liter of Milli-Q water to ensure that microbial growth was not possible.

After filtering samples (i.e. post-treatment), the source was filled with 1-2 L of heated (50 ^{o}C) 0.5 M NaOH solution. All filtrate tubing was clamped off and the solution was circulated for 60 minutes. This was for the purpose of solubilizing any residual NOM or biological constituents still present in the apparatus. After this time, the retentate tubing was placed in a disposal container. Next, 1-2 L of Milli-Q water was placed in the source, and circulated for 10 minutes. This solution was discarded and 1-2L of Milli-Q water would be circulated in the same way once more. After post treatment of the filter apparatus, all openings on the filter were sealed with parafilm and stored until further use.

2.2.1.5 Sample Ultrafiltration Procedure

As previously noted, both the control and the sample treated by freeze-thaw cycles were filtered with a 0.45µm filter followed by a 5 kDa filter. This involved adding sieved raw pore water (2-mm mesh) to the source container, and circulating this solution until a sufficient volume of filtrate was obtained. A portion of this filtrate was set aside for subsequent analyses. The rest of the filtrate was processed with the 5kDa filter. This involved decanting the 0.45µm filtrate into the source container and circulating the solution until approximately equal volumes of the 5 kDa filtrate and retentate fraction were obtained. Equal volumes were processed to minimize variability and to ensure adequate volumes for subsequent analyses.

2.2.1.6 TOC Analysis

After the filtrations were completed, each size fraction was analyzed by total organic carbon (TOC) analysis (Shimadzu TOC-L Series) to determine the concentrations of organic carbon. Samples were run by the SOWC Chemical Laboratory at the University of Guelph. Samples were run in triplicate at 680°C using a combustion catalytic oxidation method to quantify total carbon (TC), inorganic carbon (IC), and non-purgeable organic carbon (NPOC) (4-30,000 mg/L) [2].

2.2.1.7 Results & Discussion

After applying the appropriate mass corrections to the TOC values for each size fraction, according to equations 2-1 and 2-2, the distribution of carbon was compared between control and treatment samples. Graphical and tabulated values of both the percent, and total carbon distribution, in the HMW and LMW fractions are illustrated in Figures 2-3 and 2-4, and Tables 2-1 and 2-2 below. Mass balances were performed to ensure that proper performance of the filters was maintained and that no carbon was lost during the filtration process, as shown in Table 2-1 below. Filtrations yielded values of 96.2% and 102.6% (performed only once each) conserved carbon mass, respectively, for the control and FTC filtrations, as shown in Table 2-1 below.

Because the results represent only a single replicate filtration for each treatment they are not statistically significant, and therefore no conclusive statement can be made about the similarity of treatment groups. However, it was observed qualitatively that, after freezing and thawing, the relative proportion of HMW NOM increased (46.0% in treatment compared to 26.0% in control). One may be tempted to compare the absolute carbon distributions, however, because larger volumes were filtered for the control group (i.e. 4.2L starting volume for the control in comparison to 1L for the FTC samples), this is not a meaningful comparison.

There are two explanations for these results. The first is that larger fragments of NOM are produced from smaller fragments after freezing and thawing. The second is that freezing provides a physical stimulus to disrupt and release larger fragments which may have previously been associated with larger particles through weak interactions. This disruption produces new fragments to be filtered, which were previously too large to pass through the 0.45µm pore size. It is in the opinion of the author that the latter explanation is more likely to be true.

Table 2-1. Carbon Mass Balance of Control and FTC Size Fractions

Size Fractions	Control (mg C)	FTC (mg C)
0.45 µm filtrate	121.2	27.1
5 kDa retentate	44.7	20.9
5 kDa filtrate	71.9	6.9
Mass Balance %	96.2	102.6

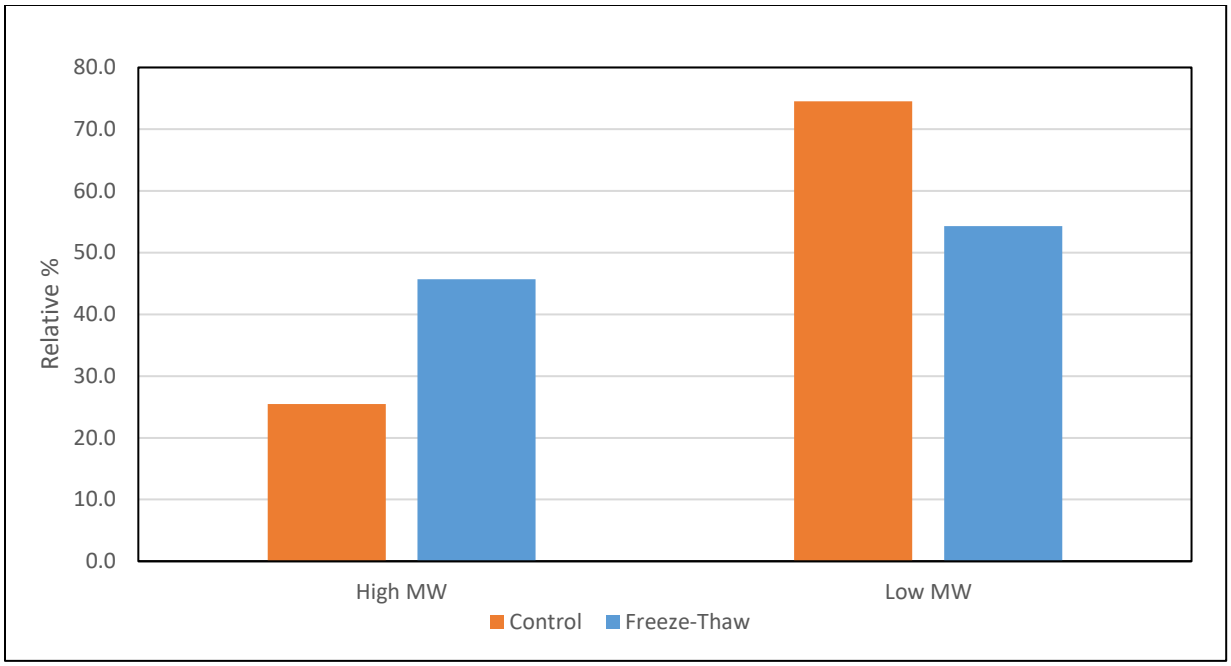

Figure 2-3. Comparison of the Relative Carbon Distribution in the high and low MW fractions of the Control and FTC treatment samples.

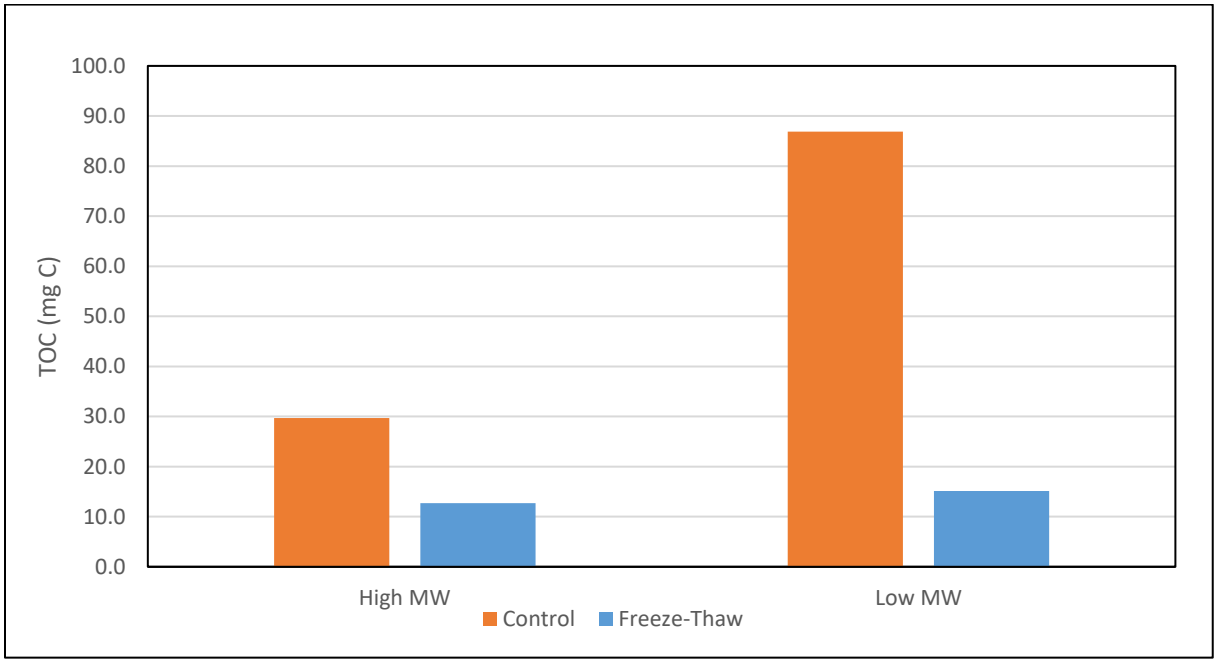

Figure 2-4. Comparison of the total carbon distribution in the high and low MW fractions of the Control and FTC treatment samples.

2.3 Fluorescence Spectroscopy

2.3.1 Introduction

Excitation-emission fluorescence spectroscopy is a tool used to study the quality of NOM [2]. Excitation emission matrices (EEMs) are produced by measuring samples over multiple excitation and emission wavelengths (i.e. 200-450 nm and 250-600 nm) [3]. The results of these measurements can provide information about the NOM's origin, seasonal variations, and trends in degradation [5, 6, 7, 8]. Specifically, EEM data can offer information regarding the composition of samples in terms of relative proportions of humic acid (HA), fulvic acid (FA), tryptophan and tyrosine. The structure for humic acid and fulvic acid components are illustrated in Figures 2-1 and 2-2 above. The tryptophan and tyrosine structures are shown in Figures 2-5 and 2-6 below.

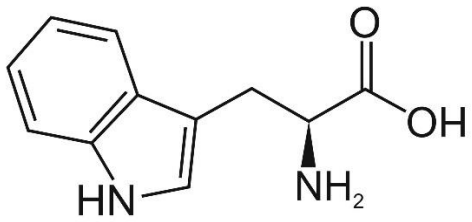

Figure 2-5. Tryptophan molecule. Trytophan-like components present within NOM represent proteinacious material containing amine groups indirectly connected to aromatic rings. Image taken from [8].

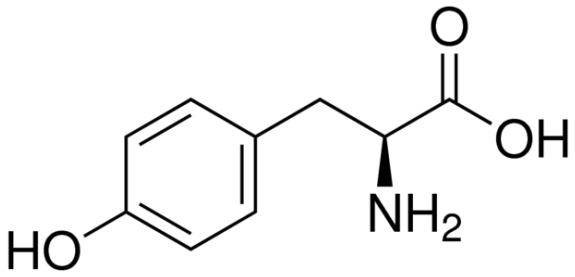

Figure 2-6. Tyrosine molecule. Tyrosine-like components present within NOM represent proteinaceous material containing amine groups indirectly connected to aromatic rings. Image taken from [9].

To obtain quantitative data from EEM measurements a multivariate analysis tool, termed ‘parallel factor analysis’ (PARAFAC), is often applied. This is a data reduction technique which reduces large matrices of data to four component relative concentrations and facilitates comparison of NOM samples.

2.3.1.1 PARAFAC Analysis

PARAFAC has proven to be effective at advancing the interpretations of EEM data. Each matrix can offer unique information by comparing specific excitation/emission wavelength pairs which correspond to characteristic molecular moieties. PARAFAC resolves this information into component spectra and relative component concentrations [11, 12, 13]. This means that, through spectral deconvolution of a ‘stack’ of fluorescent EEMs, otherwise known as a data set of EEMs from different samples, PARAFAC can quantify a minimum number of pre-defined fluorescent components to describe each EEM in a set of related samples [10]. These four components were

characterized by wavelengths at 360-390nm excitation, 320-340 nm emission (humic acid-like), 400-450 nm or 265 nm excitation, and 460-520 nm emission (fulvic acid-like), 280 nm and 230 nm excitation, 340-350 nm emission (tryptophan-like), and 280 and 230 nm excitation and emission at 300 nm (tyrosine-like) [7]. Although the resolved spectra may not result in actual concentrations of these components, PARAFAC serves as an effective tool for showing variability among samples, and illustrates relative concentrations of each component.

The relative concentration of each of the four components in the NOM samples was converted to a percent value in equation (2-3). The relative concentrations were then used to compare control and treatment samples. Results were plotted in bar graphs as shown in Figure 2.9 below.

$$\%Fluorescence_{component1} = \frac{[component1]}{[Total\ Components]} * 100 \qquad (2-3)$$

2.3.2 Experimental Details

Fluorescence spectra of the NOM samples were measured using a Varian Cary fluorescence spectrophotometer with 1cm pathlength quartz cuvettes. Measurements were made in excitation-emission mode over the wavelengths 200-450 nm and 250-600 nm.

2.3.3 Results & Discussion

PARAFAC analysis resolved four components (HA-, FA-, tyrosine-like and tryptophan-like) in the EEMs of all of the different size fractions. An example EEM and absorbance spectra is shown

in Figure 2-7 and 2-8 below. The relative percent and total composition of the NOM size fractions, normalized to mg C, as determined by EEMS and PARAFAC, are illustrated in Figures 2-9 and 2-10 below, and numerically in Tables 2-4 and 2-5 below.

The four fluorescent components identified in the pore water samples are similar to the characteristic components shown in published studies. The HA-like and FA-like components illustrated in this study are the same as two components used in a study by Holbrook et al. (denoted as components 1 and 2) and two components used in a study by Stemond et al. (denoted as components 3 and 4) [14, 15]. The trp-like component used in this study has been identified in several studies [14, 15, 16]. The tyr-like component used in this study has also been identified in another study by Stedmon et al. [16].

The control and treatment samples show similar trends throughout the percent relative composition of each component, with an increase in tyrosine-like moieties (0.45 µm control (17.6%) relative to treatment (26.0%), 5 kDa retentate control (0.0%) relative to treatment (13.5%) and 5 kDa filtrate control (35.7%) relative to treatment (45.5%)) in each of the fractions after freezing and thawing. In all three fractions of NOM, encompassing HMW and LMW NOM, HA-like components were the most abundant while Trp-like components were the least less abundant.

When comparing the total contribution of each component between the control and treatment samples, similar trends were identified. Both control and treatment samples were predominantly comprised of humic-like moieties (0.45 µm control (0.0073 AU per mg C) relative to treatment (0.0096), 5 kDa retentate control (0.0026) relative to treatment (0.0062) and 5 kDa filtrate control

(0.0105) relative to treatment (0.0154)). However, freezing and thawing of samples produced an increase in each component per unit of carbon. There is a notable increase as large as twice the intensity of the tyrosine-like component for the 0.45µm filtrate fraction, and twice the intensity of the humic-like component for the 5 kDa retentate fraction. In addition, the 5 kDa filtrate fraction shows a four-fold increase in the tryptophan-like component and a two-fold increase in the tyrosine-like component.

The results of all the fluorescence data were derived from a single sample replicate, therefore they serve as range-gathering data used to support future modifications to the experimental design.

It is interesting that different size fractions show an increase in the fluorescent components of the smallest fraction of NOM, regardless of the properties of the fluorescent component. This indicates that no correlation can be made between fluorescent moieties representing large and small molecules (e.g. large molecules such as humic acid and small molecules such as fulvic acid, tyrosine, tryptophan) and HMW and LMW size fractions. However, it can be suggested qualitatively that the humic-like and protein-like moieties increase after pore water has been frozen and thawed. Since the pore water used for the control and treatment samples were taken from the same pool of pore water, the increase in the protein-like signal is likely due to the lysis and release of microbial amino acids after freezing, which was consistent with our hypothesis (refer to Section 1.7). The increase in humic-like fluorescence after freezing and thawing was unanticipated. As previously stated at the end of Section 2.2.1.7, this suggests that larger fragments of NOM were formed from smaller fragments by freeze-thaw cycling, or that freezing disrupts weak interactions

of aggregated NOM particles particles, and releases fragments which were too large to pass through the 0.45µm filter pores before the freeze-thaw treatment.

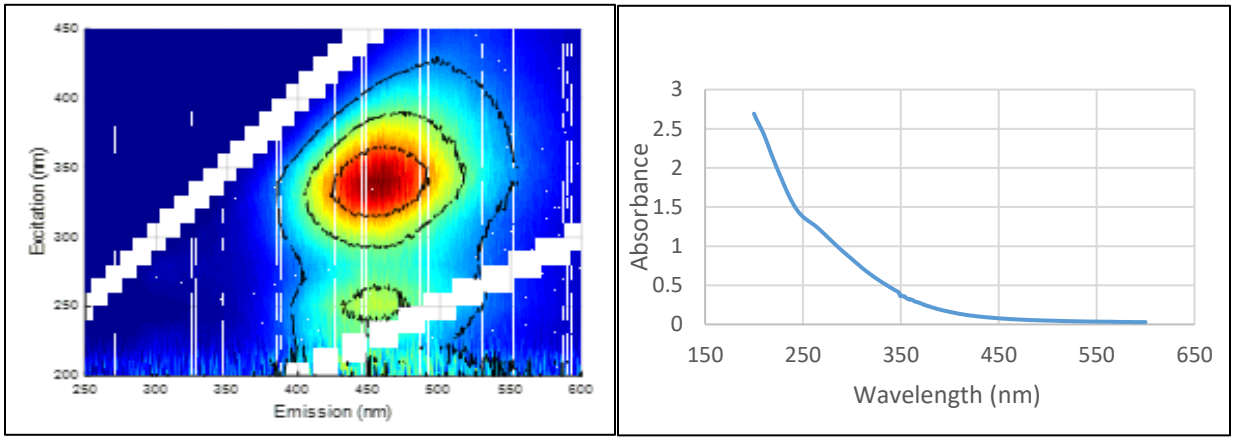

Figure 2-7, 2-8. Example Fluorescence Excitation Emission Matrix (left) and Absorbance Spectra (right) for the 5 kDa filtrate control fraction.

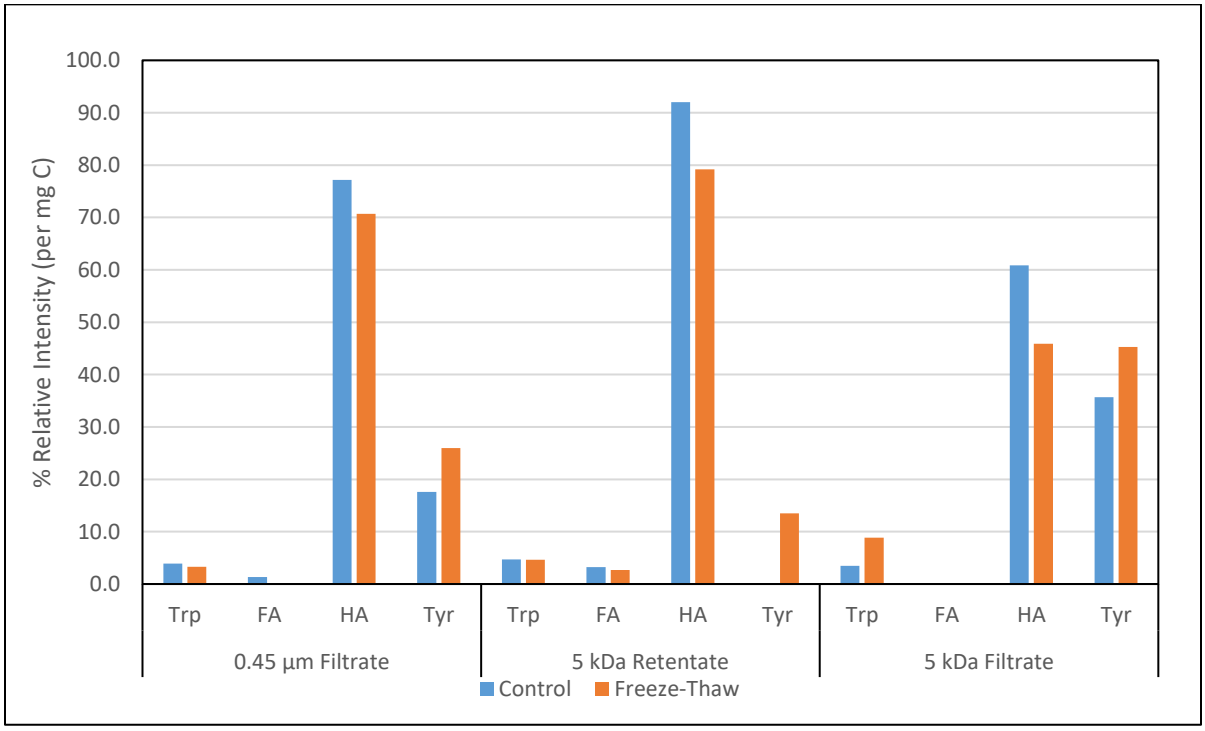

Figure 2-9. A comparison between the control and FTC treatment of the relative percent composition of four major fluorescence components, normalized to units of carbon, as determined by PARAFAC analysis.

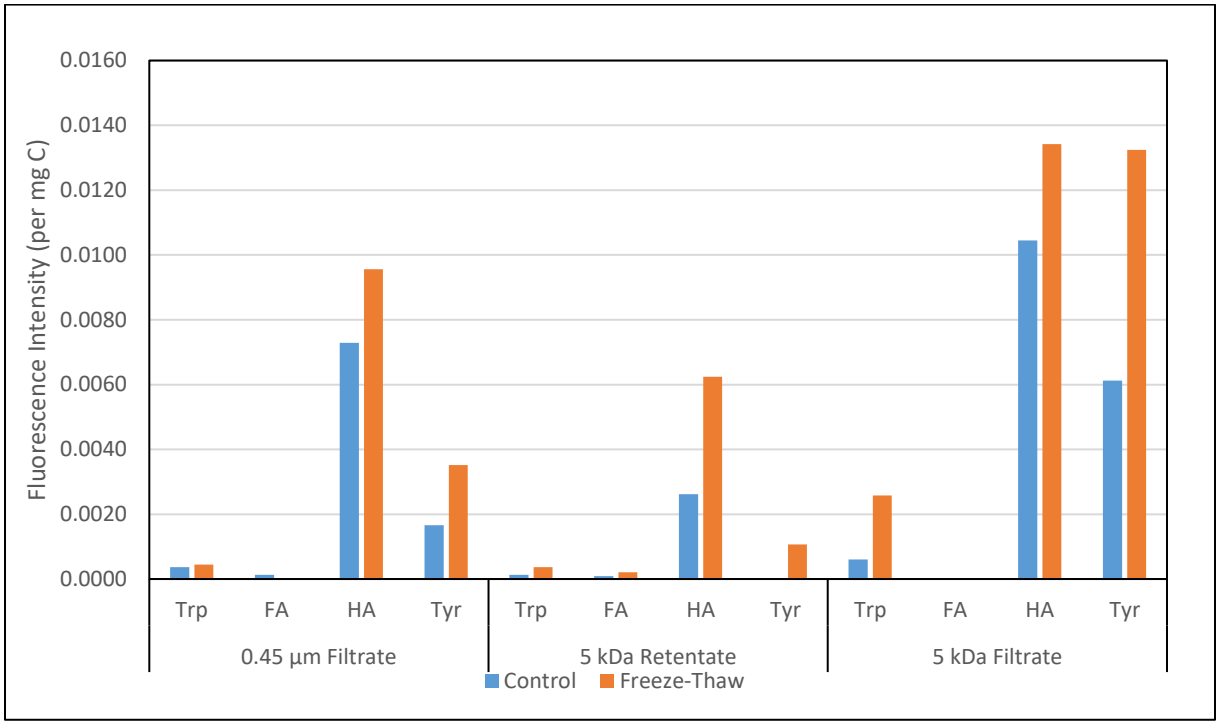

Figure 2-10. A comparison between the control and FTC treatment of the total composition of four major fluorescence components, normalized to units of carbon, as determined by PARAFAC analysis.

2.4 Potentiometric Titrations

2.4.1 Introduction

Each size fraction for the control and treatment was titrated to determine the concentration of acidic functional groups. From this, it is possible to establish any differences in the acidic functional group composition of HMW and LMW NOM fractions. This can also aid in determining whether the freeze-thaw treatment caused changes in the quality of NOM, which would be demonstrated by differing functional group compositions. It also offers implications for copper since copper binds at the same functional groups as protons. Therefore, an understanding of protein reactivity and capacity should help predict metal binding changes after freezing and thawing.

Functional group reactivity results from the deprotonation of acidic functional groups in NOM samples. As pH increases, the proportion of deprotonated sites increases. Each functional group has individual properties that depend on the type and concentration of the group, which determines its relative proton binding affinity [17]. Acid-base titrations are a unique tool that can be used to gather information about a sample by determining the pK_a values of functional groups [18]. Previous research has shown that NOM samples have functional groups which represent predominantly carboxylic and phenolic groups, with pK_a values ranging from 3-6 and 8-10 respectively [20, 21, 22]. However, it is important to note that even identical functional groups will not necessarily have identical pK_a values. This depends on the regional environment of a functional group, or on the molecules to which it is bound. This means that titration results are not used to identify individual functional groups, but rather to attain an overall distribution of the functional group spectra.

Each functional group can be characterized by an equilibrium constant for the reaction that occurs when the group is deprotonated. This is called the acid dissociation constant (Ka). A general form of the reaction for this constant is as follows:

$$HA \rightleftarrows H^+ + A^- \qquad (2-4)$$

The equilibrium constant, which can be used to calculate concentrations of each of the products and reactants in the reaction, is illustrated as follows:

$$K_a = \frac{[H^+][A^-]}{[HA]} \qquad (2-5)$$

Acid equilibrium constants can also be represented as pK_a values through the following manipulation:

$$-\log(K_a) = pK_a \qquad (2-6)$$

From a titration, we can calculate a numerical representation of the titration curve in terms of charged species. This representation is termed charge excess (b), and is the negative charge required for electroneutrality in a system. It is described by the following equation [22]:

$$b = C_b - C_a + [H^+] - [OH^-] \qquad (2-7)$$

C_b is the concentration of added base, typically the titrant (i.e. NaOH), C_a is the concentration of added acid (i.e. HCl), $[H^+]$ is the concentration of protons determined by the electrode, and $[OH^-]$ is the concentration of hydroxide ions calculated using the auto-pyrolysis equilibrium of water, which is as follows:

$$[OH^-] = \frac{K_W}{[H^+]} \qquad (2-8)$$

The concentrations and pK_a values of functional groups can be determined by fitting charge excess (b) versus pH. To estimate pK_a values of functional groups and their site densities (LT, µmol mg^{-1}), titration data in this project were fitted to a fully optimized continuous (FOCUS) model using in-house Matlab™ programs as described by Smith and Ferris [23]. Discrete ranges of specified pK_a values were defined from these fits to determine binding site concentrations within specified pK_a ranges. Using the in-house Matlab™ code this was accomplished by integrating the area under the curve to represent discrete values of acidic functional groups (pK_a <5), intermediate functional groups (5< pK_a <8.5), and basic functional groups (8.5< pK_a).

2.4.2 Experimental Details

2.4.2.1 Sample Preparation and Procedure

Prior to titration, samples were adjusted to 0.01M KNO_3 (Sigma Aldrich) and pH 4 with 1M HCl (Fisher A509-P212). 25 mL of this sample would then be added to the titration vessel. All titrations were conducted at room temperature while being purged under ultrapure N_2 gas to ensure no CO_2 absorption, using an automated titrator (848 Titrino Plus with an 801-magnetic stirrer and support

rod, Metrohm Canada) with a pH electrode (Orion 8101BNWP ROSS Half-Cell Electrode, Thermo Scientific) and a double junction Ag/AgCl reference electrode (Orion 900200 Sure-Flow Reference Half Cell Electrode, Thermo Scientific). Samples were then titrated using a solution of 0.1013M NaOH (Fluka 01968) (standardized by Gran Plot) at ~0.1 pH intervals up until pH 12.

2.4.3 Results & Discussion

The acid and base properties of control and treatment samples are represented in terms of their acidity constants (pK_a) and their densities (LT, μmol/mg C). An example pK_a spectra, illustrating typical titration data, is shown in the Figure 2-11 below. As previously stated, integration of this graphical pK_a spectra yielded proton binding capacities for each of the samples in the range of $pK_a \leq 5$ (acidic), $5 < pK_a \leq 8.5$ (intermediate) and $pK_a > 8.5$ (basic). The graphical data for the proton binding capacities of the control and treatment samples are represented in Figure 2-12 below. Each sample was titrated in triplicate due to the associated variability of this technique; however, different size fraction samples originate from only a single filtration.

Samples from both the control and treatment groups yielded spectra with concentrations of functional groups predominantly in the pK_a region of 3-4 and 10-11. This is common in NOM samples, and these observations are interpreted as contributions from carboxylic and phenolic sites [24]. The greatest difference between control and treatment samples is the decrease in basic functional group concentration in the 0.45μm filtrate fraction after freezing and thawing (7.27 ±2.07 in the control relative to 3.00 ±0.59 the treatment, at 95% confidence interval). There is also an increase in the acidic functional groups in the smallest 5 kDa filtrate treatment fraction (1.38

±0.26 in the control relative to 2.84 ±0.42 the treatment), indicating more carboxylic acid characteristics in the smaller NOM fragments after freezing and thawing. The apparent increase in total capacity (5.58 ±1.34 in the control relative to 10.02 ±3.22 the treatment) is to be expected if the smallest fraction resembles smaller fulvic acid-like molecules, because fulvic acid has a higher composition of acidic functional groups in comparison to larger humic acid-like molecules (total acidity of 10.0-12.3 meq/g for fulvic acid in comparison to 6.0-8.9 meq/g for humic acid) [25]. This is interesting because it is contrary to the predominantly humic-like fluorescent characteristics illustrated in the results of Section 2.3.3.

Titration data are variable among replicates, which can be observed by the dashed lines in pK_a spectra of Figure 2-11 below (representing ± 1 standard deviation), and by the standard error bars in Figure 2-12. The reproducibility of these titrations was poor, and there were few statistically significant differences between the control and treatment samples. For this reason, it was decided that acid-base titrations were of limited practical value for achieving the goals of this research, and this technique would not be used in subsequent research.

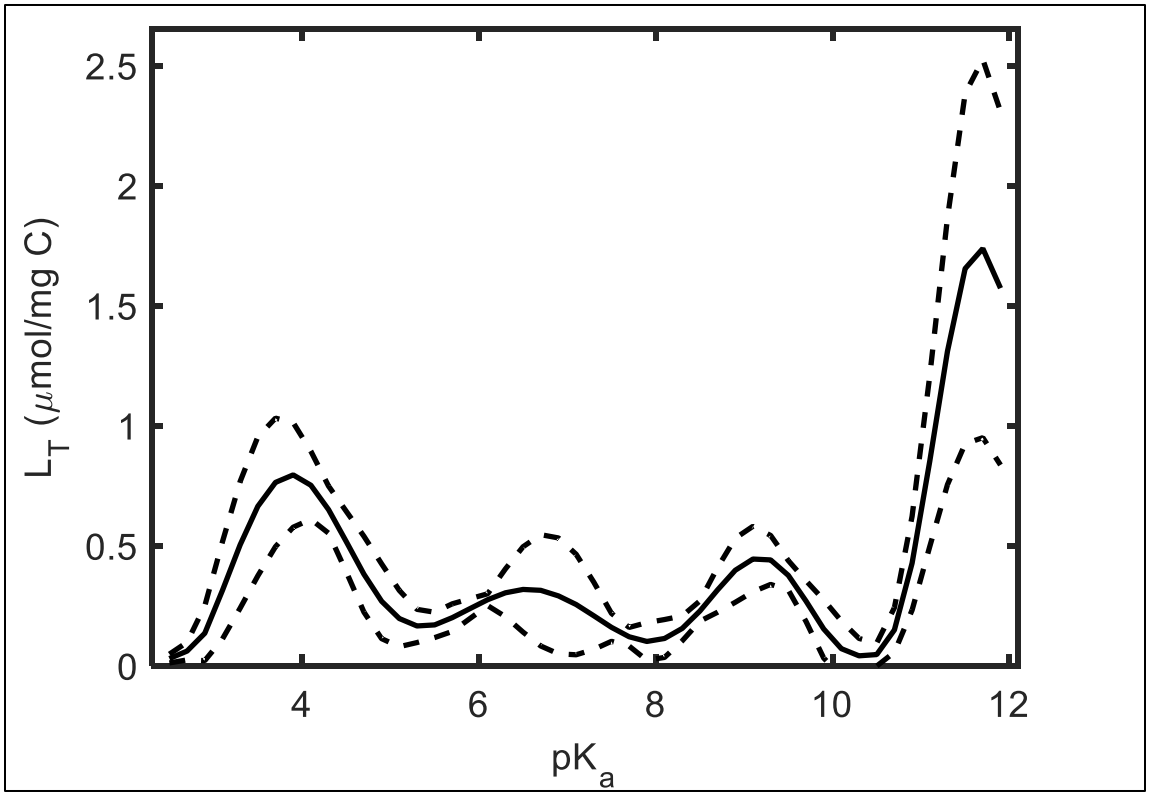

Figure 2-11. Example of pK_a spectra from acid-base titration of control 5 kDa retentate fraction.

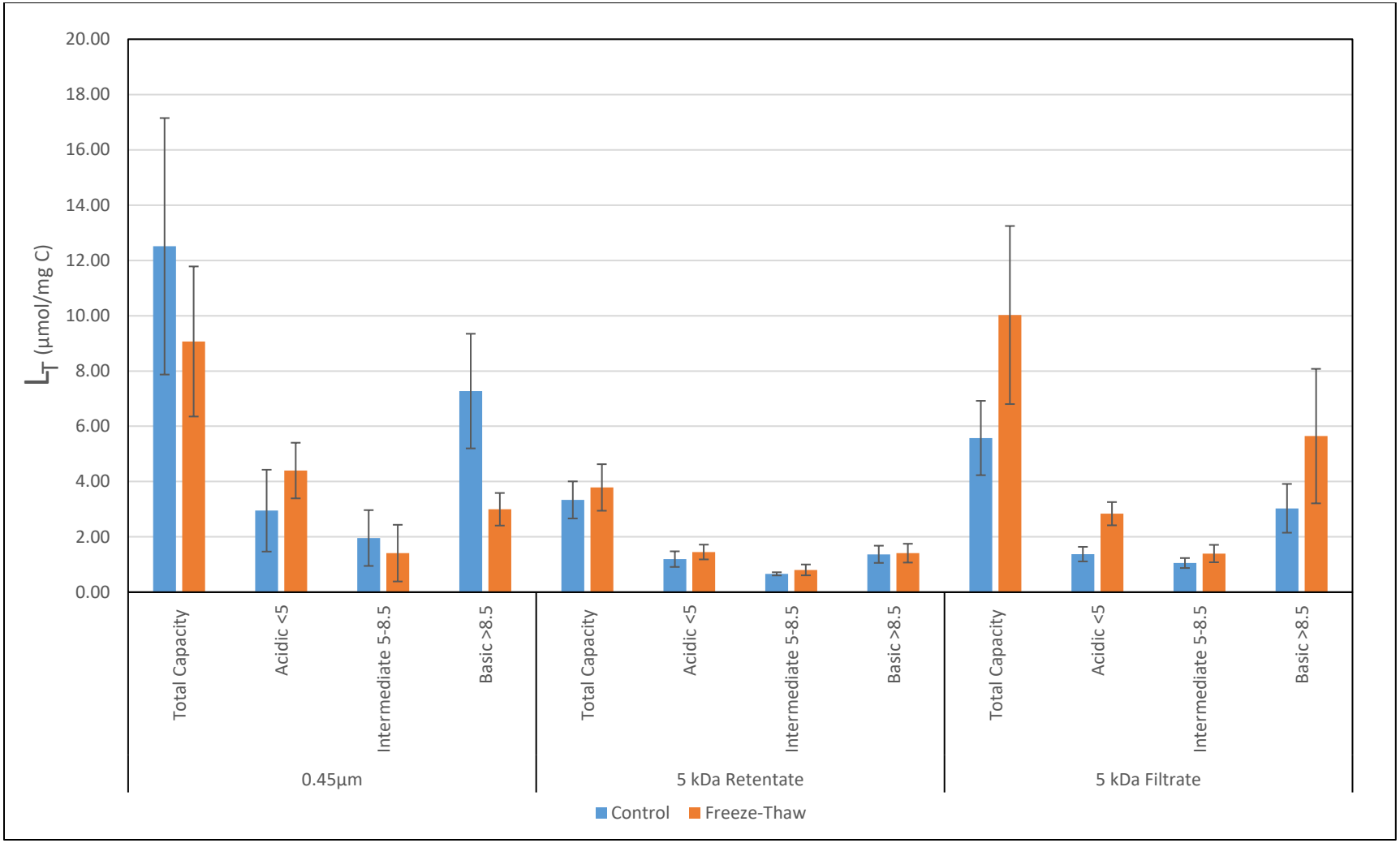

Figure 2-12. Comparison of acidic, intermediate and basic functional group concentrations in the different size fractions of the Control and FTC treatment samples. Error bars represent confidence interval at 95%.

2.5 Conclusion

The results from the TOC analyses of different size fractions clearly indicate an increase in the relative composition of HMW NOM after freezing and thawing. Further analysis using fluorescence spectroscopy indicated that the majority of NOM in all size fractions represented humic-like moieties, and this component increased after freezing and thawing. However, because the increase in humic moieties was observed for all size fractions, no correlation can be made between fluorescent properties and NOM sizes.

Freezing and thawing of NOM did, however, increase the overall contribution of fluorescence moieties per unit of carbon, which was unexpected. The FT treatment also increased the contribution of protein-like moieties, which was hypothesized and was attributed to the lysis of microbial organisms and release of their small molecular weight sugars and amino acids [27, 28]. Similarly, the largest HA-like contribution was observed for the smallest 5 kDa filtrate fraction, for both the control and treatment groups. This reaffirms the previous statement noting that no correlation can be made between fluorescent properties and NOM sizes.

As previously stated, the titration data served more as an overview of the trends of our samples, indicating no consistent differences in the functional group composition of samples after freezing and thawing. There was however an increase in the total capacity and acidic functional group concentration of the 5 kDa filtrate fractions, indicating a larger potential binding capacity for metal cations such as copper. This is unexpected since larger humic-like molecules have been shown generally to have a higher affinity for binding metal cations such as copper in comparison to smaller fulvic-like molecules [29, 30].

To conclude, this preliminary data demonstrated no major differences between the control and treatment group samples. The only trends that were observed were increases in the fluorescent and functional group properties of the smallest 5 kDa filtrate fractions, with small increases in the treatment group compared to the control. The author speculates that there are three possible reasons for this. The first potential reason is that freezing and thawing of pore water does not produce any major change to the quality of NOM. The second potential reason is that in the experimental design there was an insufficient stimulus applied for any noticeable changes to be observed. Similarly, the third potential reason is that there was an insufficient amount of NOM present in the pore water during freezing and thawing for any noticeable changes to be observed. For these reasons, steps were taken to modify how the samples were prepared and treated in comparison to this preliminary work, taking the latter two speculations into account. The following chapter will describe the results of modified experimentation which incorporated adding humified peat to pore water and applying three subsequent cycles of freezing and thawing to our samples.

2.6 References

[1] Caron, F., Manjarios, G., "Pre-assessment of the speciation of 60Co, 125Sb, 137Cs and 241Am in a contaminated aquifer," *J. Environ. Radioact*, vol. 7, pp. 29-46, 2004.

[2] Coble, P., "Characterization of marine and terrestrial DOM in seawater using excitation-emission matrix spectroscopy," *Mar. Chem*, vol. 51, pp. 325-346, 1996.

[3] Kramer, J., Smith, S., "Fluorescence analysis for multi-site aluminum binding to natural organic matter," *Environ. Int.*, vol. 25, pp. 295-306.

[4] McKnight, D., Boyer, E., Westerhoff, P., Doran, P., Kulbe, T., Adersen, D., "Spectrofluorometric characterization of dissolved organic matter for indication of precursor organic matter and aromaticity," *Limnol. Oceanogr*., vol. 46, pp. 38-48, 2001.

[5] Vodacek, A., Blough, N., DeGrandepre, M, Nelson, R., "Seasonal variation of CDOM and DOC in the middle Atlantic might: terrestrial input and photooxidation.," *Limnol. Oceanogr*., vol. 42, pp. 4, pp. 647-686, 1997.

[6] Brooks, M., Meyer, J., McKnight, D., "Photooxidation of wetland and riverine dissolved organic matter: altered copper complexation and organic composition.," *Hydrobiologia*, vol. 579, pp. 95-113, 2007.

[7] Winter, A., Fish, T., Playle, R., et al., "Photodegradation of natural organic matter from diverse freshwater sources.," *Aquat. Toxicol.*, vol. 84, pp. 215-222, 2007.

[8] Edelhoch, H., "Spectroscopic Determination of Tryptophan and Tyrosine in Proteins", *Biochem., vol. 6, pp. 1948-1954, 1967*

[9] Hubbard, S., Till, J., “Protein Tyrosine Kinase Structure and Function”, *Annu. Rev. Biochem.* vol. 69, pp 373-398, 2000

[10] DePalma, S., Arnold, W., McGeer, J., Dixon, D., Smith, D., "Protective effects of dissolved organic matter and reduced sulfur on copper toxicity in coastal marine environments.," *Ecotox. And Environ. Saf.*, vol. 74, pp. 230-237, 2011.

[11] Gheorghiu, C., Smith, S., Al-Reasi, A., McGeer, C., Wilkie, P., "Influence of natural organic matter (NOM) quality on Cu-gill binding in the rainbow trout (oncorhynchus mykiss)," *Aqua. Tox.*, vol. 97, pp. 343-352, 2010.

[12] Wood, C., Al-Reasi, A., Smith, S., "The two faces of DOC," *Aquat. Toxicol*., vol. 105, pp. 3-8, 2011.

[13] Holbrook, D., Yen, J., Grizzard, T., "Characterizing natural organic material from the Occoquan watershed (Nothern Virgina, US) using fluorescence spectroscopy and PARAFAC," *Sci. Tot. Environ.*, vol. 361, pp. 249-266, 2006.

[14] Stedmon, C., Markager, S., Bro, R., "Tracing dissolved organic matter in aquatic environments using a new approach to fluorescence spectroscopy," *Mar. Chem*., vol. 82, pp. 239-254, 2003.

[15] Baker, A., "Fluorescense excitation-emission matrix characterization of some sewage-impacted rivers," *Environ. Sci. Technol.*, vol. 35, pp. 948-953.

[16] Stedmon, C., Markager, S., "Resolving the variability in dissolved organic matter fluorescence in a temperate estuary and its catchments using PARAFAC analysis.," *Limnol. Oceanogr*., vol. 50, pp. 686-697, 2005.

[17] Martinez, R., Smith, S., Kulzycki, E., Ferris, F., "Determination of intrinsic bacterial surface acidity constants using a donnan shell model and a continuous pK_a distribution method," *J. Coll. Interface Sci.*, vol. 253, pp. 130-139, 2002.

[18] Smith, S., Ferris, F., "Specific surface chemical interactions between hydrous ferric oxide and iron-reducing bacteria determined using pK_a spectra," *J. Coll. Interface Sci*., vol. 266, pp. 60 - 67, 2003.

[19] Edwards, M., Benjamin, M., Ryan, J., "Role of organic acidity in sorption of natural organic matter (NOM) to oxide surfaces," *Colloids Surf. A*, vol. 107, pp. 297-307, 1996.

[20] Tiller, C., O'Melia, C., "Natural organic matter and colloidal stability: models and measurements," *Colloids Surf. A*, vol. 73, pp. 449-459, 1993.

[21] Gu, B., Schmitt, J., Chen, Z., Liang, L., McCarthy, J., "Adsorption and desorption of different organic matter fractions on iron oxide," *Environ. Sci. Technol.*, vol. 59, pp. 219-229, 1998.

[22] Sokolov, I., Smith, S., Henderson, S., et al., "Cell surface electrochemical heterogeneity of the Fe(III)-reducing bacteria shewanella putrefaciens," *Environ. Sci. Technol.* , vol. 35, pp. 341-347.

[23] Smith, S., Ferris, G., "Proton binding by hydrous ferric oxide and aluminum oxide surfaces interpreted using fully optimized continuous pK_a spectra," *Environ. Sci. Technol*., vol. 35, pp. 4637-4642, 2001.

[24] Smith, S., Kramer, J., "Multi-site proton interactions with natural organic matter," *Environ. Int.*, vol. 25, pp. 307-314.

[25] Tan, K., Humic Matter in Soil and the Environment: Principles and Controversies, CRC Press, 2010.

[26] Grogan, P., Michelsen, A., Ambus, P., Jonasson, S., "Freeze–thaw regime effects on carbon and nitrogen gen dynamics in sub–arctic heath tundra mesocosms," *Soil Biol. Biochem*, vol. 36, pp. 641-654, 2004.

[27] Yu, X., "Material Cycling of Wetland Soils Driven by Freeze–Thaw Effects," Springer - Northeast Institute of Geography and Agroecology, pp. 2190-5061.

[28] Ghabbour, E., Davies, G., Humic Substances: Structures, Models and Functions, Society of Chemistry, 2001, p. 161.

[29] Plaza, C., Senesi, N., Garcia-Gill, J., Polo, A., "Copper(II) complexation by humic and fulvic acids from pig slurry and amended and non-amended soils," *Chemosphere*, vol. 61, pp. 711-716, 2005.

Chapter 3: Effects of Multiple Freeze Thaw Cycles

3.1 Abstract

Experiments were performed to assess the impact of freeze-thaw cycling on the chemical and physical properties of pore water NOM. Expanding on the preliminary assessment of how NOM behaves after a single FTC in Chapter 2, Chapter 3 describes specific information regarding the fluorescent characteristics and Cu binding properties of samples pre and post freezing. Multiple cycles of freezing and thawing produce an increase in TOC in the HMW fraction relative to the control (12.6 mg C/L (± 7.5) relative to 2.3 mg C/L (± 0.45) at 95% CI). Fluorescence results indicated there were no differences in humic-like, fulvic-like and protein-like fluorescent properties of both the control and treatment samples. Copper titrations indicated trends of decreased binding affinities shown by the control 0.45 μm filtrate fraction's log K of 6.8 (+0.26/-0.29) which was larger than the treatment group's log K of 6.1 (+0.22/-0.23) at 95% CI; as well as trends of higher binding capacities shown by the treatment 0.45 μm filtrate fraction's binding capacity of 3.0 (+0.5/-0.4) μmol/mg C compared to the control group's value of 1.7 (+0.5/-0.4) at 95% CI.

3.2 Ultrafiltration

3.2.1 Experimental Details

3.2.1.1 Sampling, Storage and Selection

Samples were taken from Luther Marsh, Wylde Lake bog at coordinates 43°54'20.4"N 80°24'21.9"W. Samples were taken on January 8th, 2016. Please refer to Section 2.2.2.1 for further information related to sampling and storage.

3.2.1.2 Revised Freeze Thaw Procedure (Control and FTC Treatment)

To ensure a higher concentration of carbon in the samples and to more realistically simulate a real environmental system, peat was mixed with pore water. Peat collected from the same site as the pore water was physically mixed by hand after removing any roots, moss or larger unhumified components. A dark brown, homogenized mixture of peat remained after this process. The homogenized peat was then added to pore water, obtained as previously discussed (refer to Section 2.2.1.1), to achieve a target ratio of 300 g peat/L pore water (final ratio of 316.88 g peat/1L pore water). Samples were added to a 20L polypropylene bottle. The filled bottle was inverted 60 times to ensure mixing, and wrapped in aluminum foil to protect the samples from light degradation. The bottle was then stored for 2 weeks at 4 ^{o}C so that the pore water and peat could reach equilibrium.

After two weeks, the mixture was decanted into nine glass pyrex bottle portions (three for control replicates, three for the treatment replicates, and three for chemical extraction (to be discussed in the following chapter)). The 20 L pyrex bottle was inverted 30 times between decanting each portion to minimize particle settling. Each of the 9 portions was wrapped in aluminum foil again, and stored at 4^{o}C until further treatment.

Before each replicate filtration, the water was passed through a 2-mm sieve to remove large plant remains, and then filtered through a 1 µm polyethersulfone pre-filter (RainFresh®). This

prefiltration step helps to ensure prolonged filtration lifetime and maintain optimal ultrafiltration performance.

The pore water samples designated as the ‘multiple freeze-thaw treatment’ underwent the same pre-treatment process after the 2-week equilibration as the control samples, except these samples were frozen for 24 hours at -10 ^{o}C, then thawed at room temperature for 24 hours. The temperature and duration of the cycling was based on wetland FTC research performed by Yu et al. [1]. This process was repeated three times prior to filtration.

3.3 TOC Analysis

3.3.1 Experimental Details

Please refer to Section 2.2.2.6 for the TOC analysis method description.

3.3.2 Results and Discussion

Mass corrections were applied to the TOC values in each size fraction of the control and treatment samples to determine the mass distribution (in mg C) in HMW and LMW states (refer to Section 2.2). Graphical representations of both the relative percent, and total carbon distribution, in HMW and LMW fractions are illustrated in Figures 3-1 and 3-2. Carbon mass balances for the filtration process are represented in Table 3-1 below. It should be noted that data for the second control replicate was q-tested and identified as an outlier. Therefore, subsequent analyses based on these TOC results will not include the second control replicate. Filtration yielded average values of

96.6% (± 1.1%) and 97.4% (± 3.7%) at 95% CI conserved carbon mass, respectively, for the control and FTC filtrations, as shown in Table 3-1 below.

Figures 3-2 shows that there was a statistical increase in the proportion of HMW NOM after freezing and thawing (12.6 mg of C ± 7.5) relative to the control samples (2.33 mg of C ± 0.45).

These results show similar trends to the preliminary tests in Chapter 2. However, we cannot statistically conclude which of the two suggestions presented in Chapter 2 is correct (refer to Section 2.2.1.7). To restate the hypotheses, we had previously predicted that FTCs may disrupt larger colloidal fragments made up of NOM that is bound via hydrophobic interactions. These larger fragments would have been previously too large to pass through the first pore size prior to FT treatment. We also predicted that larger fragments of NOM are produced from smaller fragments after freezing and thawing. To conclude that the first hypothesis is correct we would expect to see an overall increased amount of released TOC after FTCs. However, the total amount of carbon after filtration (0.45 µm fraction) is not statistically different when comparing the control and treatment samples (25.77 ±13.5 mg C in control relative to 33.41 ±3.33 in the treatment). To conclude that the second hypothesis is correct we would expect to see a decrease in the LMW NOM after FTCs. However, the LMW fractions are statistically equal (22.49 ±12.34 mg C in the control relative to 20.07 ±9.14 in the treatment). However, because the confidence intervals at 95% for the 0.45 µm control fraction are so large due to the removal of an outlier replicate, we believe the data more strongly suggest that the first hypothesis is correct.

Table 3-1. Carbon mass balance of ultrafiltration size fractions for control and FTC filtration replicates.

	Control Replicates (mg C)					FTC Replicates (mg C)					
Size Fraction	Replicate 1	Replicate 3	Average	Std. Dev.	CI at 95%	Replicate 1	Replicate 2	Replicate 3	Average	Std. Dev.	CI at 95%
0.45 µm Filtrate	32.67	18.86	25.77	9.76	13.5	35.75	30.09	34.37	33.41	2.94	3.33
5 kDa Retentate	18.87	11.10	14.98	5.49	7.61	28.01	22.43	21.71	24.05	3.44	3.90
5 kDa Filtrate	12.48	7.21	9.85	3.72	5.16	8.74	5.23	11.78	8.58	3.27	3.70
Mass Balance %	96.0	97.1	96.6	0.77	1.10	102.8	91.9	97.4	97.4	3.22	3.70

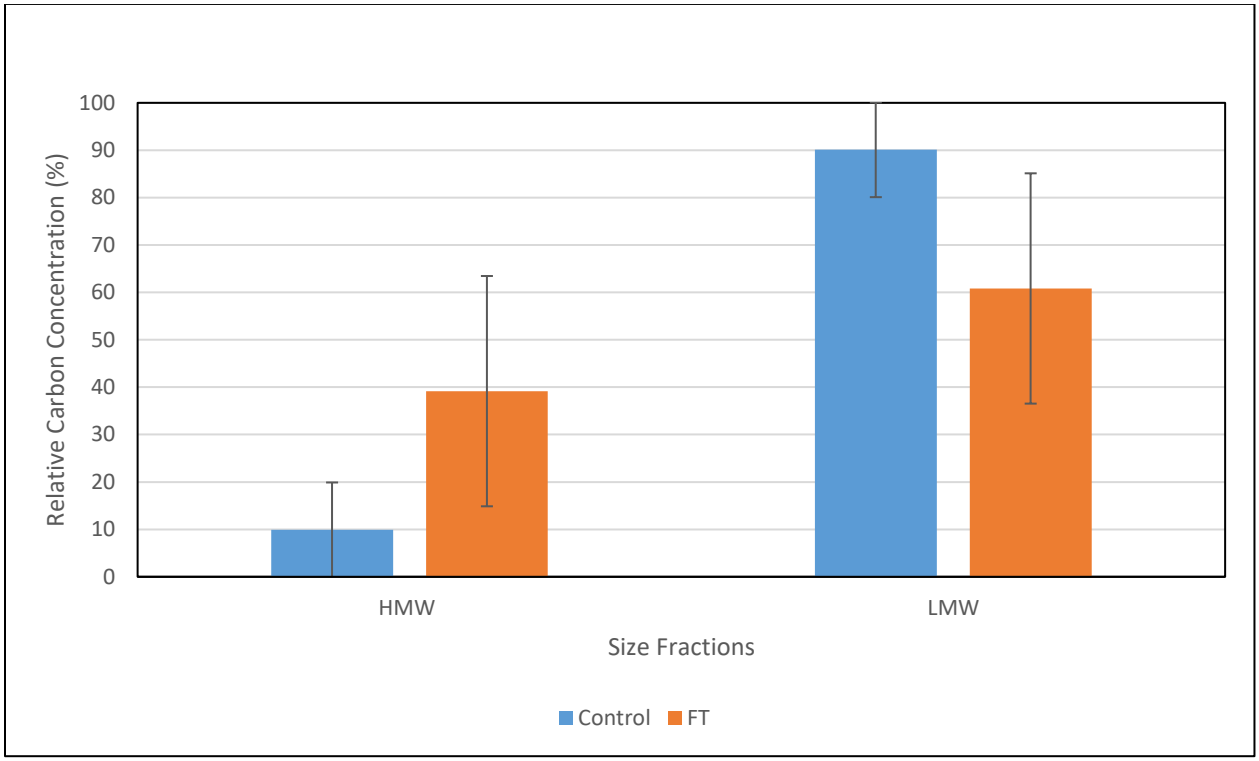

Figure 3-1. Comparison of the relative carbon distribution in the high and low molecular weight fractions of the Control and FTC treatment samples. Error bars represent confidence intervals at 95%.

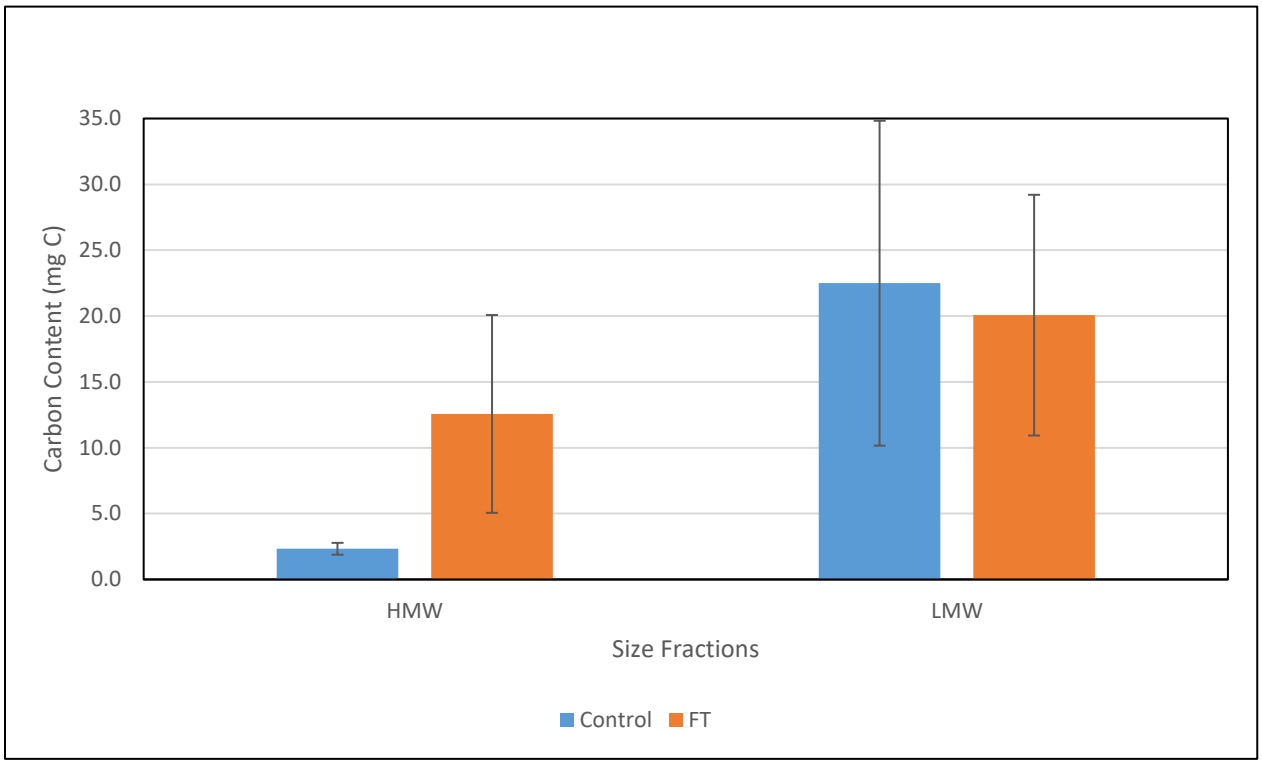

Figure 3-2. Comparison of the total carbon distribution in the high and low molecular weight fractions of the Control and FTC treatment samples. Error bars represent confidence intervals at 95%.

3.4 Fluorescence Spectroscopy

3.4.1 Experimental Details

Fluorescence analysis followed the same experimental protocol as outlined in Section 2.3.2 with the exception of a dilution step prior to analysis. Each sample was diluted to achieve <0.3 absorbance units when first analyzed by absorbance spectroscopy (Varian Cary Absorbance Spectrophotometer). This is because previous research by Ohno *et al.* has shown that diluting

samples to <0.3 absorbance units removes the potential for inner filtering effects that may diminish true fluorescent intensities [1].

3.4.2 Results & Discussion

As explained in the previous chapter, PARAFAC analysis resolved four components (HA-, FA-, tyrosine-like and tryptophan-like) in the EEMs of each of the samples. The normalized and total composition of fluorescent moieties in different NOM size fractions, as determined by EEMS and PARAFAC, are illustrated in Figures 3-3 and 3-4 below.

Like the previous chapter, HA-like and FA-like components were similar to two components published in a study by Holbrook *et al.* (components 1 and 2) who studied fresh water watershed samples, and two components published in a study by Stemond *et al.* (components 3 and 4) who studied estuarian samples [2, 3]. The trp-like component resolved in this chapter is similarly characterized to data published in several previous studies [2, 3, 4]. The tyr-like component resolved in this chapter is similarly characterized to results published by Stedmon *et al.* [5].

An evaluation of both normalized and total fluorescent data does not reveal distinct differences between the control and treatments samples. Each size fraction is dominated by FA-like and HA-like moieties. The composition of the control 0.45 µm filtrate fraction (i.e. the fraction encompassing all NOM sizes) agrees with a study that assessed filtered (0.45 µm) wetland pore water [6]. The relative compositions of each fluorescent component compared to our data are: 44% compared to 44% HA-like, 49% compared to 45% FA-like, and 7% compared to 11% protein-like [6]. An assessment of the normalized data indicates that there are also no distinct differences

between each size fraction, supporting that the apparent quality of NOM per mg C is the same regardless of size. There is, however, a larger total fluorescent contribution of FA and HA-like moieties in the 5 kDa retentate fraction relative to the 5 kDa filtrate fraction. This is most likely attributable to the fact that the 5 kDa retentate fractions contained a higher concentration of carbon (refer to Figure that shows this), which resulted in an overall more intense fluorescence response.

The data from these analyses indicate that freezing and thawing has no effect on the inherent fluorescent characteristics of NOM. We conclude from the data that no correlation can be made between the different size fractions and operationally defined molecular weights of the fluorescent components investigated in this chapter. Our findings also indicate that the increase in HMW NOM after FTCs, as outlined in Section 3.3.2, is attributed to non-flourescent NOM.

Also, because there is no apparent increase in the protein-like or FA-like moieties of samples after freezing and thawing, we can conclude that the the release of amino acids from the lysis of microorganisms, appears to be insignificant at least within the ability of fluorescence to resolve NOM quality differences.

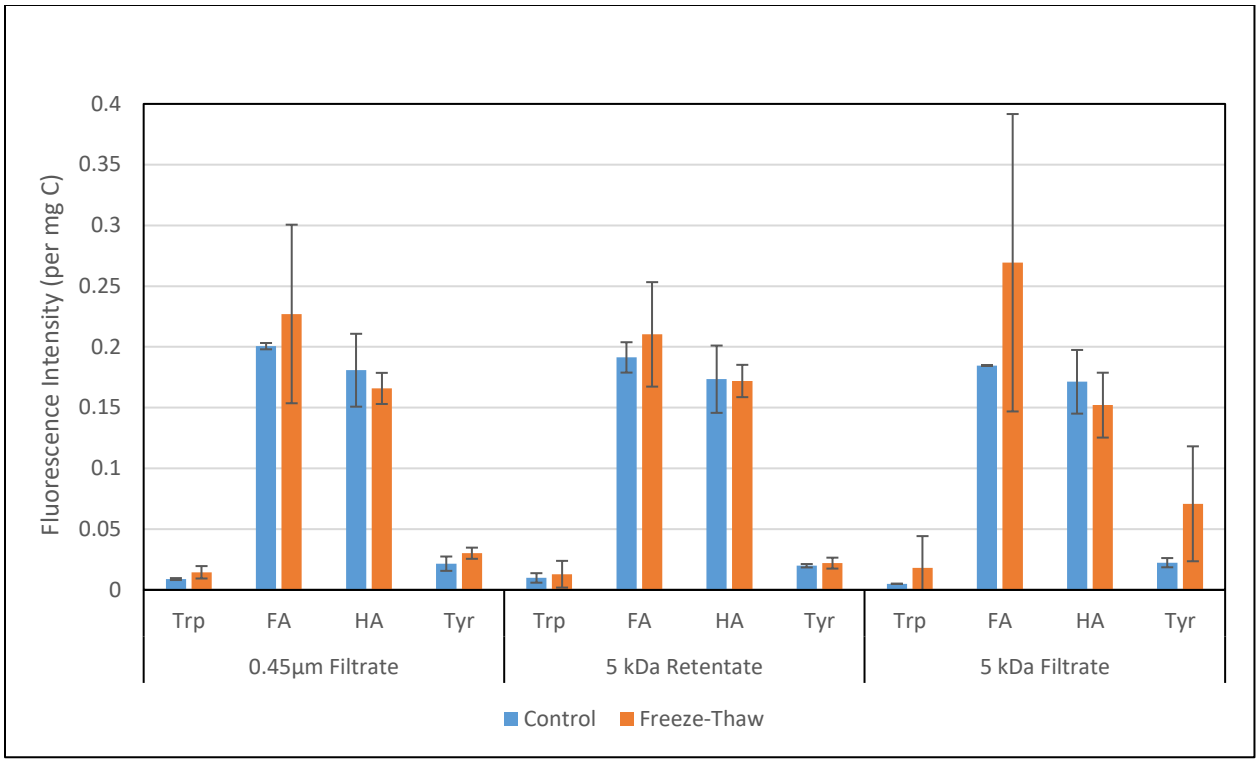

Figure 3-3. A comparison between the Control and FTC treatment samples showing the relative composition of four major fluorescence components, normalized to units of carbon, as determined by PARAFAC analysis. Error bars represent confidence interval at 95%.

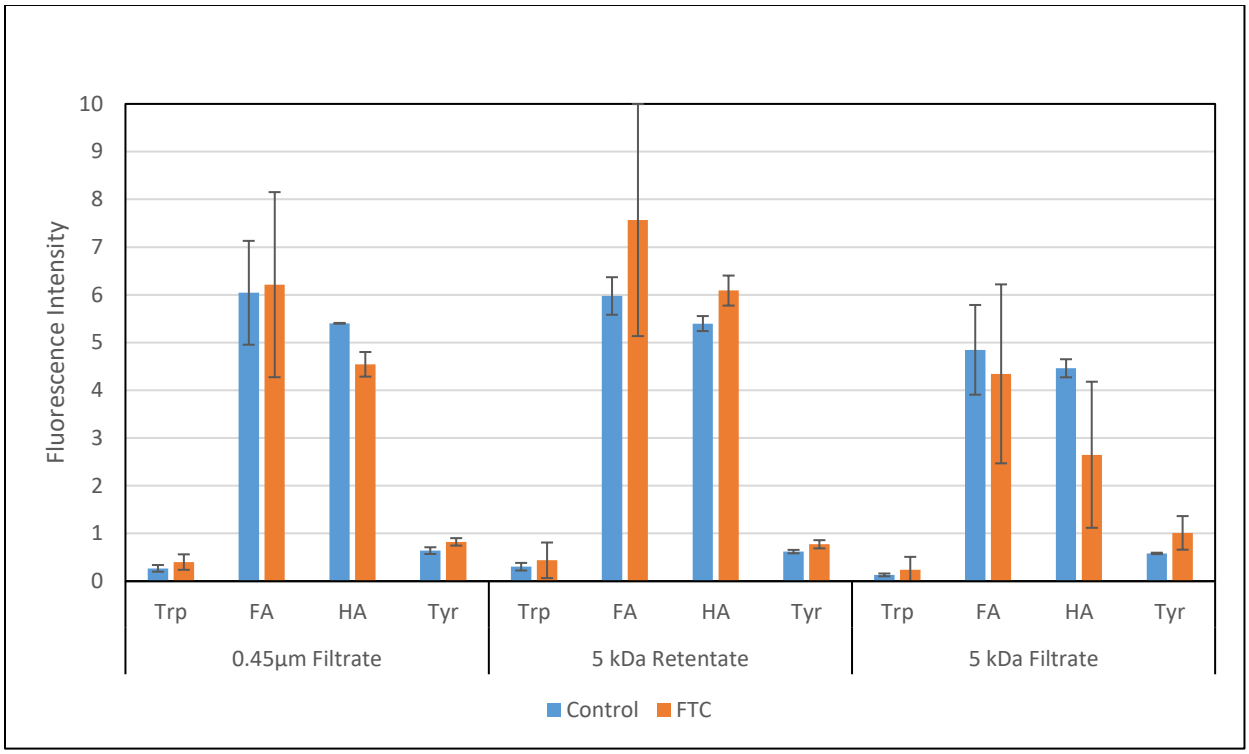

Figure 3-4. A comparison between the Control and FTC treatment samples showing the total composition of four major fluorescence components, as determined by PARAFAC analysis. Error bars represent confidence interval at 95%.

3.5 Cu Ion Selective Electrode

3.5.1 Nernst Equation

Ion selective electrode (ISE) techniques were used to assess the binding strength and capacity of the different NOM size fractions. The ISE measures the potential developed across the sensing membrane of the electrode [7]. This developed potential results as a function of the concentration of free copper in the sample. The potential is relative to a constant reference potential measured using a reference electrode. The potential resulting from the concentration of free copper can be assessed using the Nernst equation [7]:

$$E = E_o - \left(\frac{RT}{nF}\right) lnQ \qquad (3-1)$$

where E and E° are the measured electrode potential and the reference potential (constant) respectively. R is the real gas constant (8.315 J mol-1 K-1), T is the temperature in Kelvin, n represents the ionic charge number on the analyte, and F is the Faraday constant (96487 C mol-1). Q is a reaction quotient incorporating the activity of the analyte. For this Cu-ISE, this can be rewritten as:

$$E = E_o - \left(\frac{RT}{nF}\right) ln\left(\frac{1}{aCu^{2+}}\right) \qquad (3-2)$$

To further simplify this formula, we assume a temperature of 298K and convert the natural logarithm to the base ten logarithm (multiply by 2.303):

$$E = E_o + \left(\frac{0.0592}{2}\right) log(aCu^{2+}) \qquad (3-3)$$

From this we establish that the slope of the electrode will be ~29.6 mV per decade of [Cu^{2+}]. Thus, for a properly functioning electrode, the resulting slope should therefore be approximately 30 mV per decade.

3.5.2 Cu-NOM Complexation

From the free copper measured via ISE, total copper added, and TOC concentration of each sample titrated, the binding strength and capacity of each sample was determined. The concentration of bound copper in each sample was calculated using the following formula:

$$[CuL] = [Cu_{Total}] - [Cu^{2+}] - \left[Cu_{inorganic}\right] \qquad (3-4)$$

Where [CuL] is the bound copper concentration, [Cu_{Total}] is total copper concentration titrated, and [Cu^{2+}] is free copper concentration detected. Once the bound concentration of copper was calculated, inorganic complexation, denoted as [$Cu_{inorganic}$], was accounted for and subtracted from the total. This was to ensure that only Cu binding to organic ligands in the samples was considered. The data was therefore normalized to the TOC concentration for each sample. Inorganic complexation was accounted for using the equilibrium binding constants illustrated in Table 3-2 below.

Table 3-2. Equilibrium constants used to account for inorganic copper complexation in copper (II) titrations performed on NOM samples [8].

Inorganic Species	Equilibrium Constant (K)
$CuOH^+$	$10^{6.5}$
$Cu(OH)_2$	$10^{-15.2}$
$CuCO_3$	$10^{6.77}$
$Cu(CO_3)_2^{2-}$	$10^{10.2}$
$CuHCO_3^+$	$10^{1.03}$

Each inorganic complex was calculated by subbing known concentrations of each ion or molecule into its respective copper equilibrium equation. An example reaction and equilibrium equation for CuOH is shown below:

$$[Cu^{2+}][OH^-] \leftrightarrow [CuOH] \qquad (3-5)$$

$$[K_f] = \frac{[CuOH]}{[Cu^{2+}][OH^-]} \qquad (3-6)$$

3.5.3 Experimental Details

Titrations were carried out using an Orion Copper (II) ISE and an Orion double junction silver-silver chloride reference electrode (Model 900200). The general titration protocol followed the method outlined by Brooks *et al.* [8]. In brief, 50 mL solutions of each undiluted sample, adjusted

to 0.01 M KNO_3 , were titrated under Argon gas using 1000 mg/L and 10000 mg/L $CuNO_3$ (Fisher Scientific) titrant solutions. Each sample was maintained at a pH of 6 throughout the duration of the titration.

Before raw data were processed it was plotted as free versus total copper binding curves, as seen in Figure 3-5 below. This data were then manipulated into log [Cu^{2+}] and [Org-Cu] values, using an in-house MATLAB script whereby the intrinsic binding equilibria (i.e. log K values) and total binding capacities were determined. This script applied Monte Carlo analysis for each sample to account for probability distribution. The respective MATLAB script can be found in Appendix B.

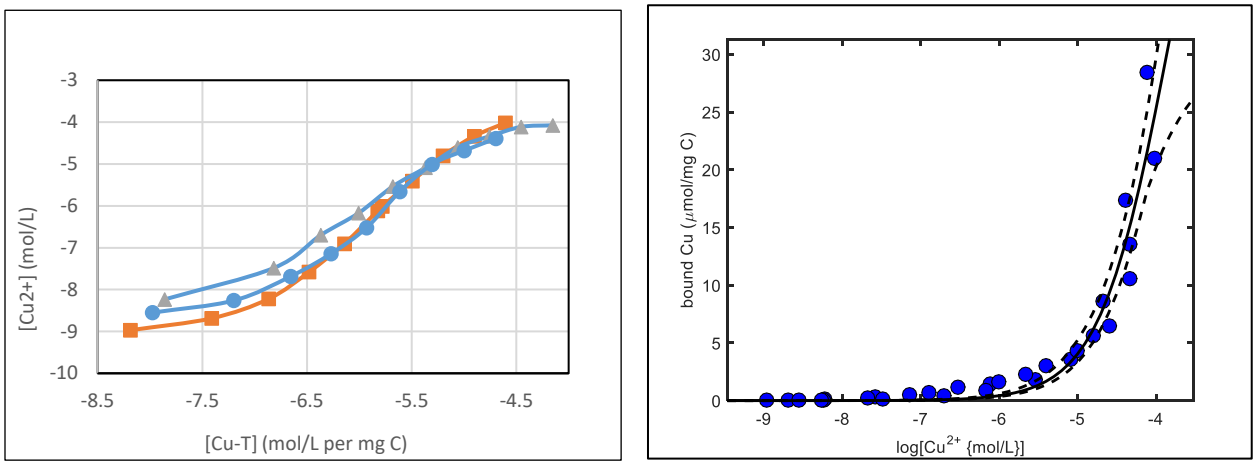

Figure 3-5, 3-6. Example of raw copper binding data illustrating detected concentration of free copper versus total copper titrated for three replicate titrations of the FT 5 kDa filtrate fraction (left); and the fitting results illustrating bound copper per unit of carbon versus free copper with best fit line (solid line) and upper and lower confidence intervals (UCI and LCI) (dotted lines) at 95% (right).

3.5.4 Results & Discussion

The copper binding affinities are illustrated in Figure 3-7 below. Overall, the control and treatment groups generally yielded equal results, with the control samples trending towards slightly higher values. The 5 kDa filtrate and retentate fractions were equal to each other between control and treatment samples. The 5 kDa filtrate fractions had a log K value in the range of 5.4-6.2. The 5 kDa retentate fractions had a log K value ranging from 5.6-6.3. The 0.45 µm filtrate fraction was the only fraction where an observable change took place after freezing and thawing. The control fraction exhibited the strongest binding strength with a log K of 6.8 (+0.26/-0.29) which was larger than the treatment NOM log K of 6.1 (+0.22/0.23) at 95% CI.

There is no research available to compare the identical size fractions that were used in this study. There are, however, examples of fresh water NOM samples which were analyzed for their copper binding affinity. In one study, nine fresh water NOM samples were treated by reverse osmosis (1µm-400 Da in size) and were tested for Cu binding affinity at circumneutral pH values (5.78-7.30); these samples yielded log K values ranging from 5.97 to 6.45 [9]. Overall, the FT treated samples ranged from 5.4 to 7.0, and the controls ranged from 5.8-7.0. Although the samples span a larger range, this is most likely attributed to variability caused by mixing of peat and pore water in the sample preparation, which this referenced study did not perform. Differences could also be attributed to the fact that their molecular weight cut-off is larger than ours. We can comment that our samples have similar binding strengths to NOM samples referenced in the literature. When considering the range of all our samples, the binding affinity is most comparable to Cu formation with CO_3^{2-} and OH^- species (log $K_{CO3(2-)} = 6.77$ and log $K_{OH(-)} = 6.5$) [8].

The total binding capacity of each sample (with upper and lower confidence intervals) is shown in Figure 3.8. These results show more variability in all size fractions and between the control and treatment groups when compared to the copper binding affinity results. Although each size fraction is not statistically equal because the data is not expressed on a logarithmic scale, the freeze thaw samples showed trends of larger binding capacities for all size fractions as shown in Figure 3.8. The 0.45 µm filtrate fractions of both the control and treatment groups showed the smallest binding capacity in the range of 1.3-3.5 µmol/mg C. The treatment sample did, however, have a higher capacity with a total ligand binding value in the 0.45 µm filtrate fraction of 3.0 (+0.5/-0.4) when compared to the control value of 1.7 (+0.5/-0.4). The 5 kDa filtrate fractions and the 5 kDa retentate fractions showed the highest binding capacities. The binding capacity of the 5 kDa filtrate fractions was in the range of 2.7-5.8 µmol/mg C. Although statistically equal because of overlapping confidence intervals, the control fraction showed a lower range of confidence at 3.4 (+0.7/-0.6) when compared to 4.8 (+1.0/-1.0) for the treated fraction. The 5 kDa retentate NOM samples ranged between 2.3-5.6 µmol/mg C. This fraction showed similar trends to the 5 kDa filtrate fraction with the control value exhibiting a value of 2.9 (+0.8/-0.6) when compared to the treatment value of 5.6 (+1.0/-1.0). It is interesting to note that there is very little difference between the 5 kDa filtrate and retentate fraction for the control, and the 5 kDa filtrate and retentate fractions for the treatment This indicates that the observed differences in copper binding capacity are most likely not due to size, but rather to the effects of freezing and thawing.

For the binding affinity results, there are few studies available to compare our Cu binding results using NOM separated by size. For the study of nine freshwater NOM samples (1µm-400 Da in size) discussed above, the binding capacities ranged from 0.93-3.52 µmol/mg C [9]. The binding

capacities of all NOM size fractions in this study ranged from 1.3-5.8 µmol/mg C, with the control samples ranging from 1.3-4.1 µmol/mg C. The binding capacity for the control treatment in our study generally demonstrated comparable results to the nine fresh water samples referenced above. The higher values that were determined could be due to the larger proportion of LMW NOM in our samples, and to their lower molecular weight cut-off (400 Da). Samples in this project contained a larger proportion of low molecular weight fulvic acid-like NOM, which has been shown to exhibit higher binding capacities than larger humic acid-like molecules [11, 12, 13].

Overall, these results agree with the hypothesis that FTC's will promote characteristics in NOM of more fulvic acid-like molecules (refer to Section 1.7). FTC samples of all NOM fractions exhibited trends of slightly lower binding affinities (treatment samples were on average 94% lower than control samples), and larger binding capacities compared to control samples (control samples were on average 64% lower than treatment samples). As previously stated, fulvic acid NOM has been shown to exhibit smaller binding affinities and larger binding capacities (refer to Section 1.7). However, we would have expected these differences to be more pronounced in the 5 kDa filtrate fraction if fulvic acid properties were also correlated with NOM size. To elaborate, we would expect there to be a larger proportion of smaller fulvic acid molecules in the smallest NOM fraction, and therefore this fraction would show different results compared to the other fractions. However, this was not the case because consistent impact of freezing and thawing was observed for each size fraction.

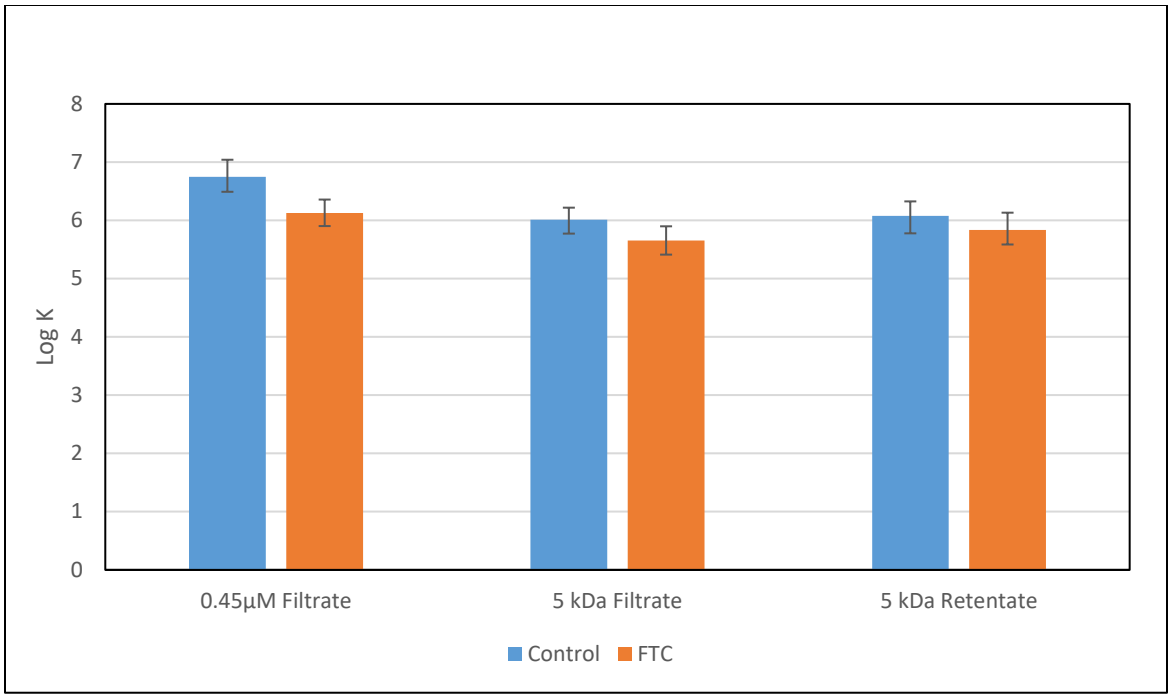

Figure 3-7. A comparison of the copper binding affinity constants (log K) for each size fraction of the Control and FTC treatment samples. Error bars represent confidence interval at 95%.

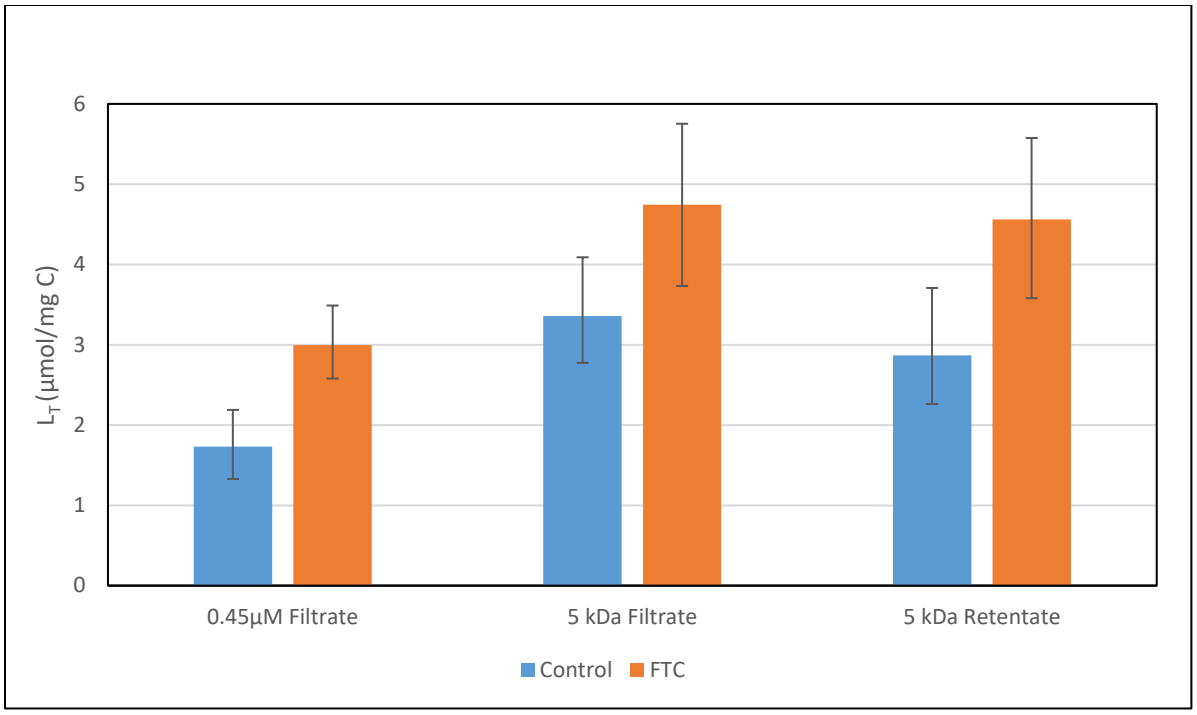

Figure 3-8. A comparison of the total binding capacity (L_T in µmol/mg C) for each size fraction of the Control and FTC treatment samples. Error bars represent confidence interval at 95%.

3.6 Conclusion

The results confirm the impact of freeze-thaw cycling on organic matter size distribution, and supports that freezing and thawing mobilizes larger NOM fragments.

Further analysis using fluorescence spectroscopy indicated that most of the NOM in all size fractions can be attributed to humic-like and fulvic-like moieties, with no differences between control and treatment groups. No correlation can be made between the size constraints put in place by the filtration pore sizes and the recognised information regarding the size of molecules represented by the fluorescent components. These results do not agree with the hypothesized increase in fulvic-acid fluorescent moieties in FTC samples. Interestingly, they also do not

correlate with the TOC-filtration results, which indicate that after freezing and thawing there is a larger proportion of HMW NOM present as shown in Figure 3-1. We therefore would have expected a larger proportion of humic-like molecules to be present and thus a larger proportion of humic-like fluorescent moieties. This indicates that there is overlap in the fluorescent properties of different size NOM fragments, and that the humic and fulvic-like components are independent of size. Also, because there is no increase in the fulvic acid-like and protein-like moieties after freezing and thawing, there is no evidence to support that freezing and thawing releases a significant amount of small molecular weight sugars and amino acids from lysis of microorganisms.

The copper titration results indicated that NOM fractions subjected to freeze-thaw cycling showed slightly lower binding affinities, and larger binding capacities, when compared to control samples. This agrees with the hypothesis, which was restated in Section 3.5.4, that NOM would be more representative of fulvic acid molecules after FTCs. Fulvic acid molecules have a lower binding affinity and higher binding capacity than larger humic acid molecules [11, 12]. Since NOM binds more copper after cycles of freezing and thawing, these findings could hold implications for increased copper mobility in northern wetland environments.

The results presented in this chapter established that NOM from different size fractions does not exhibit markedly different characteristics with respect to chemical structure, as assessed using fluorescence spectroscopy, or Cu binding titrations. The impacts of freezing and thawing generally show uniform trends across all sizes of NOM. One reason that the effects of a FT treatment are observed in all size fractions could be due to our method of separating NOM. Some of our initial

predictions were made based on information deduced from studies of humic substances and their respective model compounds, which are separated according to strictly defined chemical extraction protocols. Because a chemical extraction procedure was not used in this study, the intermolecular forces that aggregate NOM colloids were not disrupted to the same degree. Although we did observe the expected properties of humic and fulvic acid molecules, the known sizes and molecular weights of their model compounds do not correlate with our results because the NOM in our samples are aggregated via hydrophobic interactions into larger fragments. The results of chemical extraction are investigated in the Chapter 4.

3.7 References

[1] Ohno, T., "Fluorescence inner-filtering correction for determining the humification index of dissolved organic matter.," *Environ Sci Technol*., vol. 36, pp. 4, pp. 742-746, 2002.

[2] Holbrook, D., Yen, J., Grizzard, T., "Characterizing natural organic material from the Occoquan watershed (Nothern Virgina, US) using fluorescence spectroscopy and PARAFAC," *Sci. Tot. Environ.*, vol. 361, pp. 249-266, 2006.

[3] Stedmon, C., Markager, S., Bro, R., "Tracing dissolved organic matter in aquatic environments using a new approach to fluorescence spectroscopy," *Mar. Chem*., vol. 82, pp. 239-254, 2003.

[4] Baker, A., "Fluorescense excitation-emission matrix characterization of some sewage-impacted rivers," *Environ. Sci. Technol*., vol. 35, pp. 948-953.

[5] Stedmon, C., Markager, S., "Resolving the variability in dissolved organic matter fluorescence in a temperate estuary and its catchments using PARAFAC analysis.," *Limnol. Oceanogr*. , vol. 50, pp. 686-697, 2005.

[6] Agrawal, S., "Cr(VI) reduction by Fe(II)-dissolved organic matter complexes and the characterization of pore water dissolved organic matter from a coastal wetland in the Laurentian Great Lakes", *Ohio State University*, ProQuest Dissertations Publishing, 2008.

[7] Skoog, D., Holler, J., Crouch, S., Principles of Instrumental Analysis. 6th ed., Brooks & Cole: Thomson Corp. United States, 2007.

[8] Brooks, M., McKnight, D., Clements, W., "Photochemical control of copper complexation by dissolved organic matter in Rocky Mountain streams, Colorado," *Limnol. Oceanogr*.,, vol. 52, pp. 2, pp. 766-779, 2007.

[9] Hicks, K., "Using chemical, optical and biological methods to characterize Cu complexation by different natural organic matter sources collected from canadian shield waters", *Wilfrid Laurier University Thesis Archives*, 2009.

[10] Ghabbour, E., Davies, G., Humic Substances: Structures, Models and Functions, Society of Chemistry, 2001, p. 161.

[11] Plaza, C., Senesi, N., Garcia-Gill, J., Polo, A., "Copper(II) complexation by humic and fulvic acids from pig slurry and amended and non-amended soils," *Chemosphere*, vol. 61, pp. 711-716, 2005.

[12] Pettit, R., "Organic matter, humus, humate, humic acid, fulvic acid and humin: their importance in soil fertility and plant health" *Texas A&M University*, 2004.

[13] Grogan, P., Michelsen, A., Ambus, P., Jonasson, S., "Freeze–thaw regime effects on carbon and nitrogen gen dynamics in sub–arctic heath tundra mesocosms," *Soil Biol Biochem*, vol. 36, pp. 641-654, 2004.

[14] Yu, X., "Material Cycling of Wetland Soils Driven by Freeze–Thaw Effects," Springer - Northeast Institute of Geography and Agroecology, Vols. 2190-5061.

Chapter 4: Comparing Two Approaches to Studying NOM – Physical Separation *versus* Chemical Extraction

4.1 Abstract

The purpose of the research shown in this chapter is to compare two different approaches to isolating NOM. The foremost goal was to assess the reproducibility between two different separation techniques. The secondary goal was to establish if they could, therefore, be utilized in combination to characterize the quality of NOM. Using a peat-pore water mixture, a comparison was made between the 5 kDa filtrate fraction and chemically extracted fulvic acid using the traditional method from soil science literature. Comparisons were made by showing the fluorescent characteristics and Cu binding properties between physically separated and chemically extracted samples. Fluorescent analysis per unit of carbon (mg C), filtered samples exhibit a higher degree of fluorescence intensity in characteristics that were humic acid-like (0.17 (± 0.013) compared to 0.10 (± 0.0079)), fulvic acid-like (0.19 (± 0.00010) compared to 0.16 (± 00.75)) and tyrosine-like (0.022 (± 0.020) compared to 0.013 (± 0.0017)); however, fulvic acid extracts exhibited stronger tryptophan-like characteristics (0.011 (± 0.00086) compared to 0.0050 (± 0.000072)). The filtered samples also showed a lower intrinsic binding strength (log K 6.01 (+0.21/-0.24) compared to log K 6.46 (+0.22/-0.23)) and higher total binding capacity (3.36 µmol/mg C (+0.73/-0.58) compared to 1.69 µmol/mg C (+0.21/-0.23)) for copper relative to fulvic acid extracts, indicating that the NOM samples isolated using different techniques are not the same.

4.2 Introduction

The comparison of NOM isolated using different techniques is important to research on soil organic matter because there is still controversy about the most effective approach to studying NOM systems [1]. As previously stated in Section 1.5, there is a variety of techniques that can be used to study NOM. There is also a large body of published information on NOM systems. Most research in this area of soil chemistry has applied a traditional and widely accepted approach of separating humic and fulvic acids using a defined chemical extraction procedure based on pH dependent solubility. As research on soil organic matter has continued to develop, more studies using novel approaches, such as Ultrafiltration, have been applied to assess soil organic matter [1]. Currently, no research has been conducted to compare the products of ultrafiltration separation and humic-fulvic chemical extraction with respect to the chemical properties of NOM. As the breadth of this field expands, understanding how previous research can be used to further utilize current projects becomes an important topic. It becomes difficult to interpret results and to take advantage of past research without controlled comparisons. It is for this reason that physical separation by ultrafiltration – which is becoming more popular as shown by the increasing number of publications with ultrafiltration in this area of research – was compared to the traditional chemical extraction procedure for the separation of humic and fulvic acids.

To assess the transport of Cu by binding to small NOM fragments, the 5 kDa filtrate fraction from the control sample was compared to the fulvic acid fraction obtained using a standard chemical extraction protocol. These fractions were also chosen because they represent similar molecular weights (i.e. fulvic acid ranges from 200-2000 Da and the 5 kDa filtrate ranges from <5000 Da).

The ultrafiltration results (i.e. 5 kDa filtrate results) in this chapter are the same data presented in the previous chapter. NOM used for the chemical extraction was from the same source as described in the previous chapter, and was prepared the same way. For this reason, information on sample preparation and techniques related to these experiments are described in the previous chapter, as referenced,

4.3 Ultrafiltration

4.3.1 Pre-treatment of Pore Water

Samples were pre-treated in the same way as outlined in Section 3.2.1.2.

4.3.2 Ultrafiltration Apparatus Setup

Please refer to Section 2.2.2.3 for ultrafiltration apparatus setup.

4.3.3 Pre and Post Treatment, and Storage of Hollow Fiber Ultrafiltration Filters

Please refer to Section 2.2.2.4 for information related to pre and post treatment, and storage of hollow fiber ultrafiltration filters.

4.3.4 Sample Ultrafiltration Procedure

Please refer to Section 2.2.2.5 for sample ultrafiltration procedure.

4.4 Fulvic Acid Extraction

4.4.1 Pre-treatment of Pore Water

Chemical extracts (same source of NOM described in Section 3.1.2.1) were pre-treated just as the ultrafiltration samples were with the exception that no pre-filtering was applied with a 1µm filter.

4.4.2 Chemical Extraction Procedure

NOM samples were chemically extracted with the following procedure outlined in the schematic below [1].

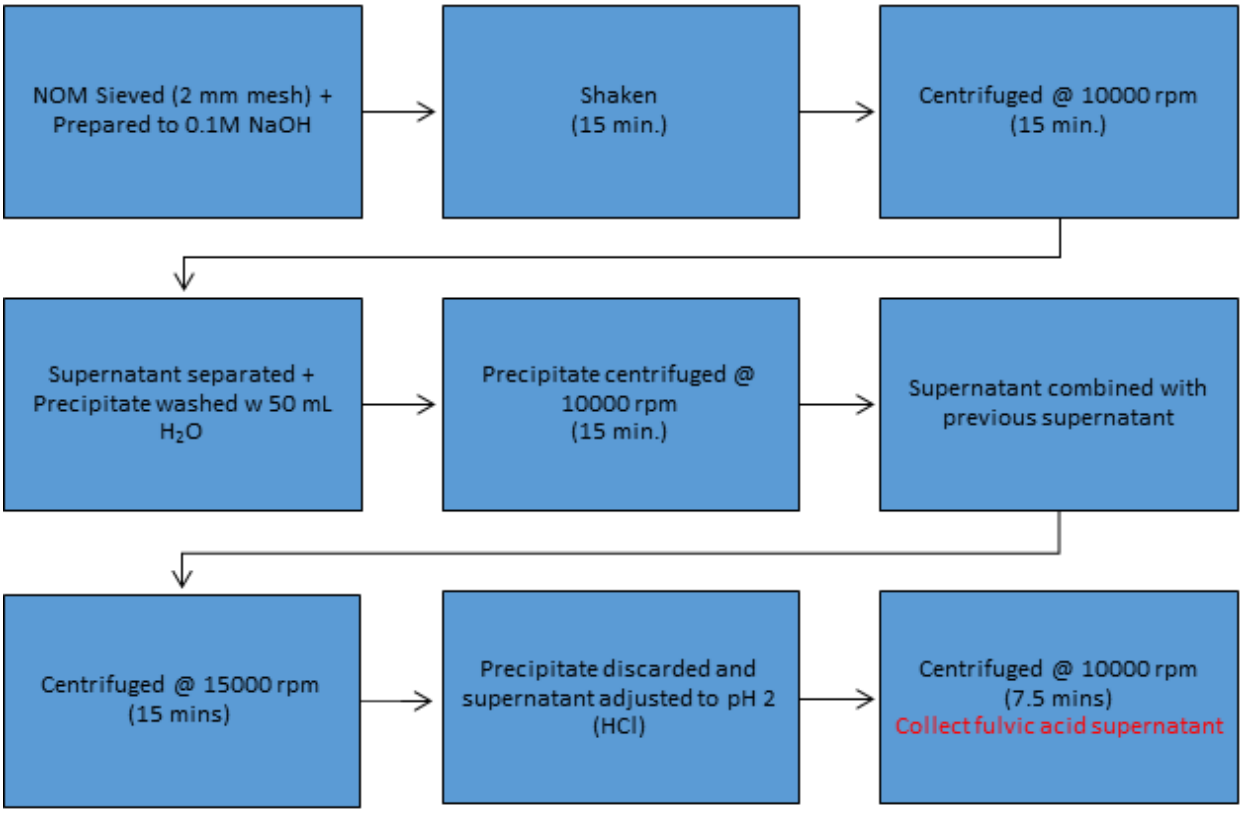

Figure 4-1. Schematic outlining the protocol performed to extract fulvic acid from pore water samples. This protocol was taken from work performed by Tan [1].

4.5 TOC Analysis

Please refer to Section 2.2.2.6 for information related to TOC analysis.

4.5.1 Results and Discussion

The tabulated concentrations of total organic carbon (mg/L) are presented in Table 4-1 below. The fulvic acid extracts, with an average total organic carbon concentration of 98.7 mg/L, were more than three times more concentrated than the 5 kDa filtrate fractions, which contained 26.2 mg C/L. The average total organic carbon content serves as a reference for the fluorescent and Cu binding experiments outlined later in this chapter since the results were normalized to carbon in order to describe the inherent characteristics of NOM in each sample. This removes the potential for biasing results based on the quantity of carbon. It should be noted that the solubilisation causing the increased carbon concentration in the FA samples represents material that would not be entirely available in a real environmental system.

Table 4-1. Total organic carbon concentrations (mg/L) for the 5 kDa Filtrate Control sample and Fulvic Acid Extract sample.

NOM Fraction	TOC (mg/L)	Standard Error
5 kDa Filtrate Control	26.2	5.12
FA Extract	98.7	16.4

4.6 Fluorescence Spectroscopy

4.6.1 Experimental Details

Fluorescence analysis followed the same experimental protocol that was outlined in Section 3.2.

4.6.2 Results & Discussion

Consistent with the results described in the previous chapters, PARAFAC resolved four components (HA-, FA-, tyrosine-like and tryptophan-like) in the EEMs of these two sample groups. The normalized and total composition of fluorescent moieties in the two NOM fractions are illustrated in Figures 4-2 and 4-3 below, and numerically in Tables 4-3 and 4-4 below.

Both fractions show similar fluorescent trends, indicating that they contain structurally similar components. Normalized data shows predominantly HA and FA-like components compositionally (44% and 35% of the 5 kDa filtrate fraction relative to 48% and 56% of the FA fraction). When compared however, the 5 kDa filtrate fraction exhibits 1.7 times more intense HA-like characteristics relative to the FA sample.

It is interesting that the properties associated with each fluorescent component, and what would be expected based on the molecular size of both NOM fractions, do not agree with our results. The separation and extraction techniques isolate small fragments relative to what was present in the initial pore water sample. It can be expected that smaller NOM fragments will exhibit a higher proportion of FA-like and protein-like characteristics [2]. However, both samples are predominantly characterized by both HA and FA-like components, exhibiting very little protein fluorescence. This is not surprising since allochthonous sources of NOM have been shown to

contain low sources of protein [3] [4]. A similar study which performed PARFAC analysis on humic-fulvic fractions extracted from allochthonous NOM showed that both fractions were predominantly characterized by fulvic-like and humic-like moieties [5]. This research further showed that the fulvic fractions had a lower concentration of protein, as shown by the 5% and 9% tyrosine and tryptophan abundances, relative to the 10% and 16% abundances in the humic fraction [5]. Similar research by Caron et al. has shown that the 5 kDa filtrate fraction in fresh water terrestrial NOM samples, similar to our samples, resembles predominantly humic and fulvic-like characteristics with protein abundances lower than 20% [6]. Also, it is interesting that the fluorescence results of the fulvic acid extracts resembled larger HA-like molecules. This could indicate that: 1) the first being that the extraction protocol does not exclusively extract fulvic acid molecules; and 2) that what is operationally defined as 'fulvic acid' also shares humic acid like properties. Previous literature has indicated that both conclusions are true [1][7].

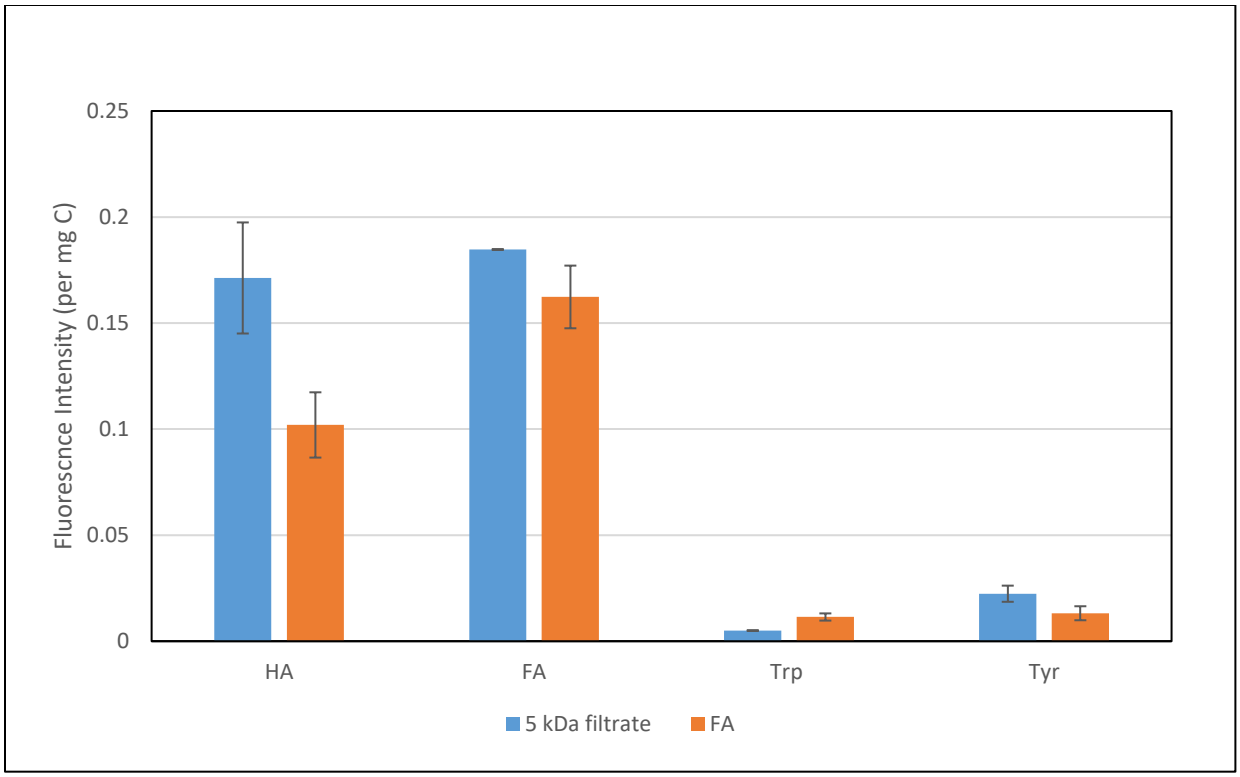

Figure 4-2. A comparison between the 5 kDa Filtrate Control and FA Extract samples of the composition of four major fluorescence components, normalized to units of carbon, as determined by PARAFAC analysis. Error bars represent confidence interval at 95%.

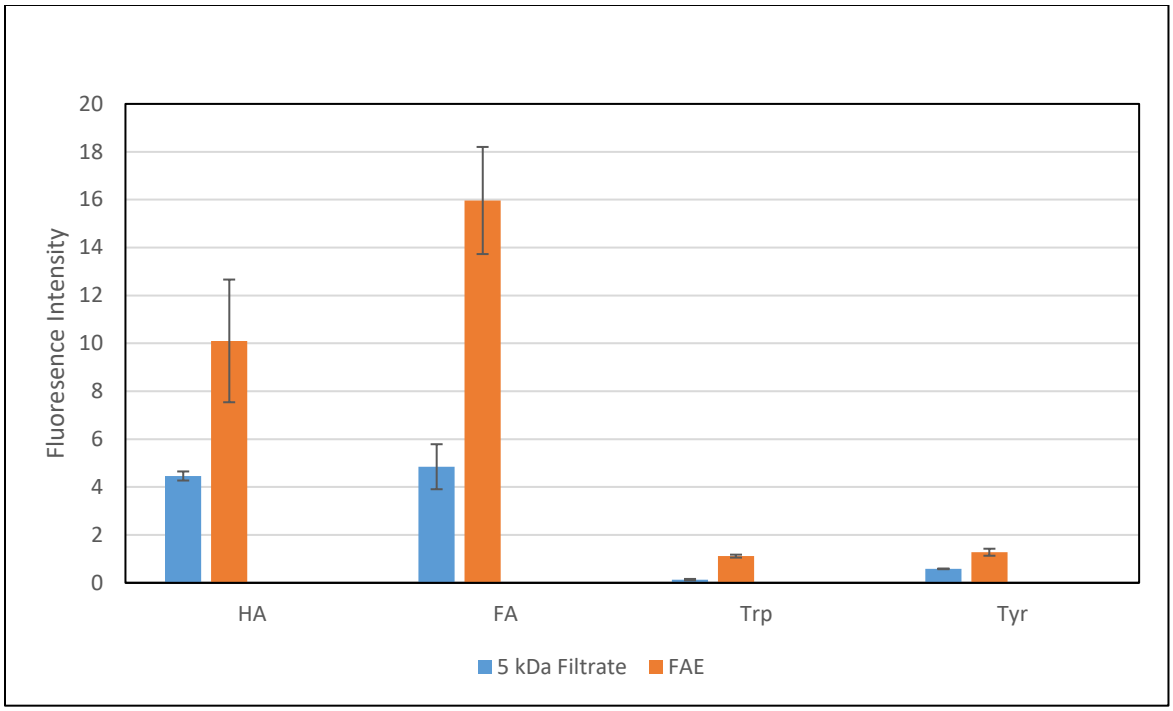

Figure 4-3. A comparison between the 5 kDa Filtrate Control and FA Extract samples of the total composition of four major fluorescence components, as determined by PARAFAC analysis. Error bars represent confidence interval at 95%.

4.7 Cu Ion Selective Electrode

4.7.1 Experimental Details

Cu-ISE analysis followed the same experimental protocol as outlined in Section 3.2.

4.7.2 Results & Discussion

As illustrated in Figure 4-5 and Table 4-4 below, the copper binding affinity of the fulvic acid extract has a larger log K value (6.46 +0.22/-0.23) than that of the 5 kDa filtrate (6.01 +0.21/-0.24). As mentioned in the previous chapter, there has been little research conducted with the same

experimental parameters for comparison. The study of nine fresh water NOM samples (1µm-400 Da in size) that was previously discussed yielded log K values ranging from 5.97 to 6.45 [3]. The results for the 5 kDa filtrate fraction, although on the lower end of this range, show similar results to that study. One reason why the 5 kDa filtrate NOM is low could be due to the higher composition of smaller NOM fragments present in our samples relative to samples in their study. Smaller fragments typically resemble fulvic acid-like molecules, which are known to have smaller log K values when compared to larger humic acid-like molecules [8]. Two comparable studies also showed fulvic acid extracts derived from NOM having log K values of 5.66 and 6.41 [5][9]. The results that were obtained for the fulvic acid extract samples are quite similar to these values. One reason that our samples are high could be attributed to differences in how the extraction was performed. In our study, we focused solely on the chemical extraction aspect, minimizing initial sample preparation steps such as filtration or XAD resin adsorption. The extraction method that was used was less specific and we speculate that some larger humic acid-like NOM components were also extracted. This ultimately resulted in a higher apparent log K since humic acid molecules have a stronger affinity for copper relative to fulvic acid molecules [8].

The total binding capacity of our samples is shown in Figure 4-6 and Table 4-5 below. The 5 kDa filtrate NOM has a much larger capacity for copper, yielding 3.36 µmol/mg C (+0.73/-0.58) when compared to the fulvic acid extracts (1.69 µmol/mg C +0.21/-0.23). For the study of 9 fresh water samples that was cited previously, the results yielded copper binding capacities ranging from 0.93-3.52 µmol/mg C [3]. Our data generally agree. One probable reason why our binding capacity is comparatively high is because the 5 kDa filtrate NOM had a larger composition of smaller NOM fragments. This means that our samples would more strongly resemble operationally defined fulvic

acid-like molecules, which have a higher binding capacity when compared to larger humic acid-like molecules [9]. For comparison, one study based on fulvic acid extracted from Canadian sphagnum peat moss at pH 4 yielded copper binding affinities of 16.1 µmol/mg C [9]. Another study based on fulvic acid extracted from organic compost at pH 7 yielded binding affinities of 2.50 µmol/mg C [10]. We can therefore conclude that the copper binding affinities are variable and perhaps characteristic of the source environments from which they are extracted. Variation may also be attributed to small differences in the extraction procedure, sample collection and storage. Therefore, no unequivocal comparison to published values can be made.

Since the results of both treatments are not equal, we can conclude that the physical separation and chemical extraction method do not yield NOM with comparable copper binding characteristics.

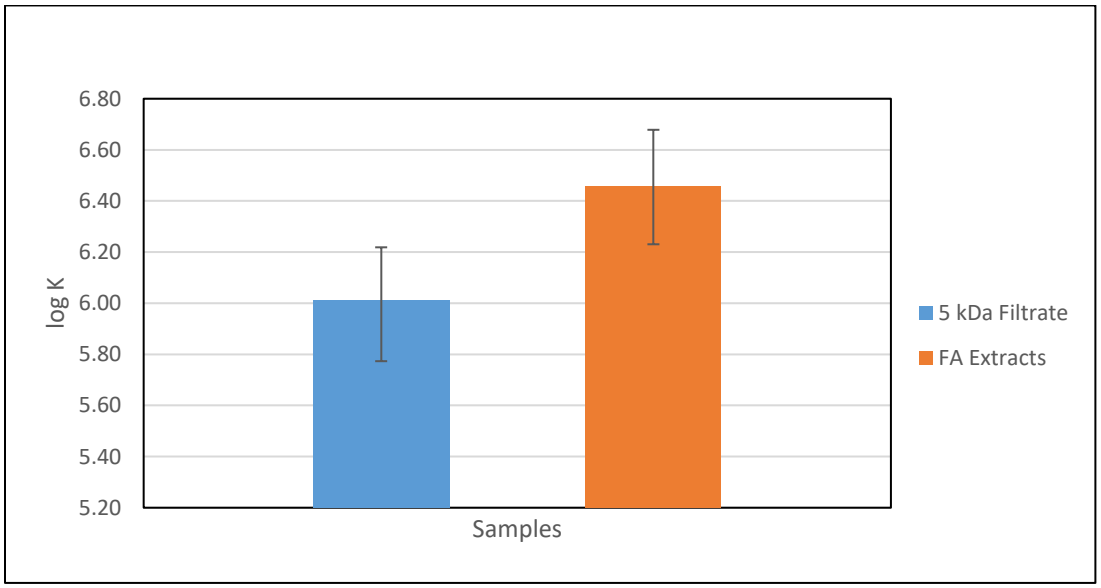

Figure 4-4. A comparison of the copper binding affinity (log K) between the 5 kDa Filtrate and FA Extract samples. Error bars represent confidence interval at 95%.

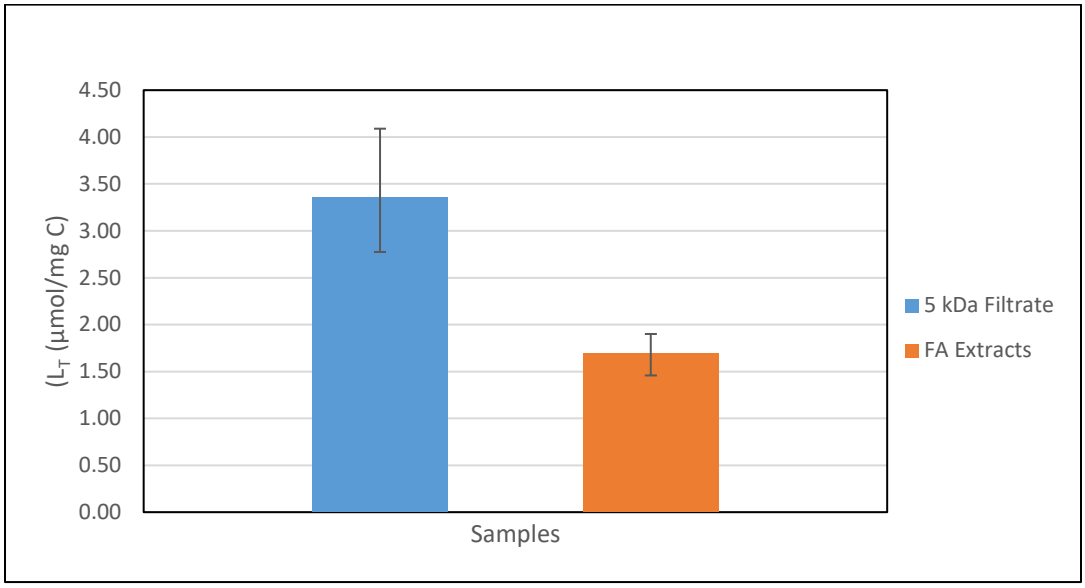

Figure 4-5. A comparison of the total binding strength (L_T in µmol/mg C) of the 5 kDa Filtrate and the FA Extract samples. Error bars represent confidence interval at 95%.

4.8 Conclusion

While no indications of quality can be drawn from the TOC results, it is noted that the FA extraction solubilized a large proportion of NOM resulting in approximately four times more TOC than our 5 kDa filtrate fractions. It is important to reiterate that while the amount cannot be quantified, a large proportion of the additional solubilized NOM would not be accessible in a real environmental system.

The fluorescent results of this chapter indicate that the NOM from the 5 kDa fraction separated by filtration and by chemical extraction show similar trends, however the quality of the NOM is not

the same. This indicates that the hypothesis that the two fractions would have the same fluorescent composition is incorrect. This is supported by the stronger intensity of the 5 kDa filtrate fraction per unit of carbon, even though both fractions were comprised mainly of HA-like and FA-like fluorescent moieties. The results from this analysis also indicate that the fluorescent components do not completely resemble their operationally defined NOM molecules. There is instead substantial overlap in the properties of different molecules. This is shown by the presence of HA-like moieties in both small NOM fractions.

The copper titration results further confirmed that the NOM samples are similar, however the inherent quality, as determined from the intrinsic binding strengths and binding capacities, is not the same. Although both isolated fractions had similar binding affinities for copper, the total binding capacities were markedly different.

We can conclude that under these experimental parameters, the two pools of organic matter isolated by different approaches do not yield products that are chemically identical. Therefore, these various approaches cannot be used in combination to characterize NOM. One could speculate that some of these differences may be attributed to the 5 kDa filtrate fraction having a slightly larger molecular weight range. However, this is most likely not the case as we would have anticipated different results, such as the exact opposite trends observed in the copper binding experiments. This has potential implications for future research which will deviate from chemical extraction techniques but at the same time base its conclusions on referencing properties of humic substances. Further implications to this research are discussed in Chapter 5.

4.9 References

[1] K. Tan, Humic Matter in Soil and the Environment: Principles and Controversies, CRC Press, 2014.

[2] Mostofa, K., Yoshioka, T., Mottaleb, A., Vione, D., Photobiogeochemistry of Organic Matter: Principles and Practices in Water Environments, Springer, 2013.

[3] Hicks, K., "Using chemical, optical and biological methods to characterize Cu complexation by different natural organic matter sources collected from Canadian shield waters", *Wilfrid Laurier University Thesis Archives*, 2009.

[4] Bieroza, M., "Fluorescence spectroscopy as a tool for determination of organic matter removal efficiency at water treatment works", Drink. Water Eng. Sci., 3, p. 63–70, 2010

[5] Wei, J., Han, L., Song, J., Chen, M., "Evaluation of the interactions between water extractable soil organic matter and metal cations (Cu(II), Eu(III)) using excitation-emission matrix combined with parallel factor analysis," *Int. J. Mol. Sci.* vol. 16, pp. 14464-14476, 2015.

[6] Caron, F., Smith, S., "Fluorescence analysis of natural organic matter fractionated by ultrafiltration: contrasting between urban-impacted water, and radio-contaminated water from a near-pristine site", *Water Air Soil Pollut*., 214:471–490, 2011

[7] Sparks, D., "Methods of soil analysis part 3 - chemical methods," *Soil Sci Soc Am J*, Inc., pp. 5, p. 1011, 1996.

[8] Ghabbour, E., Davies, G., Humic Substances: Structures, Models and Functions, Society of Chemistry, 2001, p. 161.

[9] Plaza, C., Senesi, N., Garcia-Gill, J., Polo, A., "Copper(II) complexation by humic and fulvic acids from pig slurry and amended and non-amended soils," *Chemosphere*, vol. 61, pp. 711-716, 2005.

[10] Gardea-Torresdey, J., Tang, L., Salvador, J., "Copper adsorption by sphagnum peat moss and its different humic fractions," in Proceedings of the 10th Annual Conference on Hazardous Waste Research, University of Texas at El Paso, 1995, pp. 249-260.

Chapter 5: Conclusion and Discussion

5.1 Chapter Overview

This chapter connects the objectives and hypotheses for this project to the results of the experiments that were performed. The significance of these findings are then outlined, focusing on specific implications to risk assessment and prediction for mining operations in northern peatlands, potential species of interest which may be affected by high copper concentrations, and the value in comparing different scientific approaches to studying NOM systems. This is followed by an overall conclusion and description of future work required to advance this field of study.

5.2 The Effects of Climate Change on the Quality of NOM

Some of the most valuable information regarding pore water NOM was attained during the initial method development stage of the project outlined in Chapter 2. These experiments confirmed that the NOM being studied was generally representative of NOM referenced in the literature, particularly with regards to bog wetland NOM. This could be concluded from the predominance of carboxylic acid and phenolic acid groups, as well as the humic and fulvic acid-like fluorescent characteristics.

Another relevant piece of information was outlined in the Method Development Chapter 2 as well. Studying isolated pore water NOM on its own is insufficient for observing any real effects of climate change on the quality of NOM. The decision to increase both the number of FTC's and the concentration of NOM in subsequent experimentation enabled a stronger representation of *in situ*

samples. First, this is because near-surface pore water in northern wetlands will experience multiple freeze-thaw events during the winter and early spring. Second, the pore water is part of a dynamic wetland system as explained in Chapter 1, constantly in contact with peat NOM. We had originally intended to study the effects of freezing and thawing on isolated 'blocks' of peat by simulating flowing pore water through the blocks, but it proved too difficult to control the experimental variables. For this reason, we chose to use pore water because it is more chemically and physically homogenous. We found that adding controlled amounts of peat to pore water enabled reproducible results while still allowing us to achieve our goal of assessing the response of a peat-rich environment to FT events.

We established that freezing and thawing resulted in a higher composition of HMW NOM (12.6 mg C/L (± 7.5) relative to 2.3 mg C/L (± 0.45) in the control). First, this finding disagrees with our hypothesis that freezing and thawing generates fulvic acid-like LMW fragments. Secondly, because the TOC in the LMW NOM fractions remained statistically equal, we have strong evidence to suggest that freezing and thawing disrupts intermolecular interactions between NOM fragments which would have been too large and previously excluded by filtration. Thirdly, while statistically we cannot conclude that more TOC is released after FTCs, all treatment samples did trend towards higher TOC values relative to control samples. Similar to the more pronounced results observed after adding peat to pore water in Chapter 3, we believe that in an *in situ* wetland environment, which would be even more NOM rich than our samples, that more TOC would be released after FTC's. These trends would agree with previous research showing that DOM is released after FTCs in wetland environments [1, 2]. This would therefore indicate that there will be a larger concentration of mobile NOM after freezing and thawing which implies there is an

environmental concern due to the potential for increased complexation and mobilization of copper. However, further investigation into real wetland systems would be required to validate these concerns since increased complexation and mobilization of copper does not necessarily mean increased toxicity.

Cycles of freezing and thawing had no effect on the fluorescent properties of any size fraction of NOM that was filtered. When comparing the control or treatment NOM, each size fraction represented the same fluorescent profile when normalized to carbon indicating that the quality of NOM is independent of size as well. This indicated that the imposed size constraints of the filter size could not be correlated with unique fluorescent components. These results therefore did not support the hypothesis that freezing and thawing would increase the fulvic-like and protein-like moieties. However, the hypothesized increase in protein-like moieties was based on results of studies that used peat, and was attributed to the release of cellular constituents from lysed microorganisms. The lack of observable change in the results could therefore be caused by a relatively smaller microbial population in pore water relative to the population present in whole peat soil [3, 4].

To gather more concrete information relevant to the impacts of freeze-thaw cycling on metal mobility, copper titrations were performed to establish the NOM's inherent ability to complex copper. From these results, we established that freezing and thawing elicits a decrease in the binding affinity of NOM, while also eliciting an increase in its binding capacity. Since the fluorescent properties did not change after freezing and thawing but the copper binding properties

did, there is a strong indication that FTCs only effect change in the structural conformation and intermolecular interactions of NOM fragments.

Relating our findings back to environmental impacts, we believe that differences in the copper binding results would likely be overshadowed by the probable increase in released TOC after freezing and thawing in a large-scale wetland. This has major implications when considering that, regardless of whether the nature of Cu-organic complexation changed, its mobility after freezing and thawing most certainly would. Considering this in combination with the two-fold increase in copper binding capacity (1.7 (+0.5/-0.4) µmol/mg C in the 0.45µm filtrate control relative to 3.4 (+0.5/-0.4) µmol/mg C in the treatment), Cu that has been sequestered through complexation in the upper part of soil can be expected to mobilize when northern wetlands undergo repeated cycles of freezing and thawing in spring months [4]. We should note, however, that previous research has shown a decrease in the released amount of DOC in wetlands after approximately the 4^{th} day of consecutive FTC's (-10 ^{o}C to 5 ^{o}C) [4]. One might speculate a decrease in the labile fraction of NOM if the duration of FTC's was extended over time. For this reason, we would expect to see the largest fraction of mobilized organic matter occur at the beginning of periods of consecutive FTC's.

5.3 Comparing Two Approaches to Studying NOM – Physical Separation vs. Chemical Extraction

To date, there has been no published research comparing NOM that is separated to ≤ 5 kDa using physical ultrafiltration methods to fulvic acid extracts using chemical extraction methods. Thus, it

has been impossible to assess whether findings from chemical extraction studies can be extended to research that uses less manipulative approaches.

It was hypothesized that the 5 kDa filtrate fraction from ultrafiltration separation would yield similar overall results to the fulvic acid extract from a humic-fulvic extraction procedure. As previously stated, this is because when considering the overall range of NOM fragments present in wetland enviroments, fulvic acid molecules ranging from 200-2000 Da are relatively similar to the 5 kDa filtrate fraction, which contain molecules which are equal to or less than 5000 Da [5]. We observed that although NOM separated by the two methods exhibit similar properties, they were not equal with respect to the fluorescent and copper binding properties we were assessing. The fluorescent results of the filtered samples yielded a higher degree of fluorescence intensity in characteristics that were humic acid-like (0.17 (± 0.013) compared to 0.10 (± 0.0079)), fulvic acid-like (0.19 (± 0.00010) compared to 0.16 (± 00.75)) and tyrosine-like (0.022 (± 0.020) compared to 0.013 (± 0.0017)); however, fulvic acid extracts exhibited stronger tryptophan-like characteristics (0.011 (± 0.00086) compared to 0.0050 (± 0.000072)). Similarly, the copper binding results of the filtered samples exhibited a lower intrinsic binding strength (log K 6.01 (+0.21/-0.24) compared to log K 6.46 (+0.22/-0.23)) and higher total binding capacity (3.4 µmol/mg C (+0.73/-0.58) compared to 1.7 µmol/mg C (+0.21/-0.23)).

Both the fluorescence and copper titration results confirmed that the two methods of separation resulted in NOM that was characteristically different. This research therefore illustrates that findings produced from specific techniques used for studying NOM can only benefit scientists that

are willing to carry forward the same approach. The implications for this being that Environmental researchers are further divided and forced to choose between embarking on a project using optimal techniques for their application, or using techniques which predominate the literature and which may increase their chances for publication. This should also emphasize the point that research which references properties of humic substances would be most scientifically valid only if they incorporate chemical extraction techniques into their study.

5.4 Future Direction

There are two directions of research that would extend the results of this project. The first is related to the theme of controlling variables when studying NOM. While isolated systems are useful for understanding specific mechanisms, the degree to which these mechanisms play a role in a complex natural system may never be fully articulated. There are many different factors which contribute to the dynamic nature of the geochemistry of peat wetlands, and therefore an excess of variables which makes experimentation difficult to control for. It is for this reason that research should be directed towards *in situ* field studies. To start, these same separation techniques and tools for analysis could be used to analyze real samples that have naturally undergone multiple freeze-thaw cycles in a peat bog. In the author's opinion, this will be the most effective way of determining the relevance and contribution of findings from isolated studies. The second direction, as previously stated, is to apply these findings to specific applications. This research has established a foundation for assessing one possible effect of climate change on metal transport in wetlands, however the validity of our findings will only be established once a connection can be made to a specific application. For example, research has previously shown that concentrations of

copper can negatively affect growth, or increase mortality rates for various fresh water species and organisms such as algae, diatoms, rotifers, molluscs, and aquatic insects [5, 6, 7, 8, 9]. Future research should therefore consider assessing these toxicological factors on such species in real world environments. We would also need to establish how our findings are connected to other factors such as wetland size, where these organisms live, what bodies of water are in the vicinity, and the degree of anthropological impact.

To extend the implications of this research to risk assessment it is important to connect findings on the mobility and transport of metals in wetlands to toxicological profiles of specific organisms. Conclusions about risk assessment will be region specific, and encompass a multitude of other factors such as copper concentrations, hydrologic flow paths and species at risk [10, 11]. If it was desired, our research could be continued by applying the Biotic Ligand Model to our data to establish a link between bioavailable copper and the risk for toxicity of an organism [12].

5.5 References

[1] Amrhein, C., Strong, J, "Effect of deicing salts on metal and organic matter mobility in roadside soils," *Environ. Sci. Technol*., vol. 26, pp. 703-709, 1992.

[2] Wang, B., "Organic and inorganic nitrogen leaching from incubated soils subjected to freeze–thaw and flooding," *Can. J. Soil Sci.*, vol. 74, pp. 201-206, 1994.

[3] Grogan, P., Michelsen, A., Ambus, P., Jonasson, S., "Freeze–thaw regime effects on carbon and nitrogen gen dynamics in sub–arctic heath tundra mesocosms," *Soil Biol. Biochem.*, vol. 36, pp. 641-654, 2004.

[4] Yu, X., "Material Cycling of Wetland Soils Driven by Freeze–Thaw Effects," Springer - Northeast Institute of Geography and Agroecology, Vols. 2190-5061.

[5] Niessen, W., "Liquid Chromatography-Mass Spectrometry, Third Edition," CRC Press - Taylor & Francis, vol. 97, p. 216.

[6] Haynes, K., "Hydrological controls on mercury mobility and transport from a forested hillslope during spring snowmelt", Department of Geography, University of Toronto, 2012.

[7] Bearup, L., "Changing flow, transport, and geochemistry in the mountain pine beetle-killed forests of Rocky Mountain National Park, Colorado", Colorado School of Mines, 2014.

[8] Schafer, H., Hettler, H., Fritsche, U., et al., "Biotests using unicellular algae and ciliates for predicting long-term effects of toxicants.," *Ecotoxicol. Environ. Saf.*, vol. 27, pp. 64-81, 1994.

[9] Janssen, C., Ferrando, M., Persoone, G., "Ecotoxicogical studies with the freshwater rotifer Brachionus calciflorus. IV. Rotifer behavior as a sensitive and rapid sublethal test criterion," *Ecotoxicol. Environ. Saf*, vol. 28, pp. 244-255, 1994.

[10] US EPA, "Ambient water quality criteria for copper," US Environmental Protection Agency, 1980.

[11] Cheng, T., "Use of Copper as a Molluscicide.," Copper in the Environment. Part 2. Health Effects. John Wiley, pp. 401-432, 1979.

[12] Buhl, K., Hamilton, S., "Comparative toxicology of inorganic contaminants released by placer mining to early life stages of salmonids," *Ecotoxicol. Environ. Saf.*, vol. 20, pp. 325-342, 1980.

Appendix A – Supplementary Information, Figures & Tables for Chapters 2 to 4

Chapter 2 Supplementary Information

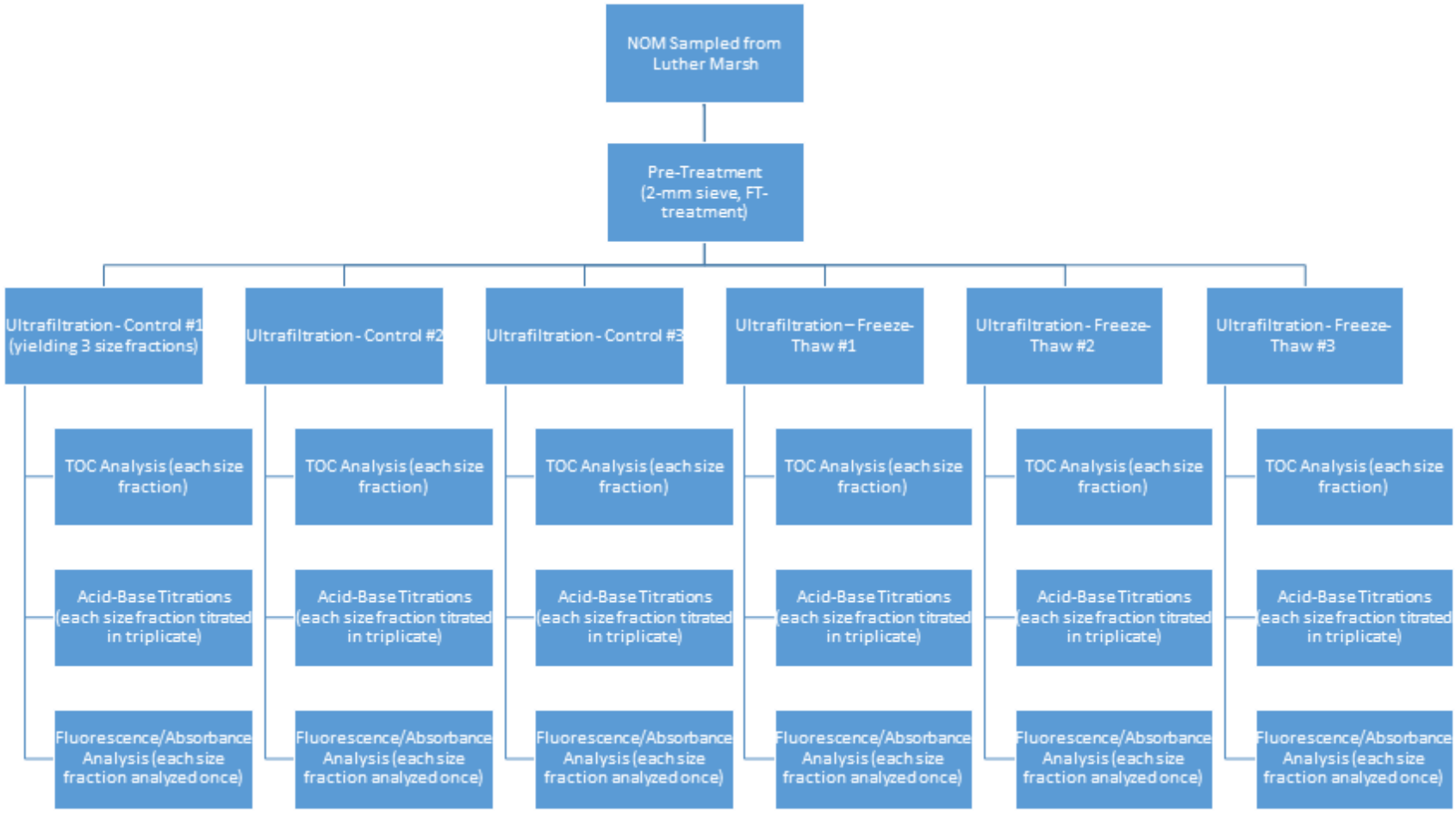

Figure A1. Schematic of Experimental Workflow for Chapter 2.

Table A1. Relative HMW and LMW TOC composition for ultrafiltration treatments. Standard error not included due to lack of replicates for Chapter 2 data. Supplementary to data illustrated in Figure 2-3.

Size Fraction	Control TOC (%)	FTC TOC (%)
High MW	25.5	45.6
Low MW	74.5	54.4

Table A2. Mass correction yielding HMW and LMW NOM carbon content for ultrafiltration treatments. Standard error not included due to lack of replicates for Chapter 2 data. Supplementary to data illustrated in Figure 2-4.

Size Fraction	Control TOC (mg C)	FTC TOC (mg C)
High MW	29.7	12.7
Low MW	86.9	15.1

Table A3. Tabulated values comparing the percent relative fluorescent components in different size fractions of control and FTC samples, normalized to units of carbon, as determined by PARAFAC analysis. Standard error not included due to lack of replicates for Chapter 2 data. Supplementary to data illustrated in Figure 2-9.

Fluorescent Components	Size Fractions					
	0.45µm Filtrate		5 kDa Retentate		5 kDa Filtrate	
	Control	Freeze-Thaw	Control	Freeze-Thaw	Control	Freeze-Thaw
Trp	3.9	3.3	4.7	4.6	3.5	8.8
FA	1.3	0.0	3.2	2.7	0.0	0.0
HA	77.2	70.7	92.0	79.2	60.8	45.9
Tyr	17.6	26.0	0.0	13.5	35.7	45.3

Table A4. Tabulated values comparing the total composition of fluorescent components in different size fractions of control and FTC samples, normalized to units of carbon, as determined by PARAFAC analysis. Standard error not included due to lack of replicates for Chapter 2 data. Supplementary to data illustrated in Figure 2-10.

Fluorescent Components	Size Fractions					
	0.45µm Filtrate		5 kDa Retentate		5 kDa Filtrate	
	Control	Freeze-Thaw	Control	Freeze-Thaw	Control	Freeze-Thaw
Trp	0.0004	0.0004	0.0001	0.0004	0.0006	0.0026
FA	0.0001	0.0000	0.0001	0.0002	0.0000	0.0000
HA	0.0073	0.0096	0.0026	0.0062	0.0105	0.0134
Tyr	0.0017	0.0035	0.0000	0.0011	0.0061	0.0132

Table A5. Comparison of Acidic, Intermediate and Basic Functional Group concentrations in the different size fractions of the Control and FTC treatment samples. Standard error not included due to lack of replicates for Chapter 2 data. Supplementary to data illustrated in Figure 2-12.

	0.45µm (L_T (µmol))				5 kDa Retentate (L_T (µmol))				5 kDa Filtrate (L_T (µmol))			
	Total Capacity	Acidic <5	Intermediate 5-8.5	Basic >8.5	Total Capacity	Acidic <5	Intermediate 5-8.5	Basic >8.5	Total Capacity	Acidic <5	Intermediate 5-8.5	Basic >8.5
Control	12.5	2.95	1.96	7.27	3.33	1.19	0.66	1.369	5.57	1.37	1.05	3.03
Freeze-Thaw	9.06	4.39	1.41	2.99	3.79	1.45	0.80	1.41	10.02	2.84	1.40	5.64
S.D. Control	8.03	2.56	1.74	3.59	0.94	0.39	0.08	0.44	1.90	0.37	0.25	1.24
S.D. Freeze-Thaw	3.83	1.42	1.44	0.83	1.19	0.37	0.27	0.48	5.57	0.72	0.54	4.21
S.E. Control	4.64	1.48	1.01	2.07	0.67	0.28	0.06	0.31	1.34	0.26	0.18	0.88
S.E. Freeze-Thaw	2.71	1.01	1.02	0.59	0.84	0.27	0.20	0.34	3.22	0.42	0.31	2.43

Chapter 3 Supplementary Information

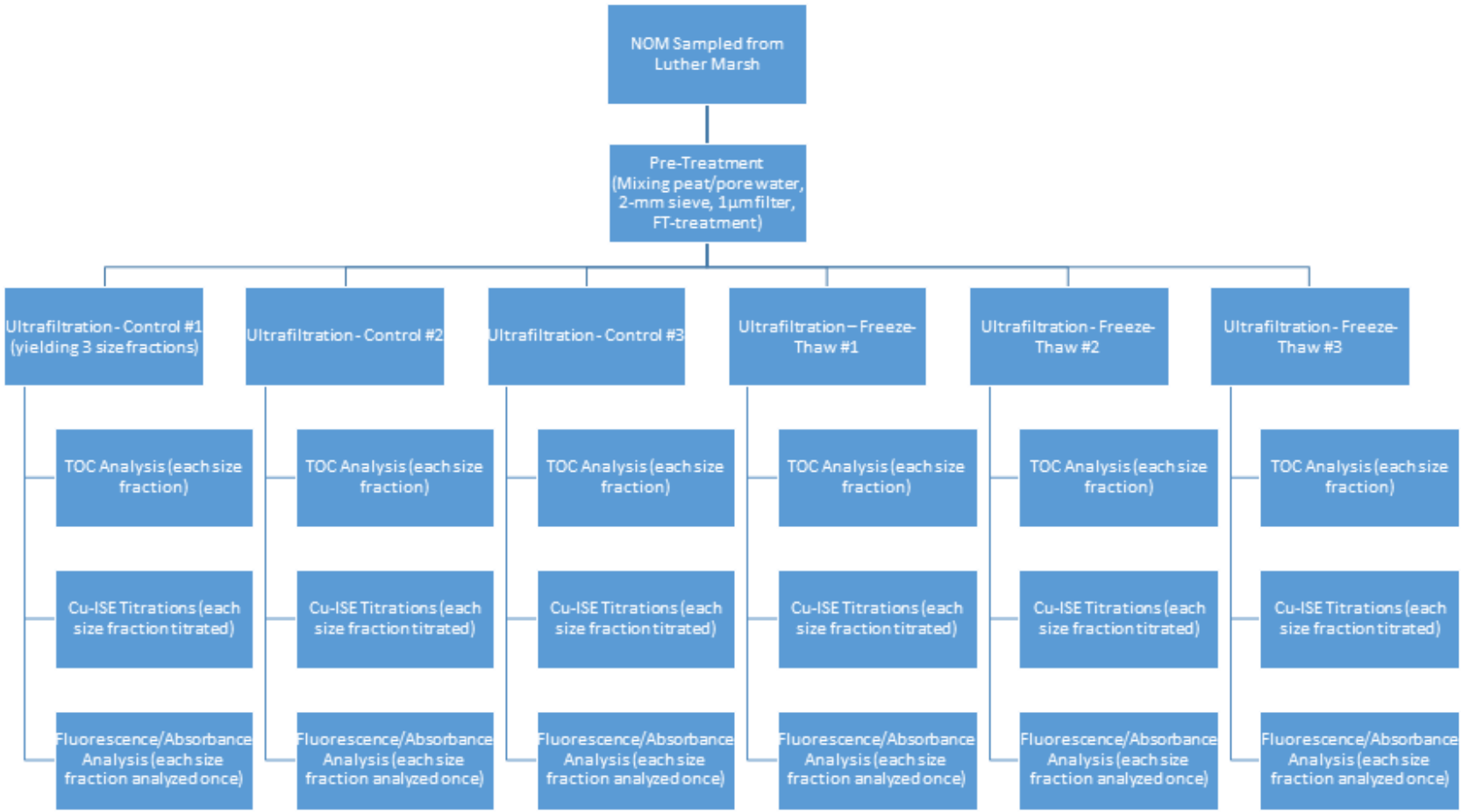

Figure A2. Schematic of Experimental Workflow for Chapter 3.

Table A6. Relative high and low molecular weight NOM composition for ultrafiltration treatments. Supplementary to data illustrated in Figure 3-1.

Size Fraction	Control TOC (%)	Standard Error	FTC TOC (%)	Standard Error
High MW	9.9	3.33	39.17	24.29
Low MW	90.1	3.33	60.83	24.29

Table A7. Mass correction yielding high and low molecular weight carbon content for ultrafiltration control and FTC treatment samples. Supplementary to data illustrated in Figure 3-2.

Size Fraction	Control TOC (mg C)	Standard Error	FTC TOC (mg C)	Standard Error
High MW	2.3	0.4	12.6	7.5
Low MW	22.5	12.3	20.1	9.1

Table A8. Tabulated values comparing the intensity of fluorescent components in different size fractions of Control and FTC samples, normalized to units of carbon, as determined by PARAFAC analysis. Supplementary to data illustrated in Figure 3-3.

	Size Fractions					
	0.45µm Filtrate		5 kDa Retentate		5 kDa Filtrate	
Fluorescent Components	Control	FTC	Control	FTC	Control	FTC
Trp	0.0090	0.014	0.010	0.013	0.005	0.018
FA	0.20	0.23	0.19	0.21	0.19	0.27
HA	0.18	0.17	0.17	0.17	0.17	0.15
Tyr	0.022	0.030	0.020	0.022	0.022	0.071

Table A9. Tabulated values comparing the total intensity of fluorescent components in different size fractions of Control and FTC samples, as determined by PARAFAC analysis. Supplementary to data illustrated in Figure 3-4.

	Size Fractions					
	0.45µm Filtrate		5 kDa Retentate		5 kDa Filtrate	
Fluorescent Components	Control	FTC	Control	FTC	Control	FTC
Trp	0.27	0.40	0.30	0.44	0.13	0.24
FA	6.04	6.21	5.98	7.57	4.85	4.34
HA	5.40	4.54	5.40	6.09	4.46	2.65
Tyr	0.64	0.82	0.62	0.77	0.58	1.01

Table A-10. Tabulated values comparing the relative copper binding affinity (log K) for each size fraction of the control and FTC treatment samples. Supplementary to data illustrated in Figure 3-7.

Size Fraction	Treatment	Log K	CI (±)
0.45 µm Filtrate	Control	6.75	0.29/0.26
	FTC	6.13	0.23/0.22
5 kDa Filtrate	Control	6.01	0.21/0.24
	FTC	5.65	0.25/0.24
5 kDa Retentate	Control	6.08	0.25/0.30
	FTC	5.83	0.300.25

Table A-11. Tabulated values comparing the total binding strength (L_T in µmol/mg C) of the control and FTC treatment samples for the 0.45 µm filtrate, 5 kDa filtrate and 5 kDa retentate fractions. Supplementary to data illustrated in Figure 3-8.

Size Fraction	Treatment	L_T (µmol/mg C)	CI (±)
0.45 µm Filtrate	Control	1.73	0.46/0.40
	FTC	2.99	0.49/0.41
5 kDa Filtrate	Control	3.36	0.73/0.58
	FTC	4.75	1.01/1.01
5 kDa Retentate	Control	2.87	0.84/0.60
	FTC	4.56	1.01/0.98

Chapter 4 Supplementary Information

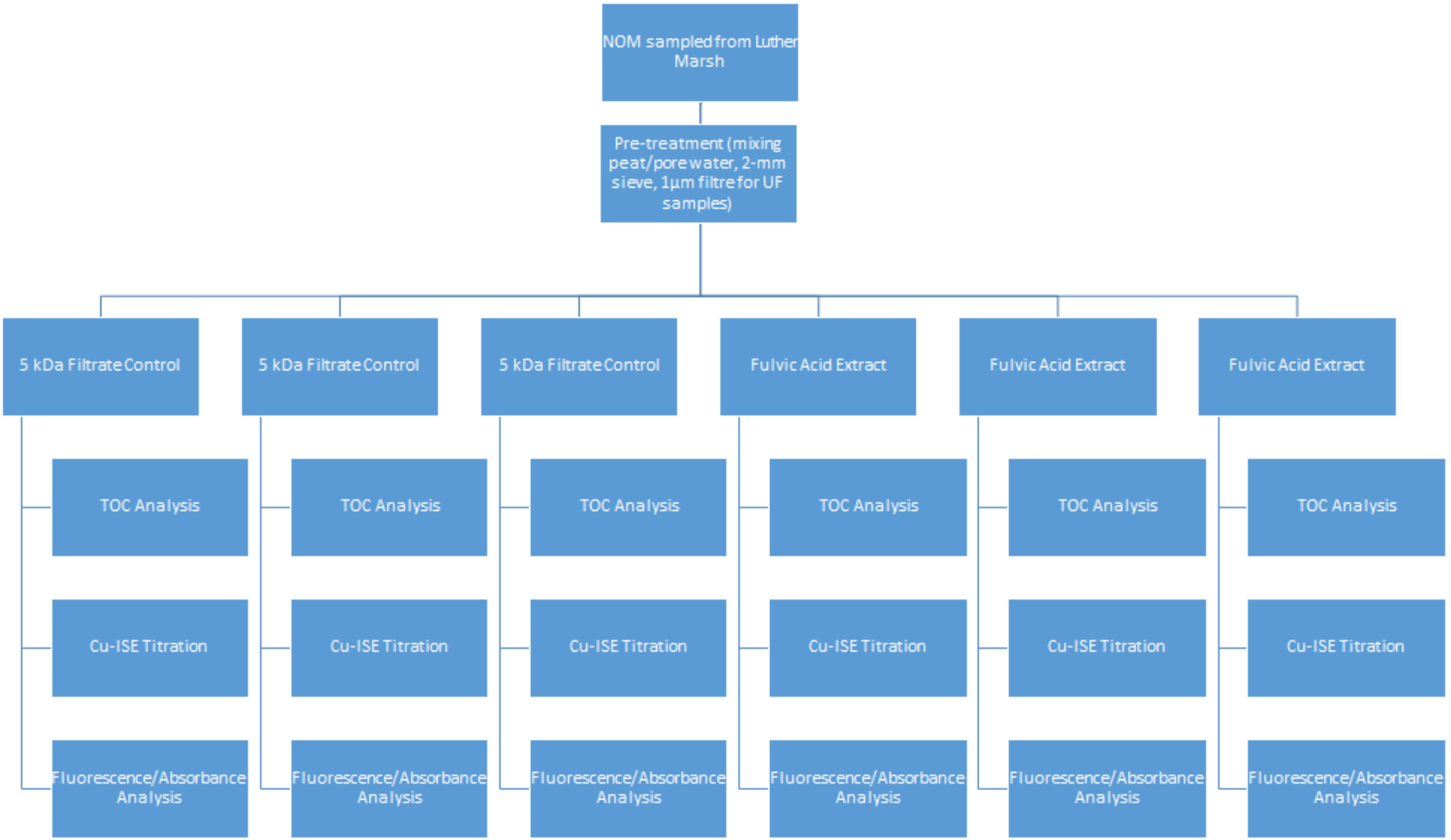

Figure A3. Schematic of Experimental Workflow for Chapter 4.

Table A-11. Tabulated values comparing the fluorescent components of the 5 kDa Filtrate control and FA Extract samples, normalized to units of carbon, as determined by PARAFAC analysis. Supplementary to data illustrated in Figure 4-2.

Fluorescent Components	NOM Fractions	
-	5 kDa Filtrate	FA Extract
Trp	0.005	0.011
FA	0.19	0.16
HA	0.17	0.10
Tyr	0.022	0.013

Table A-12. Tabulated values comparing the total fluorescent components of the 5 kDa Filtrate control and FA Extract samples, as determined by PARAFAC analysis. Supplementary to data illustrated in Figure 4-3.

Fluorescent Components	NOM Fractions	
-	5 kDa Filtrate	FA Extract
Trp	0.13	1.11
FA	4.8	15.9
HA	4.4	10.1
Tyr	0.58	1.28

Table A-13. Tabulated values comparing the relative copper binding affinity of the control and FTC treatment samples for the 0.45 µm filtrate, 5 kDa filtrate and 5 kDa retentate fractions. Supplementary to data illustrated in Figure 4-4.

Size Fraction	Log K	CI (±)
5 kDa Filtrate	6.01	0.21/0.24
FA Extract	6.46	0.22/0.23

Table A-14. Tabulated values comparing the total binding strength (L_T in μmol/mg C) of the 5 kDa Filtrate and the FA Extract samples. Supplementary to data illustrated in Figure 4-5.

Size Fraction	LT (μmol/mg C)	CI (±)
5 kDa Filtrate	3.36	0.73/0.58
FA Extract	1.69	0.21/0.23

Appendix B – MATLAB Processing Scripts

B1 - MATLAB Script for PARAFAC Processing of Fluorescent Samples to Produce Percent HA, FA, TYR and TRY-like components.

```
function II=PARAFAC_process_Matts_data

prefix='Matt'; %EXX=220:10:450;

%----- start preprocessing ---------------------- %
 %preprocess so strange data resolution can have same dimension as the rest
%load SS1_scott_sept7_2007_filtered.mat
%EM=em; EX=ex;
%name='SRFA'; txt=['load ',name,'.mat']; eval(txt);
[FF,weight]=resample(ex,em,F,EX,EM); FSRFA=FF; F=FF;
%save FSRFA.mat
% ----- end preprocess

% took out

%'Nov23_2006_Hamilton3'

% start real processing
%'Tyr_5e-7M_and_Trp_25e-8M_Apr12_2008.mat', ...
%'Tyr_5e-7M_Apr10_2008.mat', ...

names=strvcat(...
'FAE1.mat', ...
'FAE2.mat', ...
'FAE3.mat', ...
'FT1-5kdaFiltrate.mat', ...
'FT1-5kdaRetentate.mat', ...
'FT1-045um.mat', ...
'FT2-5kdaFiltrate.mat', ...
'FT2-5kdaRetentate.mat', ...
'FT2-045um.mat', ...
'FT3-5kdaFiltrate.mat', ...
'FT3-5kdaRetentate.mat', ...
'FT3-045um.mat', ...
'nFT1-5kdaFiltrate.mat', ...
'nFT1-5kdaRetentate.mat', ...
'nFT1-045um.mat', ...
'nFT4-5kDaFiltrate.mat', ...
'nFT4-5kDaRetentate.mat', ...
'nFT4-045um.mat', ...
'nFT5-5kdaFiltrate.mat', ...
'nFT5-5kdaRetentate.mat', ...
'nFT5-045um.mat', ...
'Trp_25e-8M_Apr12_2008.mat', ...
'Tyr_5e-7M_and_Trp_25e-8M_Apr12_2008.mat', ...
'Trp_25e-8M_Apr12_2008.mat', ...
```

Sample Data

```
'Tyr_5e-7M_and_Trp_25e-8M_Apr12_2008.mat', ...
'Tyr_5e-7M_Apr10_2008.mat');

firstdimension=size(names,1);
name=names(1,:); txt=['load ',name]; eval(txt);
seconddimension=size(F,1)-2
thirddimension=size(F,2)

EMM=em; EXX=ex(3:26);

Fnew=ones(firstdimension,seconddimension,thirddimension); Fnew=Fnew*NaN;

for ii=1:size(names,1)
    name=names(ii,:);
    txt=['load ',name]; eval(txt);

    F=F(3:26,1:351);

    %meantst=nanmean(nanmean(F));
    %stdtst=nanstd(nanstd(F));

    %for i=1:size(F,1)
    %    for j=1:size(F,2)
    %        if F(i,j)>=meantst+12*stdtst; F(i,j)=NaN; end
    %    end
    %end


    %Fii=F./(max(max(F)));
    Fnew(ii,:,:)=F;

    %FI(ii)=Fii(18,201)/Fii(18,251);
%     contour(EMM,EXX,(F),10)
%     k=waitforbuttonpress;

end

f=dataset(Fnew);

f.author='Scott Smith';
f.label{1}=[names];
f.axisscale{1}=[1:1:firstdimension];
f.axisscale{2}=EXX;
f.axisscale{3}=EMM';
f.axisscalename{1}='Sample number';
f.axisscalename{2}='Emission wavelength';
f.axisscalename{3}='Excitation wavelength';
f.title{1}='Sample mode';
f.title{2}='Emission mode';
f.title{3}='Excitation mode';

numberofcomponents=5;
options=parafac('options');
options.stopcriteria.relativechange=1e-8;
```

```
%options.constraints{1}.nonnegativity=1; % constrain positive concentrations

 for i=1:3
     istr=num2str(i);
     txt=['options.constraints{',istr,'}.type=''nonnegativity''']; eval(txt);
 end

model=parafac(f,numberofcomponents,options);

%load six
%load resix;
%load four.mat
%load five.mat
%load seven.mat

for i=1:numberofcomponents
    istr=num2str(i);
    txt=['emspec',istr,'=(model.loads{2}(:,',istr,'));']; eval(txt)
    txt=['exspec',istr,'=(model.loads{3}(:,',istr,'));']; eval(txt)
    txt=['conc',istr,'=(model.loads{1}(:,',istr,'));']; eval(txt)
    txt=['surf',istr,'=emspec',istr,'*exspec',istr,''';']; eval(txt)
end

if numberofcomponents==1; fname=[prefix,'one']; end
if numberofcomponents==2; fname=[prefix,'two']; end
if numberofcomponents==3; fname=[prefix,'three']; end
if numberofcomponents==4; fname=[prefix,'four']; end
if numberofcomponents==5; fname=[prefix,'five']; end

txt = ['save ',fname,'.mat']; eval(txt);

end

%%%%%%%%%%%%%%%%%%%%%%%%%%%%%%%%%%%%%%%%%%%%%%%%%%%%%%%%%%%%%%%%%%%%%%%%55-
function [II,W]=resample(ex,em,F,EX,EM);

c=0; cc=0; x=[]; y=[]; z=[];

for i=1:size(ex,2)
    for j=1:size(em,1)
            tst=isnan(F(i,j));
            if tst==0
            c=c+1;
            x(c)=ex(i);
            y(c)=em(j);
            z(c)=F(i,j);
            end
            if tst==1
            cc=cc+1;
            xc(cc)=ex(i);
            yc(cc)=em(j);
            zc(cc)=0.01;
            end
```

```
    end
end

[xx,yy]=meshgrid(EM,EX);
zz=griddata(x,y,z,yy,xx,'cubic',{'QJ'}); %linear cubic nearest v4
II=zz;

[xx,yy]=meshgrid(EM,EX);
zzweight=griddata(xc,yc,zc,yy,xx,'linear',{'QJ'}); %linear cubic nearest v4
for i=1:size(zzweight,1)
    for j=1:size(zzweight,2)
        tst=isnan(zzweight(i,j));
        if tst==1; zzweight(i,j)=1; end
    end
end
W=zzweight;

End
```

B2 - MATLAB Script for Fully Optimized Continuous (FOCUS) Processing Template used to Produce Concentrations of Functional Groups in Discrete Ranges of pK_a Values from Acid-Base Titrations.

```
function [II,GG,HH,QQ]=FOCUS_BestLts(pH,b)

warning off

% select pKas defined by the data (first choice)
% or fix pKa range (usefull if planning on linear combination of pKa
% spectra
n=size(pH,1); delta=mean(diff(pH));
pKs=min(pH)-1:delta:max(pH)+1;
%pKs=[3.2:0.2:10.6];

So=0; Lts=zeros(size(pKs'));

p0=[Lts' So];
maxpH=max(pH); minpH=min(pH); % can change these values to only fit portion
of data
[pH,b,origin,p0]=return_data_for_process([pH],[b],maxpH,minpH,pKs,Lts,So);
n=size(p0,2); Lts=p0(1:n-1)'; So=p0(n); % now reenter to make sure p0
estimate is a good one
[pH,b,origin,p0]=return_data_for_process([pH],[b],maxpH,minpH,pKs,Lts,So);

lambdaguess=1; OPTIONS=optimset('fminsearch');
OPTIONS.MaxFunEvals=50000; OPTIONS.Display='off';

best_lambda=fminsearch('minimize_distance',lambdaguess,OPTIONS,p0,pH,b,origin
,pKs);
```

```
[distance,bestLts]=minimize_distance(best_lambda,p0,pH,b,origin,pKs);

% best-fit line

% make A matrix add a site with zero conc on either end

%delta=pKs(2)-pKs(1);
[n,m]=size(pKs);
pKs_mod=[pKs(1)-3*delta pKs(1)-2*delta pKs(1)-delta pKs pKs(m)+delta
pKs(m)+2*delta pKs(m)+3*delta];

K=10.^(-1*pKs_mod); H=10.^(-1*pH);

for i=1:size(pH,1)
        for j=1:size(pKs_mod,2)
              A(i,j)=K(j)/(K(j)+H(i));
        end
end

[n,m]=size(p0); %s=p0(1:m-1); so=p0(m); s=[0 0 0 s 0 0 0];
s=bestLts(1:m-1); so=bestLts(m);s=[0 0 0 s 0 0 0];

q=A*s'+so; bsd=ones(size(b));

II=bestLts(1:m-1);
GG=pKs;
HH=q;
QQ=so;

end
```

B3 - MATLAB Script for Langmuir Isotherm Template by Monte Carlo Analysis used to Produce Log K and Copper Binding Capacities from Copper Binding Titrations.

```
% fitting Langmuir isotherm data TEMPLATE

clear

% ----------------------------  INPUT DATA  -----------------

% three things to input DOC, titration data (in format I describe below
% and initial guess (described below)

DOC=1; % measured DOC in mg C/L

% first column is log of free Cu (measured in mol/L)
% second column is bound Cu calculated as
% CuT-[Cu meas] - sum Cu inorg (calc from Cu meas)
```

```
% NOTE take out data at the beginning of the titration if free Cu (mV) are
% constant.  that means the free Cu is below detection for that level of
% buffering

% for replicate data just put in all the points in two columns

DATA=[...

-9.629285714    1.7947E-09
-9.307857143    1.07787E-08
-8.522142857    3.77108E-08
-8.165          9.15886E-08
-7.415          1.9907E-07
-6.879285714    4.13686E-07
-6.200714286    8.39364E-07
-5.486428571    1.67199E-06

-9.874642857    1.67538E-09
-9.588928571    1.00581E-08
-8.7675         3.51947E-08
-8.231785714    8.54546E-08
-7.5175         1.85802E-07
-6.910357143    3.86031E-07
-6.124642857    7.81767E-07
-5.303214286    1.54155E-06

-10.4438701     1.59056E-09
-10.29404053    9.54506E-09
-9.657264861    3.34073E-08
-8.945574409    8.11259E-08
-8.12151178     1.76517E-07
-7.484736113    3.67173E-07
-6.885417837    7.48009E-07
-6.023897816    1.50339E-06
 ];

% initial guess should be LT guess where the data plateaus (data normalized
% to DOC because that is the way I wrote the fitting).  the logK guess
% should be 1/[Cu2+] at half saturation.  (or -1*log[Cu] at half sat.).
% YOu will see this from the preliminary data plot I generate below.

logK=6.8; LT=5.5; %LT in umol/mg C (I intentionally set an initial guess off
the best fit so you can see the improvement
K=10.^logK;

% monte carlo analysis number of steps

MC=1000; % should be 1000 for the final determination. but can make smaller
while figuring it out
error=0.1; % relative error.  currently set to 5% of the max OrgCu
flag=0; % set to zero so you don't see MC graphs.  set to 1 to see them

% ------------------ PARAMETER FITTING ----------------
```

Example Data

```
% start by plotting data and initial guess.  Run the program manually
% changing initial guess until you get a good initial guess (CTRL C to
% cancel after making each initial guess you don't like).  click on the
% figure window if you like the initial guess and want to proceed.

logCu=DATA(:,1); Cu=10.^logCu;
OrgCu=(1e6*DATA(:,2))./DOC; % bound in units umol/mg of C

figure(1); clf; plot(logCu,OrgCu,'ko','markersize',10,'markerfacecolor','b')
set(gca,'linewidth',2,'fontsize',12)
xlabel('log[Cu^{2+} \{mol/L\}]','fontsize',12)
ylabel('bound Cu (\mumol/mg C)','fontsize',12)

% add initial guess line

interval=(max(logCu)-min(logCu))./50;
logCuplot=min(logCu)-5*interval:interval:max(logCu)+5*interval;
Cuplot=10.^logCuplot;
OrgCumodel=(Cuplot*LT*K)./(1+K*Cuplot);

hold on; plot(logCuplot,OrgCumodel,'k','linewidth',2)
axis([min(logCuplot) max(logCuplot) 0 1.1*max(OrgCu)])

k=waitforbuttonpress; % fitting will not continue until figure window is
clicked

langmuir=@(p) log10(sum((OrgCu-(10.^p(1)*10.^p(2)*Cu)./(1+10.^p(2)*Cu)).^2));
% sum of squares error function

pguess=log10([LT K]); % optimize as log so that LT is that both are forced to
be nonzero

lb=[log10(LT)-3 log10(K)-3]; ub=[log10(LT)+3 log10(K)+3]; % prevent "crazy"
parameter values
options = optimoptions('fmincon','Display','iter','Algorithm','sqp');

%popt = fmincon(fun,x0,A,b,Aeq,beq,lb,ub,nonlcon,options)
[popt,fval] = fmincon(langmuir,pguess,[],[],[],[],lb,ub,[],options);

LTopt=10.^popt(1)
logKopt=popt(2)
Kopt=10.^logKopt;

%R2 = 1.0 - (SSres/SStot) =1.0-4165/62735= 0.9336

SSres=10.^fval; SStot=sum((OrgCu-mean(OrgCu)).^2); N=size(OrgCu,1)

R2 = 1.0 - (SSres)./(SStot)
R2adjust= 1.0-(SSres/(N-2))./(SStot/(N-1))

%R squared from http://www.graphpad.com/guides/prism/6/curve-
fitting/index.htm?reg_diagnostics_tab_7_2.htm
```

```
% verify fit

bestOrgCumodel=(Cuplot*LTopt*Kopt)./(1+Kopt*Cuplot);
plot(logCuplot,bestOrgCumodel,'b--','linewidth',2)

k=waitforbuttonpress;

% add in boostrap MC analysis for parameter confidence ----------------------
----------------------

% define error function for MC

for i=1:MC
    i
    % remove 1/3 of the data
    MCOrgCu=OrgCu;
    fraction=round(N/3);
    selections=randperm(N,fraction);
    for j=1:size(selections,2)

MCOrgCu(selections(j))=(Cu(selections(j))*LTopt*Kopt)./(1+Kopt*Cu(selections(
j)))+error*max(OrgCu)*randn(1);
    end
    if flag==1
    figure(2);
    plot(logCu,OrgCu,'ko','markersize',10);
    hold on
    plot(logCuplot,bestOrgCumodel,'b--')
    plot(logCu,MCOrgCu,'k.','markersize',10);
    %k=waitforbuttonpress;
    end
    % FITTING
    MClangmuir=@(p) log10(sum((MCOrgCu-
(10.^p(1)*10.^p(2)*Cu)./(1+10.^p(2)*Cu)).^2)); % sum of squares error
function
    options = optimoptions('fmincon','Display','off','Algorithm','sqp');
    [popt,fval] = fmincon(MClangmuir,pguess,[],[],[],[],lb,ub,[],options);
    LToptVECTOR(i)=10.^popt(1); logKoptVECTOR(i)=popt(2);

bestOrgCumodelMATRIX(:,i)=((Cuplot*LToptVECTOR(i)*10.^logKoptVECTOR(i))./(1+1
0.^logKoptVECTOR(i)*Cuplot))';
end

% SEM = std(LToptVECTOR)/sqrt(length(LToptVECTOR));              % Standard
Error
% ts = tinv([0.025  0.975],length(LToptVECTOR)-1);      % T-Score % this is
95% CI
% CI = mean(LToptVECTOR) + ts*SEM;                      % Confidence
Intervals
% %LTandCI=[mean(LToptVECTOR) CI]
% LTplusminus95CI=[mean(LToptVECTOR) CI(2)-mean(LToptVECTOR)]
%
%
% SEM = std(logKoptVECTOR)/sqrt(length(logKoptVECTOR));               %
Standard Error
```

```
% ts = tinv([0.025  0.975],length(logKoptVECTOR)-1);      % T-Score % this is
95% CI
% CI = mean(logKoptVECTOR) + ts*SEM;                      % Confidence
Intervals
% logKplusminus95CI=[mean(logKoptVECTOR) CI(2)-mean(logKoptVECTOR)]
%
% m = mean(logKoptVECTOR);
% dist = abs(logKoptVECTOR - m);
% [sortDist, sortIndex] = sort(dist);
% index_95perc = sortIndex(1:floor(0.95 * numel(logKoptVECTOR)));
% x_95percent = logKoptVECTOR(index_95perc); n=size(x_95percent,2);
% logKandCI=[mean(logKoptVECTOR) x_95percent(1) x_95percent(n)]

logKandCI=[mean(logKoptVECTOR) prctile(logKoptVECTOR,[2.5 97.5])]
LTandCI=[mean(LToptVECTOR) prctile(LToptVECTOR,[2.5 97.5])]

k=waitforbuttonpress;

% ------------------ GRAPHING ------------------------

figure(1); clf; plot(logCu,OrgCu,'ko','markersize',10,'markerfacecolor','b')
set(gca,'linewidth',2,'fontsize',12)
xlabel('log[Cu^{2+} \{mol/L\}]','fontsize',12)
ylabel('bound Cu (\mumol/mg C)','fontsize',12)
hold on
plot(logCuplot,bestOrgCumodel,'k','linewidth',2)
plot(logCuplot,min(bestOrgCumodelMATRIX'),'k--','linewidth',2)
plot(logCuplot,max(bestOrgCumodelMATRIX'),'k--','linewidth',2)
axis([min(logCuplot) max(logCuplot) 0 1.1*max(OrgCu)])

figure(2); clf;

subplot(211);
histfit(LToptVECTOR,10); set(gca,'linewidth',2)
xlabel('L_T (\mumol/mg C)','fontsize',12)
ylabel('frequency','fontsize',12)
subplot(212);
histfit(logKoptVECTOR,10); set(gca,'linewidth',2)
xlabel('logK','fontsize',12)
ylabel('frequency','fontsize',12)

% ---------------- EXPORT DATA ----------------------

dataexport=[...
    logCuplot' bestOrgCumodel'
    ]

% cut and paste from matlab window into excel
% or import the text file into excel (this file will be overwritten each
% time unless you change the name

save bestfitlangmuir.txt dataexport -ascii
```